UiT The Arctic University of Norway

Department of Arctic and Marine Biology

Vegetation-environment analysis of areas with peat accumulation and hummock formation in the context of NiN (Natur i Norge)

A study from Laggu, Gamvik municipality, Troms and Finnmark county

Elin Karin Plathe

Master's thesis in Biology … BIO-3950 … May 2021

Elin Karin Plathe
elinplathe@gmail.com
+47 934 99 486

Supervisors:

Lennart Nilsen
lennart.nilsen@uit.no
Northern population and ecosystems research group,
UiT Arctic University of Norway

Rune Halvorsen
rune.halvorsen@uhm.uio.no
Geo–ecological research group (GEco)
Natural History Museum, UiO

Geir Arnesen
geir@sallirnatur.no
Sállir natur AS

Master of Science in biology:
Northern Populations and Ecosystems
Department of Arctic and Marine Biology
UiT The Arctic University of Norway

Front page: Hummock formations on an esker in Laggu, Troms and Finnmark county.
Photo by Elin Karin Plathe

“Nothing in biology makes sense except in the light of evolution.”
–Theodosius Dobzhansky

Abstract

A conspicuous type of heath and forest with peat accumulation and hummock formation in terrestrial systems has been investigated in Laggu, Gamvik municipality in northern Norway (70°57' N 27°38' E). The aim was to describe vegetational composition, soil depth and hummock distribution, and identify environmental factors that cause terrestrial peat accumulation.

Vascular plants, bryophytes and lichens were registered in 58 plots of 1×1 meter, located within seven transects that covered terrestrial peat accumulating areas and a gradual transition into their surrounding nature types. 26 explanatory variables were registered in each plot. To identify compositional turnover along the main gradients and relate the explanatory variables to the observed pattern, parallel ordination with DCA and GNMDS was applied. Land cover–mapping of the transects and their surrounding nature types was also conducted. Additionally, peat depth and maximum hummock height in areas surrounding each transect was recorded.

The results discovered three distinct gradients along the investigated transects. The main gradient was related to a well-known gradient from forest to exposed ridges. The second gradient was related to peat accumulation. The third gradient was related to the presence and cover of the allelopathic evergreen shrub *Empetrum nigrum*.

The results from this study indicate that peat accumulation rates is likely a result of a cold climate, the low decomposition rate of the soil and in a positive feedback–loop with the allelopathic properties of *Empetrum nigrum* and the intrinsic slow decomposition rates of *Polytrichum juniperinum*, in addition to effects caused by frost processes. Regarding the NiN-system, this study concludes that there exists a peat accumulation gradient in terrestrial systems, similar to the LEC Peat accumulating ability (TE) in wetland systems. Further research is needed to describe the details of the hummock and evaluate the snow cover and frost processes that is connected to terrestrial peat accumulation.

Keywords: Terrestrial peat accumulation, hummock, Nature in Norway (NiN), gradient analysis, *Empetrum nigrum*, *Polytrichum juniperinum*.

Abbreviations

DCA – Detrended Correspondence Analysis
DEM – Digital Elevation Model
EDU – Ecological Distance Unit
GAP – Gradient Analytic Perspective
GIS – Geographic Information System
GPS – Global Positioning System
GNMDS – Global Non–Metric Multidimensional Scaling
LEC – Local environmental complex–variable
NIN – Natur i Norge, 'Nature in Norway'
NDVI – Normalized Difference Vegetation Index

Acknowledgements

Takk til mine veiledere for gode diskusjoner og et spennende prosjekt! Takk til Sissel Kaino for god hjelp og tilrettelegging på lab, til Kari–Anne Bråthen for bruk av NIRS metodikk, til Jane Jepsen for datering av bjørkemålerangrep og til Arve Elvebakk for hjelp til artsbestemmelse av moser og lav.

Stor takk til gamle og nye venner i Ung Botaniker Tromsø for en god blanding av faglig og sosialt påfyll, også gjennom en pandemi! Takk til mamma Hilde og pappa Erik for urokkelig støtte gjennom et langt studieløp. Takk til gode venner for motivasjon gjennom hele løpet.

Takk også til min pelskledde feltassistent Primus for en måneds selskap i felt. Og takk for at du kom tilbake etter 10 timer på frifot på Finnmarksvidda og ikke gjorde feltarbeidet alt for spennende...

Sist men ikke minst, takk til min fine kohort; Brynjar og de to firbeinte Primus og Brautin.

Elin Plathe

Elin Karin Plathe
Tromsø, may 2021

Contents

List of Figures

List of Tables

1

Introduction

Plant communities are characterized by being dynamic and spatially heterogeneous systems (White, 1979; Sousa, 1984). The dynamics in natural communities are expressed through changes in relative species abundances over time, which is mediated by ecosystem-level processes and disturbances (Økland & Bendiksen, 1985). Traditionally disturbances have been defined as irregular and uncommon events causing abrupt changes in natural communities (Sousa, 1984; White, 1979) or removing or damaging biomass (Grime, 1979). More recent publications has recognized that a strict determinism is inadequate for referencing complex environmental systems, and defines disturbance in broader terms as a process or event both regular and irregular, with a damage intensity that is either negligible or extreme (Barristi, Poeta, & Fanellu, 2016). Disturbances can be both natural and anthropogenic, and affect both the vegetation and the organization of a system below the ground (Barristi et al., 2016).

A type of natural disturbances is peat accumulation, a well-known process in wetland systems. Joosten, Tanneberger, and Moen (2017) defines peat as a material that has accumulated in situ, i.e. is produced and accumulated in the same location, and that consists of at least 30 % dead organic material. Several plant species may contribute to peat formation, e.g. sedges, grasses, bryophytes such as *Sphagnum* spp., and woody plants (Joosten et al., 2017), forming a wide variety of botanical peat types. Peat accumulation is a slow, subtle process with large annual variation. An area with naturally accumulated surface peat layer is referred to as a peatland (Joosten et al., 2017). The definition of peatland

varies between countries and sectors when it comes to the thickness of the peat (Joosten et al., 2017), however a minimum peat depth of 30 cm is commonly used (Joosten et al., 2017; Halvorsen, 2016). Fens, bogs and mires are types of peatlands defined based on a set of defining characteristics (Joosten et al., 2017).

A large and complex set of environmental variables are responsible for peat accumulation on wetland and at what rate it occurs (Halvorsen, 2016). The processes involved are a part of a system of feedback mechanisms, which makes the description and identification of peatland challenging, and has resulted in a variety of classification methods across countries and focus of interests (Joosten et al., 2017).

At the broadest level, peat accumulation is a result of a net production of organic matter that is higher than net decomposition rates. Decay-resistance of the dead plant material and the presence of water are considered the most important factors in controlling decomposition (Joosten et al., 2017). Decay-resistance is affected by several factors, such as soil acidity, nutrient availability and vegetation composition, while the presence of water is affected by peat stratigraphy, fluctuations in and distance to the water table and the origin of the water (Joosten et al., 2017). Water in peatland can have different sources, either by direct contact with the water table (minerogenous) or trough precipitation (ombrotrophic). Areas with a cold climate have occurrences of peatland in areas with less precipitation and humidity than temporal areas, as warmer air temperatures decrease the amount of water in peat through evapotranspiration processes (Joosten et al., 2017).

Peatland that have ombrogenous origin of water are often referred to as ombrotrophic bogs (Joosten et al., 2017). They are nutrient-poor due to the somewhat acidic properties in rainwater and a lack of access to minerals from the ground, which causes a species poor flora and fauna (Joosten et al., 2017; Vitt, Halsey, & Zoltai, 1994). Ombrotrophic bogs and other forms of peatland can form a feature called hummocks, which are accumulations of peat raised 20–50 cm above the surface, characterized by dry-occurring vegetation such as dwarf shrubs, certain bryophytes and lichens (Joosten et al., 2017). The height level relative to the surface causes a change in the vegetation because of variation in moisture conditions, water table fluctuations and peat firmness (Joosten et al., 2017).

Hummocks can have different cores, consisting of rocks, mineral or even ice (Vliet-Lanoë & Seppala, 2002; Tarnocai & Zoltai, 1978; Seppala, 1997). Hummocks with an ice core are called palsas, and occur in regions with discontinuous permafrost, such as in parts of northern Norway (Gisnås et al., 2017). Formation of palsas is a product of the thermal conductivity of peat, which is low

in dry peat and considerably higher in saturated peat (Seppala, 1997). Palsas are caused by the deep seasonal freezing causing frost heave, mass wasting and frost sorting of peat, combined with cold temperature in winter, especially during snow-free periods (Seppala, 2006). The dry outer peat layer of a palsa insulates the iced core from heat and thawing during warmer months (Seppala, 2006). Snow depth is considered the most critical factor for permafrost formation (Seppala, 2006, 1997), as a thin snow cover will promote penetration of frost.

Another variation of peatland in regions with permafrost is a polygonal arrangement of peat deposits, often referred to as polygonal mire (Joosten et al., 2017). They occur when frost processes form cracks in accumulated peat, causing permanently broken soil. Other ecosystems may also be locally peat forming, such as snow beds, heathlands and salt marches (Joosten et al., 2017). Ice wedges can occur in peatland areas with permafrost (Kokelj et al., 2014).

A system that describes and classifies peatland is Nature in Norway (further referred to as NiN), which is a system for classifying Norwegian nature. NiN is an implementation of the EcoSyst framework, which is a principle- and rule-based system for organizing natural variation in a standardized manner (Halvorsen, Skarpaas, et al., 2020). In NiN, variation in nature is described on three levels, encompassing microhabitat, ecosystem and landscape (Halvorsen, Bryn, & Erikstad, 2016). At the ecosystem level variation is hierarchically sorted in a type system, compromising major-type groups, major types and minor types (Halvorsen et al., 2016). In addition, NiN contains a non-hierarchical attribute system where objects and other observable characteristics that is not expressed by the type system can be described, such as regional variation, man-made objects or species composition (Halvorsen et al., 2016). The first version of NiN, named ”Nature types in Norway”, was released in 2009 (Halvorsen et al., 2009), and a revised second version was released in 2015, renamed ”Nature in Norway” (Halvorsen et al., 2016).

NiN is has its theoretical foundation in the gradient analytic perspective (GAP). Three main points of GAP is summarized by Halvorsen (2012): (1) external factors do not influence species one by one, but act on the species in concert as complex gradients, (2) a few major complex–gradients normally account for most of the variation in species composition that can be explained by environmental factors, and (3) species occur within a restricted interval along each major complex-gradient.

In NiN, major complex-gradients are called local environmental complex-variables (further referred to as LECs). Some central LECs (hLECs) that describe variation and create major types on peatland are peat accumulating ability (TE), mire expanse character (MF), duration of period without inundation (TV)

and lime–richness (KA). Variation along these LECs explain the continuous variation in vegetation pattern and environmental variation in peatland. The amount of variation explained by a system along an LEC is what separates peatlands into different major types within in the major-type group wetland (V). Wetland (V) in NiN is defined as ground with water table sufficiently close to the ground surface, or that is so abundantly supplied with surface water, that organisms that are adapted to life under water saturated conditions or that demand a stable access of water occur frequently (Halvorsen et al., 2016). In NiN, bog (V3) and open fen (V1) are major types, while palsa mires and polygon fens are described as landforms in the attribute system (3TO-PA and 3TO-OP, respectively) (Halvorsen et al., 2016).

While definitions and causal factors of peatland in wetland have been thoroughly investigated and described, terrestrial peat accumulation largely lacks a description in the literature. In this study, a conspicuous type of terrestrial peatland with and without tree cover on convex landforms is investigated. The systems accumulated terrestrial peat depth up to 70 cm, had hummock formations and a pedology resembling ombrotrophic bog.

A similar case of terrestrial peatland is described by Edvardsen et al. (1988), which describes a heath with peat accumulation located on the coast near Tromsø, northern Norway. In addition, a study from Fenton (1980) described mainland peat accumulation in moss banks in Antarctica, attributing the accumulation to permafrost and the intrinsic slow decomposition rates of some bryophytes. However few studies focus on the processes behind terrestrial peat accumulation, and more research is required to establish a better understanding and description of the systems. Regarding the NiN system, there is a lack of description of terrestrial peat accumulation, and this study aim to investigate this.

Aims

The motivation for this master thesis was to investigate the environmental and vegetational gradient patterns in areas with terrestrial peat accumulation. The aims of this study can be summarized by the following research questions:

i) Which ecological gradients can be identified on terrestrial peatland?
ii) Which environmental factors impact these systems, and how can they explain and affect terrestrial peat accumulation?
iii) Is the peat producing areas associated with a unique composition of plant species?
iv) How should this terrestrial peat accumulation be described in the NiN system?

2

Study area

2.1 Location

The study area is located in Langfjorddalen/Laggu (70°57' N 27°38' E) in Gamvik municipality, Troms and Finnmark county, see figure 2.2. Field sites are situated north-east of the Lákkomohkki area, see figure 2.1. The area is within the northern boreal bioclimatic zone and the weak oceanic bioclimatic section (Moen, 1999). Annual precipitation is 480–555 mm, based on measurements from Lebesby and Karlmyhr during two separate periods from 1948 to 1980 in Lebesby and from 1981 to 1990 in Karlmyhr (Førland, 1993). Mean annual temperatures are between 0°C and –2 °C (Moen, 1999). Mean January temperatures are –4 °to –6 °C, while mean July temperatures are 8 °C to 12 °C (Moen, 1999). The length of the growing season is 120–130 days, defined as the number of days when normal temperatures exceed 5 °C (Moen, 1999).

The Laggu valley was established as a nature reserve as defined by the nature richness act of Norway on 29th of June 2007, with the purpose of conserve the rich, northern deciduous forest in the area (Lovdata, 2007).

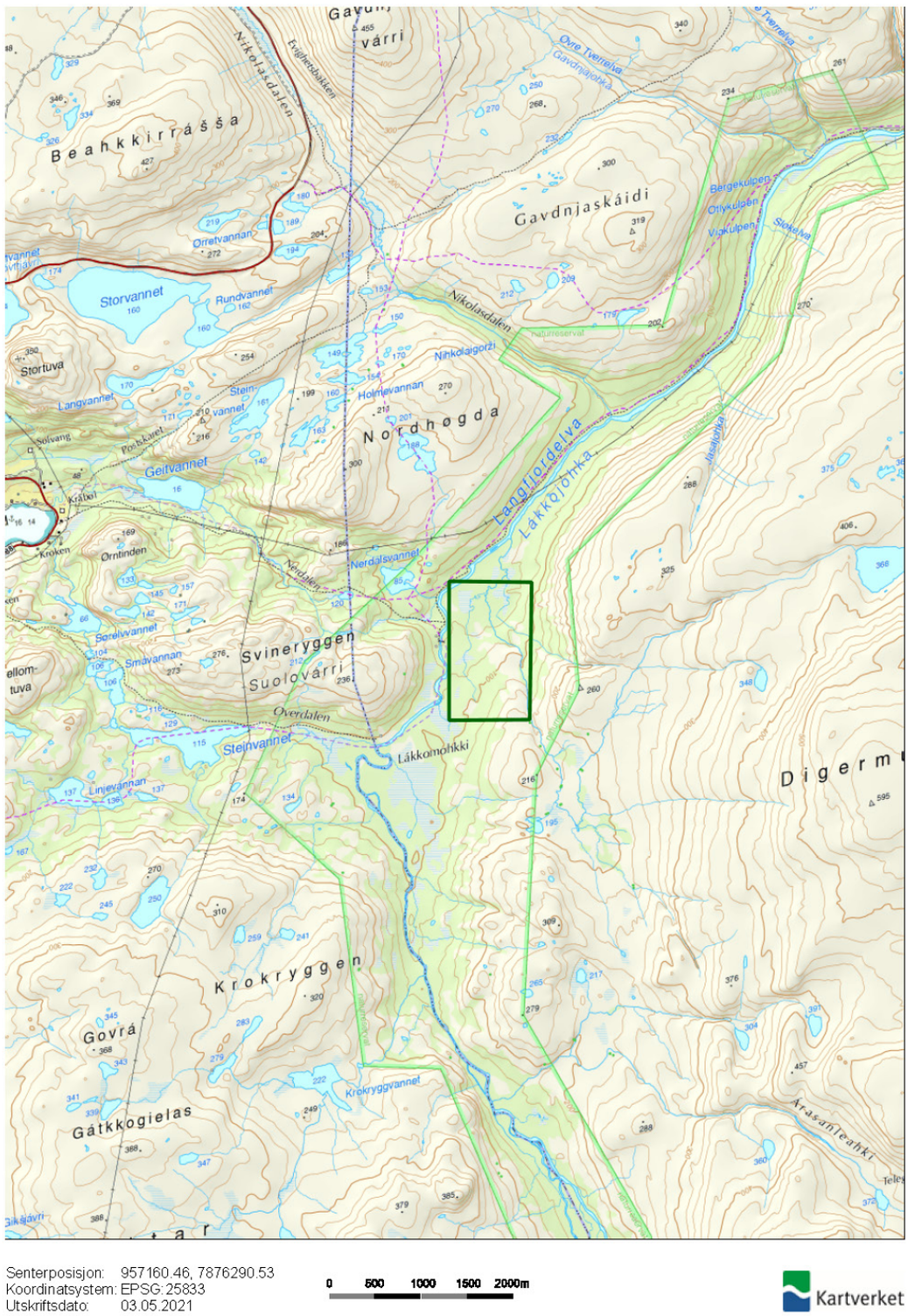

Figure 2.1: Map illustrating Laggu nature reserve. Lákkomohkki area marked in the middle of the map. Dark green lines indicate the study area. Map downloaded from Kartverket.no

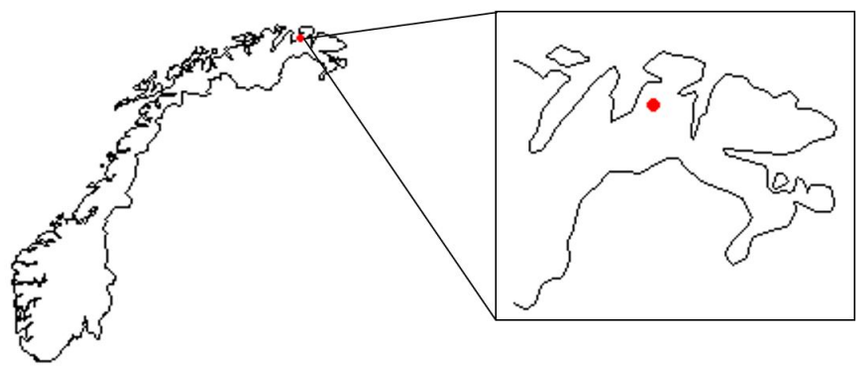

Figure 2.2: Location of study area in Troms and Finnmark county, northern Norway.

2.2 Geology and deglaciation

The bedrock is a coarse-grained sedimentary conglomerate dominated by granite, quartzite, and greenstone (NGU, 2017a), with form acidic mineral soil. The upper layer is covered with an incoherent or thin cover of loose materials, usually less than 0,5 meters (NGU, 2017b). The sediment is usually hard packed and poorly sorted and can contain all grain sizes from clay to rocks and blocks (NGU, 2017b).

During the last ice age, approximately 12 800 years ago, Finnmark was covered in an ice sheet cover that has influenced the geology and natural systems when it comes to its age, development, origin and distribution (Lilleøren, Etzelmüller, Schuler, Gisnås, & Humlum, 2012). When the ice cover pulled back, glacifluvial deposits formed the landscape. These were landforms such as eskers, which are a deposition of remains of sand, gravel and rocks that were transported in the tunnels of melt water below the glacier (Sigmond, Bryhni, & Jorde, 2013).

After deglaciation, the post-glacial respond has caused a land rise in large parts of Norway (Lilleøren et al., 2012). The climate post deglaciation was cold and humid in Nordic regions (P. Oksanen, 2006). Climatic conditions factoring permafrost and permafrost landforms existed both before and after climatic optimum during Holocene, the epoch that followed the last ice age (Lilleøren et al., 2012). During Holocene, a climatic shift towards warmer and wetter conditions occurred, which favored accumulation of organic material on wetland (P. Oksanen, 2006).

Permafrost and palsa mires

Permafrost is defined as ground with temperatures at or below 0 °C during more than two consecutive years or more (Joosten et al., 2017). Modeling of permafrost distribution in Norway by Gisnås et al. (2017) indicate occurrences of sporadic permafrost out to the coast in northern Norway (Gisnås et al., 2017). Sporadic permafrost consist of areas where 10–50% of the surface area is likely to have permafrost (Gisnås et al., 2017).

Permafrost is a solely thermally defined phenomenon and is not necessarily visibly on the ground surface, therefore local phenomena related to permafrost can give indication of a permafrost layer. In northern Norway the permafrost is often located in mires, producing palsas and peatland (Gisnås et al., 2017). Other types of landforms that indicate permafrost, existing or former, are rock glaciers, ice-cored moraines and ice-wedge polygons (Lilleøren et al., 2012). Active rock glacier down to sea level have been documented at Nordkinnhalvøya (Lilleøren et al., 2012), and palsa mire has been located in Laggu (Johansen, Tandstad, Arnesen, & Finne, 2020; Kristiansen, 2006).

2.3 History and natural disturbances

2.3.1 Settlement and use

Laggu is a popular destination for arctic salmon (*Salmo salar*) fishing during the summer season. The valley is uninhabited today, but had a permanent resident located across the river from Lákkomohkki during the first half of the 20th century until 1945 (Køste, 2006). At most 2 adults and 13 children resided here, possessing a horse, several cows and sheep (Køste, 2006). According to Køste (2006) the surrounding area was utilized for outlying fields for grazing, ditching of bogs for growing food for the livestock, breaking soil to grow potatoes and wood for fuel.

Laggu is an important spring and summer pasture for domesticated reindeer (*Rangifer tarandus*) (NIBIO, 2020). The luxuriant vegetation in the area makes a good grazing area in summer. The area is also utilized during autumn relocation of the herds from summer to winter pasture (NIBIO, 2020). The area is within reindeer grazing district 13, Siskkit Čorgašja Lágesduoyyar/ Ifjordfjellet and reindeer grazing district 9 Nordkinnhalvøya/Vestertana (NIBIO, 2020).

2.3.2 Geometrid moth mass outbreaks

Geometrid moth mass outbreaks have been documented in Laggu in 2003, 2004 and 2015 using NDVI (Normalized Difference Vegetation Index) satellite data as described in Jepsen et al. (2009). Two species of geometrid moth; *Operophtera brumata* and *Epirrita autumnata*, have occurred in in large cyclic outbreaks every 7–15 year in large parts of north–eastern Fennoscandia (Jepsen, 2013). Their life cycle is based around *Betula pubescens* where the eggs overwinter attached to branches, capable of surviving in temperatures down to –35 °C (Ammunét, Kaukoranta, Saikkonen, Repo, & Klemola, 2012). They hatch with the sprouting of the first birch leaves in spring and during the larval state of 4–8 weeks they graze on birch leaves (Jepsen et al., 2013). The two species hatch at a few weeks' separate intervals, causing an extension of the total grazing–period. When outbreaks occur several years in a row, the consequence can be fatal to a birch forest. Less severe outbreaks can cause a major range shift in the understory vegetation, causing *A. flexuosa* to take over in large quantities just a few years after an outbreak (Jepsen et al., 2013; Karlsen, Jepsen, A., Ims, & Elvebakk, 2013). Research shows that dwarf shrubs such as *E. nigrum* and *V. myrtillus* are affected when the larvae drop to the ground beneath the tree and feed off the understory vegetation (Karlsen et al., 2013). Attacks on *E. nigrum* can subject the plant to fungi infections that can cause the plant to die (Olofsson, Ericson, Torp, Stark, & Baxter, 2011).

3

Materials and Methods

3.1 Study design

Field work was carried out in July, August and September 2020.

3.1.1 Sampling design

The process of selecting sampling units was based on three steps described in the following sections.

i) Area selection
Convex landforms with terrestrial peat accumulation were discovered in Laggu in 2019 (documented in Johansen et al., 2020). In addition to the registered areas discovered in 2019, possible terrestrial peatland was identified by evaluating orthophotos prior to field work. The areas were then sought out in person and evaluated.

ii) Transect selection
Seven transects were placed along areas containing varying degree of peat accumulation, hummock size and tree cover. The aim was to cover variation in soil depth and to cover the gradual variation from areas with peat accumulation to surrounding nature types, i.e. major types as defined in the NiN–system according to (Halvorsen et al., 2016). The transects ranged from 54 to 132 meters in length. Table 3.1 gives an overview of major types contained in each

transect. Transect positions are shown in figure 3.1 and 3.2.

iii) Plot selection

Plots in the shape of 1×1 m quadrats were placed along each transect line. An absolute rule of ≥ 2 meters between the outer corner of plots, and ≥ 1 meter from a zone limit to the outer corner of a plot was established. A rule was established of one plot per 10 m within a zone. A special rule of 4 plots for zones between 30–50 meters and maximum 5 plots per zone was established. Plot position within a zone was decided using random numbers. Plots with tree stems and coverage of large roots (>50 %) were rejected. A total of 58 plots were placed along seven transects.

Regarding the NiN system, the transects were placed to cover gradual variation based on major type in NiN or, if they did not fit into the NiN–system, they were assigned a supplementary minor type. These were T3–C–15 Peat heath and T4–C–21 Peat forest. T3–C–15 Peat heath was defined as terrestrial areas without permanent tree–cover, with mean soil depth >25 cm or hummock formation. T3–C–15 Peat forest was defined as terrestrial areas with mean soil depth >25 cm or hummock formation. Other nature types that were covered in the transects were T4 Forest, T14 Exposed Ridge and T3 Arctic–alpine heath and lee side.

The plots were numbered according to the transect they belong to and their position along the transect from north to south. For instance, plot 103 corresponds to a plot in transect 1, position nr 3.

Table 3.1: Overview of the transects and their nature types. T4–C–21 and T3–C–15 were applied as supplementary nature types for terrestrial peat accumulation and are not defined in the NiN system. A msl refers to meters above mean sea level.

Transect	Number of plots	Nature types					Altitude (a msl)
		T4	T4–C–21	T3	T3–C–15	T14	
1	12	5		4	1	2	84–95
2	8	3	2		3		91–94
3	12	4	3		5		101–105
4	6	2	2		2		102–106
5	8	4	1		3		95–100
6	6	2			4		62–71
7	6	2	1		3		62–72

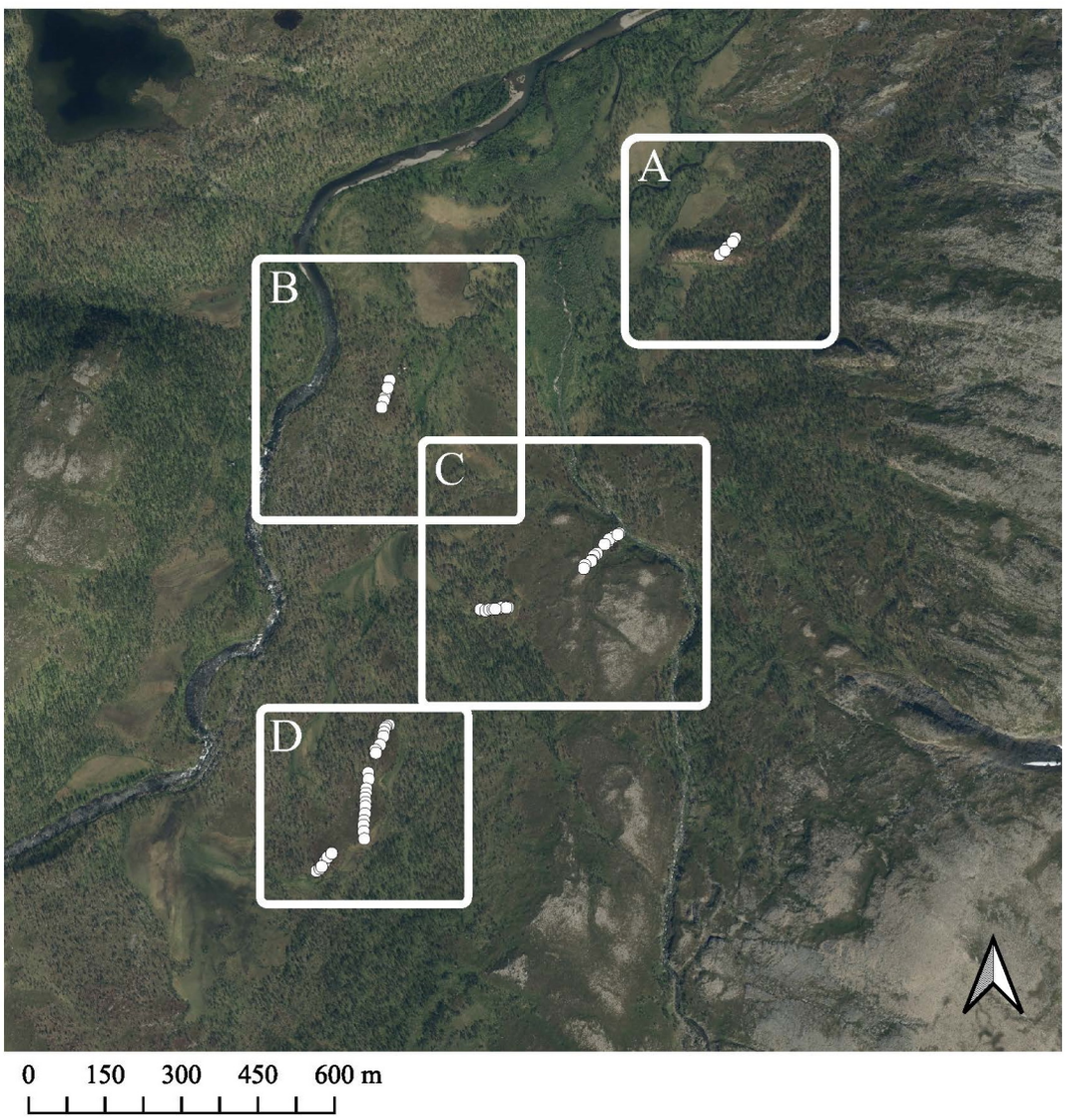

Figure 3.1: An overview of all 7 transects. Corresponding crops shown in figure 3.2 are marked with white squares and assigned a letter. Figure made with QGIS version 3.10.4.

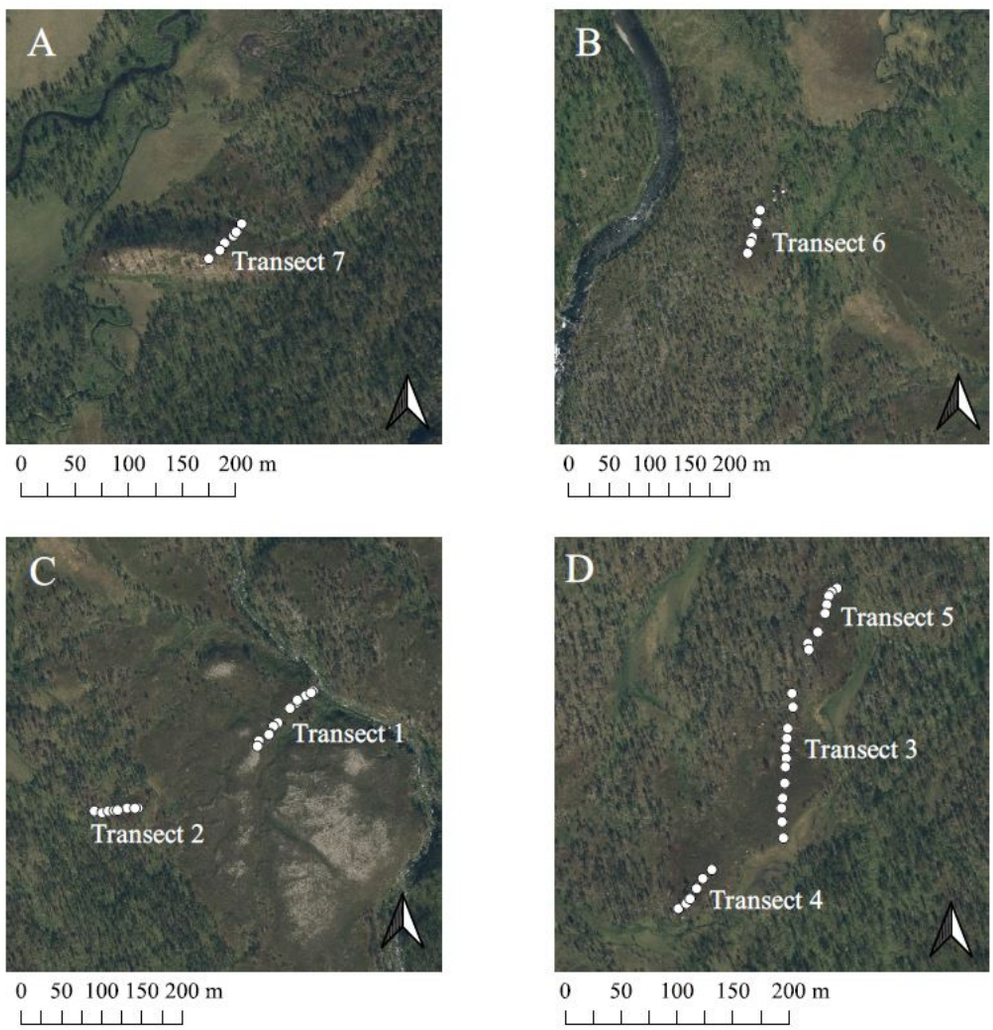

Figure 3.2: An overview of all 7 transects and their 58 plots. Figures A–D correspond to positions in figure 3.1. Figures made with QGIS version 3.10.4.

3.1.2 Species data recording

Plant composition was recorded in 1×1 m plots. The plots were further divided into 16 subplots of 25×25 cm. The subplots were marked manually with sticks, see figure 3.3. Species data was registered in terms of frequency (0–6) and coverage (0–4) as described in table 3.2 and 3.3. The sum of recoded frequency and coverage was used in analyses, resulting in total species cover on a 0–10 scale.

Table 3.2: Recorded species frequency with reference to sub-plot occurrences.

Recorded frequency	0	1	2	3	4	5	6
Number of sub-plots	0	1	3	3–4	5–8	9–14	15–16

Table 3.3: Recorded coverage with reference to percent coverage in an entire plot.

Recorded coverage	0	+1	+2	+3	+4
Percent cover in plot	< 6,25 %	6,25–12,5 %	12,5–25 %	25–50 %	> 50

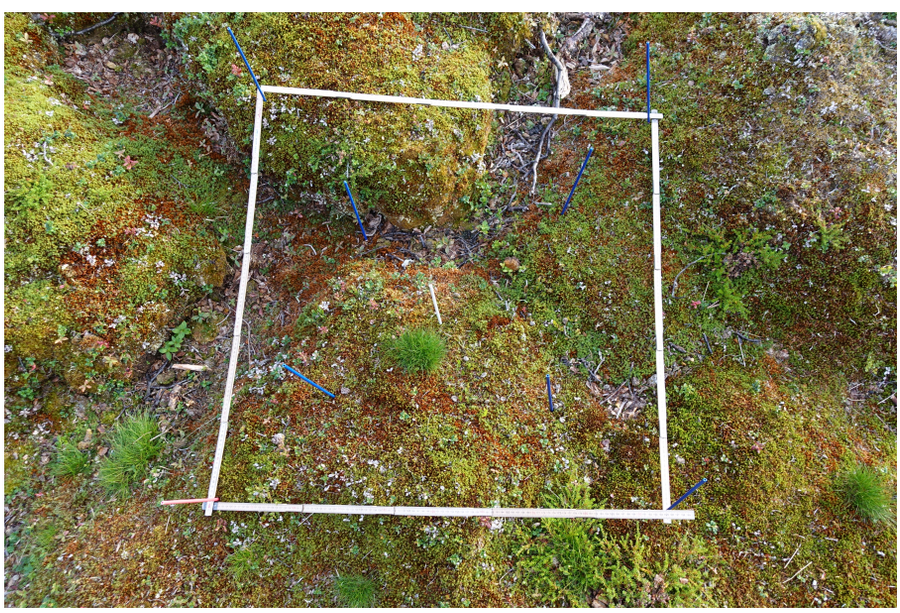

Figure 3.3: Picture of plot 103. Exemplifying a 1×1 m plot, with sticks marking 25×25 cm quadrants. The red stick in the lower left corner marks the plot position along the transect.

The nomenclature of vascular plants, bryophytes and lichen follow Artsdatabanken (Artsdatabanken, 2015, accessed 01.02.2021). For some genera further identification was not possible, and they were considered as aggregated (agg.) or as species pluralis (spp.). Species growing directly on rocks, wood or on animal droppings were not registered. Entire species list can be accessed in Appendix 7.

3.1.3 Explanatory variables

Recorded in field

In all plots 26 explanatory variables were recorded in a standardized way, described in detail in Appendix 2.

Aspect and slope were measured using a compass and a clinometer. Aspect was recorded on a 0–360°scale. Curvature was subjectively estimated by spanning a line of length 3 meters centered on the plot. Curvature was assessed in the horizonal and vertical direction with reference to the transect. It was registered on an 9–step scale ranging from –2 to +2, where –2 referred to strongly concave curvature, +2 referred to strongly convex curvature and 0 was no curvature.

The main LECs for each main type were considered by subjective consideration of elementary segments (described in Halvorsen, 2016). They were risk of severe drought (UF), wind-mediated disturbance intensity (VI) and lime richness (KA). KA was not applied in further analyses as there was a lack of variation between plots within this variable.

Microtopography was recorded at three points in the vertical and horizontal direction (see illustration in figure 3.4) to describe variation in topography within a plot. A chain with a length of 2 meters was used. The chain followed the terrain within each plot, and the length of the chain exceeding 1 meter was registered. A sum of the three recorded values in the horizontal and vertical direction was then calculated.

Tree crown cover was recorded in four directions, standing in the middle of a plot. It was registered using a Spherical Densiometer (Lemmon, 1956) with 24 squares. Each square was visually counted in four sub–squares, creating a maximum of 96 squares. The occurrence of living and dead tree branches was registered for each sub–square as two separate variables.

Soil depth was measured at five positions in each plot, illustrated in 3.4. In this

study, the term *soil* when referring to soil depth is used to describe to the layer of peat, soil, sand, gravel, pebbles and cobbles that a soil rod could penetrate until it stopped.

Soil samples were collected from four quadrants in each plot, illustrated in figure 3.4. Samples were collected in varying positions to cover within–plot variation, e.g. on top of a hummock and in a depression. Collection was made using a 5 cm cylinder. In plots with a thick peat layer samples were collected up to 15 cm below the surface. In plots where the soil depth was scarce within the plot, i.e. on exposed ridges, patches surrounding the plot was collected. The samples were mixed in a paper box, stored at room temperature, and aired-dried from the day of sampling until analyses.

A second set of soil samples were collected for soil moisture. For each sample, two collections were made from separate parts of a plot to cover within-plot variation. Collection was made using 5 cm cylinders. Soil moisture samples were collected to determine how water retention varies along the transects. The samples should ideally be collected after a longer dry period of several days, to represent the water retention abilities of the soil. All soil moisture samples were collected on August 13th. The samples were stored in a paper bag within two plastic bags to maintain moisture and stored at room temperature until analysis.

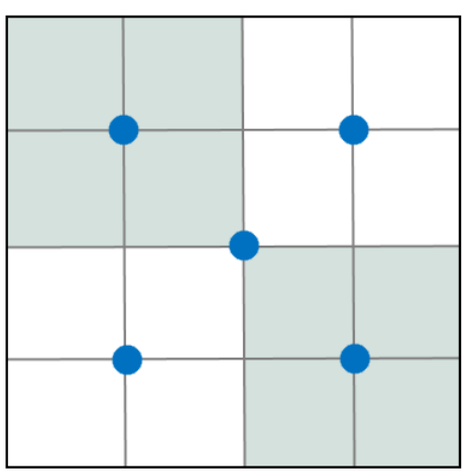

Figure 3.4: Illustration of a 1×1 m plot. Grey lines illustrate the three horizontal and three vertical lines for microtopography measurements. Blue points show position of soil depth measurements. White and green backgrounds show the four quadrants where soil–samples were taken.

Derived from chemical analyses

Chemical soil analyses were conducted at UiT The Arctic University of Norway in October and November 2020.

Soil samples
Prior to analyses the soil samples were dried, crushed by hand in a mortar and sieved through a steel sieve with 2 mm mesh width. Sieve and mortar were thoroughly cleaned before treatment of each sample.

Loss on ignition (LOI) was used to estimate organic matter content. Approximately one tablespoon of soil was kept in a drying cabinet at 60 °C for 24 hours. The soil was then weighed in a previously weighed cubicle and placed in a muffle furnace oven at 550 °C for 3 hours. After cooling down in an desiccator to avoid water retention during the cooling process, the samples were weighed again. Loss on ignition was expressed in percent, see formula in Appendix 4.

For pH measurements, 5 g of dry soil was mixed with 25 ml of distilled water. The samples were then shaken for 5 minutes and left overnight. The next day they were shaken again for 5 minutes. When the solution stabilized pH was measured using a Bluelab soil pH pen. The pen was calibrated with buffer solutions of pH 4 and pH 7 and recalibrated for every 10th sample.

All soil samples were analyzed for nitrogen and phosphorous content using near-infrared spectroscopy (further referred to as NIRS). NIRS is an indirect method for measuring constituents in plants, based on visible and near infrared light absorption in the organic bonds in molecules (Murguzur et al., 2019). By evaluating the combined light absorptions at different wavelengths, information about nutrient content is retrieved (Murguzur et al., 2019).

A NIRS method for leaf and soil nutrient prediction has been developed at UiT, with most of its research conducted on leaf content (e.g. Petit Bon, Böhner, Kaino, Moe, & Bråthen, 2020; Murguzur et al., 2019). The method uses models based on samples from Finnmark and Svalbard (Murguzur et al., 2019), which have been developed by comparing results from NIRS analyses to results from chemical analyses. As discussed in Murguzur et al. (2019), the precision of the NIRS calibrations depend on the precision and bias of the analytical techniques that the NIRS spectra are fitted to. Since the resulting values for nitrogen and phosphorus content were not crosschecked with traditional methods, the results from NIRS analyses were treated as estimates.

Prior to analysis one tablespoon of each sample of pre-sieved soil were kept in a drying cabinet at 60 °C for 48 hours to ensure completely dry samples,

as water interferes with the NIR spectra (Givens, de Boever, & Deaville, 1997). The soil sample was then placed in a small petri dish and scanned using a Muglight connected to a Fieldspec 3. Each sample was scanned 5 times, rotated after each scan, and mixed once during analysis. A baseline was taken before scanning and every 30 minutes with a white reference spectralon.

The NIR spectra were converted to nitrogen and phosphorous content by applying prediction models developed with samples from Finnmark and Svalbard, described in Murguzur et al. (2019). The calculations were conducted in R version 1.4.1103 (RCoreTeam, 2021). For each sample, a mean of the 5 scans was calculated. Scans that deviated strongly were excluded to avoid outliers affecting the data. Scanning and data calibration was done two separate times for all samples, and a mean was calculated. Appendix 12 contains NIRS estimates for TotN and TotP, and appendix 13 contains LOI values from NIRS estimates and analyses in muffle oven.

Soil moisture samples
For soil moisture each sample was weighed in wet state, then dried in a drying cabinet at 105 °C for 24 hours and weighed again. Soil moisture content was then determined and expressed in percent. See formula in Appendix 3.

Precipitation data from Lebesby–Karlsmyhr weather station located approximately 15 km from the study area in the preceding days to sample collection are shown in table 3.4 (Norsk klimaservicesenter, 2020, retrieved 17.02.2021). A large amount of precipitation on August 10th in addition, temperatures averaged 12 °C during this period (Norsk klimaservicesenter, 2020, retrieved 10.05.2021). Low temperatures cause slower evaporation of soil moisture after precipitation. There was some variation expressed within the soil moisture samples, however the variation within this variable was not emphasized when evaluating the results.

Table 3.4: Precipitation at Lebesby–Karlsmyhr weather station in the days preceding soil moisture. Data retrieved from Norsk klimaservicesenter.

Date	Precipitation, per day (mm)
09.08.2020	0
10.08.2020	22.1
11.08.2020	0.5
12.08.2020	0
13.08.2020	0

Derived from external digital sources

Altitude data for each plot was retrieved form the Høydedata database (Kartverket, 2021) post field work using plot coordinates.

Snow cover was visually evaluated using data from the Sentinel-2 satellite, retrieved from ESA remote sensing data (European Space Agency (ESA), 2021). The interpretation of Sentinel-2 data was done by the use of a normal color image that consist of three channels of green, blue and red, that were treated in QGIS version 3.14 (QGIS Development Team, 2021). The resulting image had a 10 m pixel resolution. The relatively low resolution of this information compared to plot precision, makes for an uncertainty in the data.

A variable for snow cover was created by evaluating six scenatios from the period of snow melt in 2020. Each plot was assigned a value ranging from 0–6, by summing the observations for each scenario. Pixels with snow cover was assigned a score of 1 and pixels without snow was assigned a score of 0. The dates each scenario was taken from were March 4th, May 26th, June 2nd, June 13th and July 15th. Due to a cloud cover above transect 7 on June 2nd, a supplementary photo from May 2019 with similar snow conditions was used for this scenario. Appendix 11 contains all images used for the evaluation.

3.2 Soil depth and maximum hummock height measurements

Soil depth and maximum hummock height was registered along grids consisting of points. Grids were created with each transect as a baseline and a plot in each transect was selected as basis for the grid, see details in table 3.5. Points in the grid were placed with 7 meter distance to each other, along perpendicular and parallel lines to each transect. A Silva Compass Ranger was used to measure perpendicular lines from the transect. Figure 3.6 shows an overview of the grids.

Soil depth was measured at four points approximately one meter from a grid point, see figure 3.5. Post fieldwork, a mean was calculated to represent soil depth at each point. Maximum hummock height was measured within a radius of two meters of a grid point. It was measured as the greatest distance from the top of a hummock to the nearest depression. Appendix 4 contains details on the process.

Table 3.5: Details on grids corresponding to each transect.

Transect	Plot of origin	Nr of points in grid
1	106	102
2	204	63
3	306	192
4	403	73
5	503	94
6	605	129
7	705	103

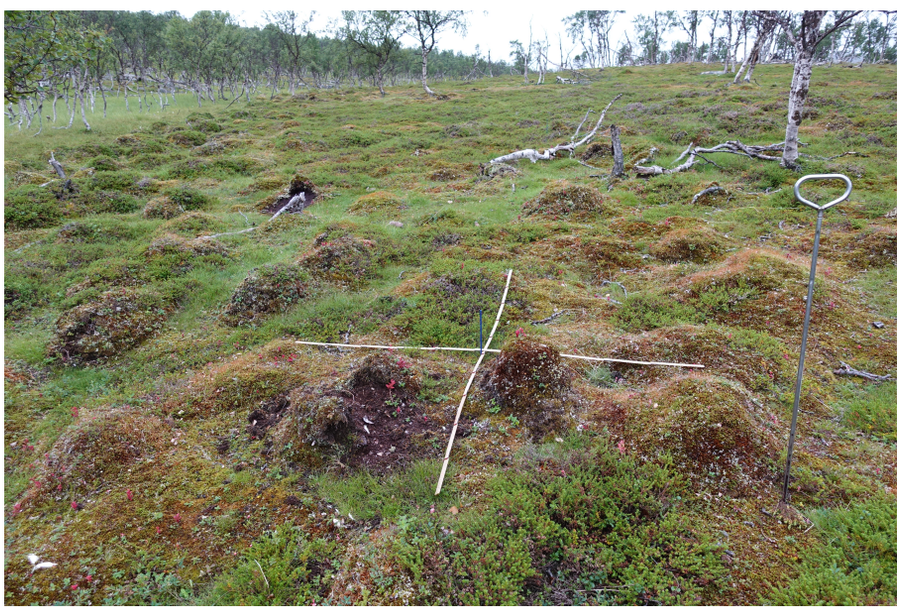

Figure 3.5: Image of a point for soil depth measurements, using metersticks of 2 meter to find 1 m distance from the center.

3.3 Land–cover mapping

Land-cover mapping was conducted in September 2020 according to instructions for NiN land-cover mapping to scale 1:5000 in (Bryn, Halvorsen, & Ullerud, 2018). The aim was to identify the nature types surrounding the transects. A Getac-touchpad (Getac F110, Windows 10 Pro 64 bits) with integrated GPS was used. Data were recorded in a QGIS 3.14 project with a NiN mapping application (described in Horvath, Nilsen, & Bryn, 2019). Polygons with nature types were digitized using orthographic photos from 2018 and contour lines

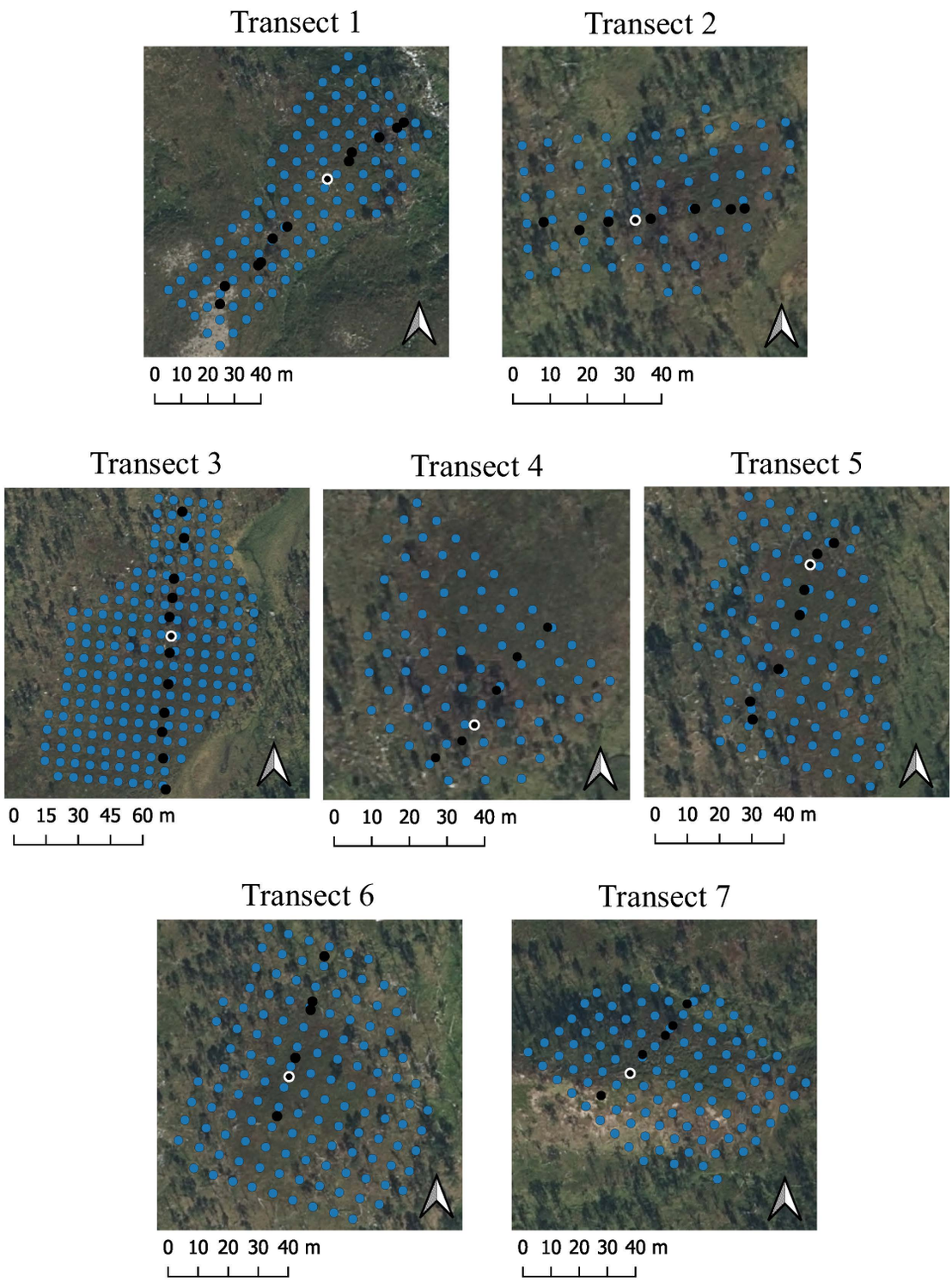

Figure 3.6: Grid visualizing measurement points surrounding all transects. Blue points illustrate points of measurements. Black points indicate positions for the plots in each transect. Black point with white ring indicates plot of grid origin in the transect.

with equidistance of 1 m as a background.

The minimum size of polygons when land-cover mapping to scale 1:5000 is 250 m^2 (Bryn et al., 2018) In some areas the protocol of minimum width for a forest-polygon of 7,5 m was broken to describe important ecological traits about the nature surrounding the transects, a procedure in land-cover mapping that is discussed in Halvorsen, Wollan, Bryn, Bratli, and Horvath (2021, p. 104).

Areas with peat accumulation were recorded as supplementary basic types T3–C–15 Peat heath and T4–C–15 Peat forest, as defined in section 3.1.1.

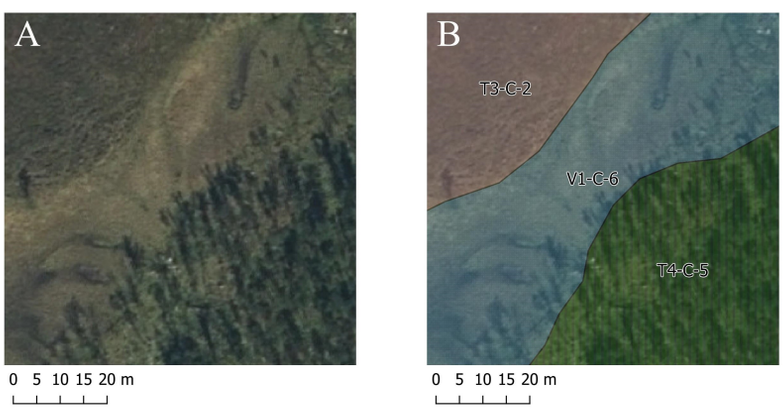

Figure 3.7: Example of digitization of land–cover mapping. Figure A shows orthophoto used as base, while figure B shows digitized land–cover mapping of nature types, i.e. basic types in the NiN–system.

3.4 Obtaining historical information

Historical information about anthropogenic activity was obtained through *En søring nordpå* by Køste (2006) and *Fortellinger fra Langfjorddalen* by Jensen (2012).

Dating of geometrid moth outbreaks was documented using Normalized Difference Vegetation Index (NDVI) anomalies as described in Jepsen et al. (2009). NDVI data are calculated by comparing visible and near-infrared light reflected from the vegetation (Jepsen et al., 2009). Healthy vegetation absorbs most visible light and reflect most near-infrared light, while unhealthy vegetation reflects more visible light and less near-infrared light. NDVI anomalies are an expression for the relative decrease in NDVI one year, compared to what would be expected from a year with high productivity.

3.5 Data analysis

3.5.1 Data manipulation

Zero-skewness standardization was applied to all continuous explanatory variables, following to Halvorsen, Økland, and Rydgren (2001). Zero-skewness variables were obtained by subjecting them to the following formulas.

$$y = ln(c + x) \tag{3.1}$$

$$y = e^{cx} \tag{3.2}$$

$$y = ln(c + ln(c + x)) \tag{3.3}$$

$$y = e^{c}e^{cx} \tag{3.4}$$

The constant c was manually changed until the standardized skewness of the standardized variable was $<10^{-5}$. For negative skewness values of untransformed data, the exponential formula was used, and for positive skewness values the logarithmic formula was used. Formula 3.1 or 3.2 was tested first. If they could not be used to obtain standardized skewness, formula 3.3 or 3.4 were used. Finally, the transformed values y were ranged from 0–1 using formula 3.5.

$$y_{scaled} = \frac{y - y_{min}}{y_{max} - y_{min}} \tag{3.5}$$

Appendix 5 and 6 contain the untransformed and the transformed and ranked variables respectively. Table 3.6 contains a summary of explanatory variables and their associated characteristics.

Table 3.6: Overview of explanatory variables used in the ordinations.

Variable	Abbreviation	Details	Untransformed		Transformed	
			Range	Mean	Type	*c-value*
Altitude	Altitude	Plot altitude in meters above sea level.	61.1–105.5	91.0	e^cx	0.06159751
Aspect	Aspect	Aspect favorability on a 0–360° scale.	4 – 335	127.4	ln(c+x)	3.8539
Bottom layer	BotLayer	Percentage (%) cover of the bottom layer.	24 – 98	78.0	e^cx	0.03951803
Convexity (horizontal)	ConvH	Horizontal convexity of plot, –2 is strongly convex.	–0.5 – 2	0.0	e^cx	1.030311
Convexity (vertical)	ConvV	Vertical convexity of plot, –2 is strongly convex.	–1 – 0.5	0.0	e^cx	0.659082
Droppings from reindeer	DroppingsRangifer	Fraction of droppings from reindeer (*Rangifer tarandus)*.	0 – 14	5.6	ln(c+x)	5.6452
Field layer	FieldLayer	Percentage (%) cover of the field layer.	4 – 89	48.4	e^cx	0.0104485
Loss on ignition	LOI	Loss on ignition, percentage (%) of soil organic matter.	24.0 – 98.3	91.9	e^cx	0.82699
Microtopography (horizontal)	MicrotopoH	Average horizontal microtopography in cm.	0 – 10	2.5	ln(c+x)	1.7132
Microtopography (vertical)	MicrotopoV	Average vertical microtopography in cm.	0 – 6	2.3	ln(c+x)	1.64946
pH	pH	Soil pH measured in distilled water.	3.1 – 3.8	3.3	ln(c+x)	-3.053129
Risk of severe drought	UF	Based on the elementary segments for the LEC in NiN.	2–8	4	ln(c+x)	-0.742838
Slope	Slope	Inclination inside plots.	1 – 34	9.4	ln(c+x)	2.97976
Snow cover	Snow Cover	Estimated snow cover based on Sentinel-2 satellite photos from six scenarios during the snow melting season in 2020.	1-4	2.1	e^cx	0.1792086
Soil depth	SoilDepth	Mean soil depth in cm.	3.5 – 39	18.2	ln(c+x)	36.189
Soil moisture	SoilMoisture	Percentage (%) of moisture in soil.	21.3 – 78.0	71.3	e^cx	0.161783
Total nitrogen	TotN	Total nitrogen, percentage (%) of organic matter.	6.6 – 24.4	14.3	ln(c+x)	17.4737
Total phosphorous	TotP	Total phosphorous, percentage (%) of organic matter.	0.2 – 5.4	0.7	ln(c+ln(c+x))	0.5273836
Density of alive trees	TreeDensAlive	Density of alive tree branches above the plot, measured by densitometer of 92 small quadrats recorded in four directions.	0 – 182	39.0	ln(c+x)	0.972275
Density of dead trees	TreeDensDead	Density of dead tree branches above the plot, measured by densitometer of 92 small quadrats recorded in four directions.	0 – 81	13.8	ln(c+x)	0.044911
Dead wood	DeadWood	Prescence (1) or absence (0) of dead wood, e.g. tree stems or large branches.	0–1	0.2	Binary	-
Droppings from rodents	DroppingsRodent	Fraction of droppings from small rodents.	0–1	0.5	Binary	-
Mineral cover	Mineral	Fraction of loose rocks with a diameter > 6 cm.	0–1	0.2	Binary	-

3.5.2 Statistical analyses

All statistical analyses were conducted using R version 1.4.1103 (RCoreTeam, 2021). The vegan package version 2.5–7 (J. Oksanen et al., 2020) was used for multivariate analyses.

All continuous explanatory variables were subjected to pairwise correlations using Kendall's rank correlation coefficient τ. To obtain p–values for pairs of continuous and factor variables, a Wilcoxon test was used. For factor variables, a χ^2–test was used to obtain p–values between pairs.

For statistical analyses, the raw species–abundance data with sub–plot frequencies (0–10) was used. Raw data can impact the results of the ordination results (van Son & Halvorsen, 2014; Økland, 1990). However, uncertainties are related to the subjectivity of the alternative which is abundance/dominance data (van Son & Halvorsen, 2014; Økland, 1990).

As suggested in van Son and Halvorsen (2014), multiple parallel ordination of detrended correspondence analysis (DCA) (Hill & Gauch, 1980) and global-nonmetric multidimensional scaling (GNMDS) (Kruskal, 1964b, 1964a) was performed. To obtain DCA axes, the Decorana function (Hill, 1979) was run with four rescaling cycles and 26 segments per cycle. DCA axes was scaled in standard deviance units (S.D. units). GNMDS in three dimensions obtained, where the distance matrix was compared to Bray Curtis dissimilarities. New geodesic distances were calculated with step across $\epsilon = 0.8$ for unreliable distances. 8. Maximum amount of iterations were 200 and a stress convergence criterion of 1×10^{-7}. GNMDS axes were rescaled to half-change units (H.C. units) and subjected to varimax rotation. All ordinations were screened for artefacts such as the tongue effect in DCA and the horseshoe effct in GNMDS. Correlations between GNMDS and DCA ordination axis resulted in a three-dimensional GNMDS ordination being used for interpretations.

For purposes of ecological interpretation of the results, biplots with vectors showing direction of maximum increase for significant continuous variables and positions of optimum for factor variables along the axis were made. Biplots with isoline representations of the most important significant variables was also made using the *envfit*–function. Correlations between explanatory variables and ordination axes were calculated for all continuous environmental variables. For factor variables a Wilcoxon test was conducted to show the relationship with the ordination axes.

4

Results

4.1 Transect characteristics

In total 70 species were recorded in all 58 plots. Of these 21 were vascular plants, 24 bryophytes and 25 lichens. Figure 4.1 shows the mean species richness expressed in vascular plants, bryophytes and lichens for each transect. Appendix 10 contains the registered sub-plot frequencies and coverage of species for all transects.

All transects were located within 1 km^2 and differences in species richness between transects were largely dependent on nature types rather than between-transect variation. Of vascular plants, *Vaccinium myrtillus, Vaccinium vitis-idaea, Chamaepericlymenum suecicum, Lysimachia europaea, Empetrum nigrum and Avenella flexuosa* were frequent in all transects. Regarding bryophytes, *Dicranum fuscescens* was registered in all 58 plots and *Polytrichum juniperinum* occurred with high frequency and coverage in almost all plots (56 of 58 plots total). Livermosses *Barbilophozia floerkei, Barbilophozia lycopodioides, Calypogeia neesiana, Cephalozia* agg., *Pohlia nutans* agg. and *Lophozia ventricosa* occurred frequently in all transects. In addition, *Pleurozium schreberi* occurred with high plot frequency but low cover in all transects. Lichens occurred in high frequencies but low coverage, and were largely represented by *Cladonia* spp.. *Betula pubescens* occurred as young sprouts of less than 10 cm in all transects except transect 7.

Forest plots were dominated by *A. flexuosa* in the field layer and livermoss

B. floerkei in the bottom layer. Most forest plots had low management intensity (HI–a) reflected by species such as *Nardus stricta* and *Carex brunnescens*. In addition, *Listera cordata, Lycopodium annotum, Dryopteris expansa* and *B. lycopodioides* occurred mainly in forest plots.

Transect 1 spanned from forest via heath to exposed ridge. It was the most wind exposed of the transects, which was reflected by a larger species richness of lichen than most of the other transects, see figure 4.1. *Ochrolechia* spp., *Cetraria islandica, cetraria aculeata, Sphaerophorus globosus, Ptilidium ciliare, Polytrichum pilfierum* and *Juncus trifidus* reflect these conditions.

Transect 2 and transect 3 had some plots located close to mire with occurrences of water-loving species such as *Mylia anomala*, see figure 4.2. These transects also had a higher cover of *Vaccinium uliginosum* than the other transects. Transect 3 had the highest frequency of *V. myrtillus*, occuring in 10 of 12 plots total. This transect also had the highest frequency of young sprouts of *B. pubescens*, occuring in 6 plots.

In contrast to the other transects, transect 4 had a low frequency and cover of *E. nigrum* and did not have occurances of *V. uliginosum*. The transect was located on woodland and the bottom layer was dominated by *P. juniperinum*. Transect 7 had more species of lichen than most of the the other transects due to a plot in windy positioning. It also had a relatively high frequency of *Nephroma arcticum* and *Rubus chamaemorus* on peatland.

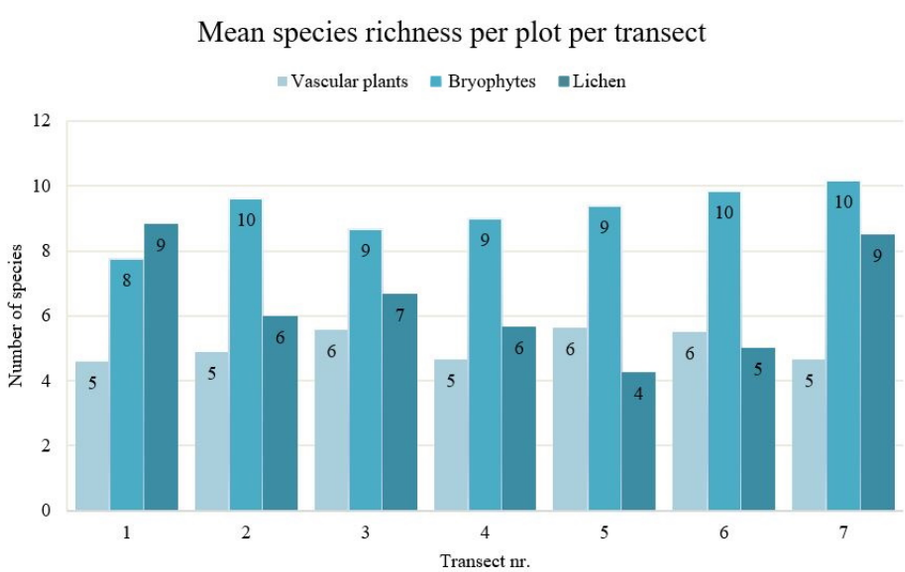

Figure 4.1: Mean species richness per plot per transect. Averages are rounded to integers.

Figure 4.2: Images displaying the south end of transect 3 with hummock formation bordering with mire.

4.2 Characteristics of terrestrial peatland

Nine plots were identified as T4–C–21 Peat forest and 21 plots as T3–C–15 Peat heath. Figures showing species frequencies and mean species abundances per plot in Peat heath and Peat forest can be found in Appendix 11.

Thhe bottom layer was dominated by *Polytrichum juniperinum* all investigated terrestrial peatland plots, with a cover of 9.6 in Peat forest and 7 in Peat heath. The livermosses *Pohlia nutans* agg. *Calypogeia neesiana* and *Barbilophozia floerkei* typically grew in between the thick covers of *P. juniperinum*, and occurred with higher cover in Peat forest than in Peat heath. *Vaccinium vitis-idaea* had high frequency but low cover in all terrestrial peatland plots. *Dicranum fuscescens* had high frequency and medium cover in both Peat forest and Peat heath. Lichens that occurred with high frequency but low cover were mainly *Cladonia* spp., in particular *C. rangiferina, C. uncialis, C. gracilis* and *C. squamosa*.

E. nigrum occurred in all Peat heath plots with an average cover of 8.5. In transects 1, 2, 3, 5 and 7, plots with Peat heath had occurrences of *R. chamaemorus* with low cover on hummocks. Transect 3 and 7 had a few occurrences of *Hylocomium splendens* on Peat heath. See figure 4.4 for hummock formation

on Peat heath.

E. nigrum occurred with low cover in 4 of the 9 Peat forest plots, with an average plot cover of 3.3. Plot number 7 in transect 3 deviated from the other Peat forest plots with respect to *E. nigrum*, which had a cover of 9 in this plot. It was located close to the transition zone between Peat forest and Peat heath, and had less tree cover than the other Peat forest plots. See figure 4.5 for hummock formation in Peat forest.

A gradient in species composition from the top of hummocks to the depressions and vertical parts of hummocks was observed. In and around depressions, there was a dominance of *C. neesiana*, *P. nutans* and *L. ventricosa* and high frequency of *Cladonia* spp. The upper parts of hummocks were dominated by *P. juniperunim* and dwarf shrubs such as *E. nigrum, V. uliginosum and V. vitis-idaea* in addition to lichen, mainly *Cladonia* spp. and *Nephroma arcticum*. *Rubus chamaemorus* also occurred on hummocks in many Peat heath plots.

In addition to hummock formation, there were observed cracks resembling ice-wedges in the terrestrial peatland, see figure 4.3. The cracks were located around several of the transects.

Figure 4.3: Cracks in terrestrial peatland, resembling ice-wedges.

Figure 4.4: Terrestrial hummock formation on Peat heath on a convex landform along transect 2.

Figure 4.5: Peat accumulation and hummock formation in Peat forest areas along transect 4.

4.3 Soil depth and maximum hummock size

Figure 4.6 shows mean soil depth on a grid around each transect. Figure 4.7 shows maximum hummock size within a radius of 2 meter of each point in the grid. The top side of all the maps in the figures faces north.

Figure 4.6 show that soil depth increases towards the upper part of convex landforms and on slopes. One exception is transect 7, where the largest soil depths and hummock sizes of all the transects was registered in and around a concave landform on an esker. The soil depth map around transect 7 also shows a relatively sharp gradient in decreasing soil depth on the south facing side of the esker, and when moving from east to west along the esker.

Comparing figure 4.6 and 4.7 shows how the larges hummock sizes occur in areas with high soil depth. Figure 4.7 shows how the size of the hummock in the concave landform in transect 7 are compared to the other transects. Large hummock sizes are also registered in the east side of transect 5, which is in the transition zone towards a mire. A large hummock occuring around ares without other hummocks and with relatively low soil depths (5-1 cm) is visible on the south-east side of the grid around transect 3.

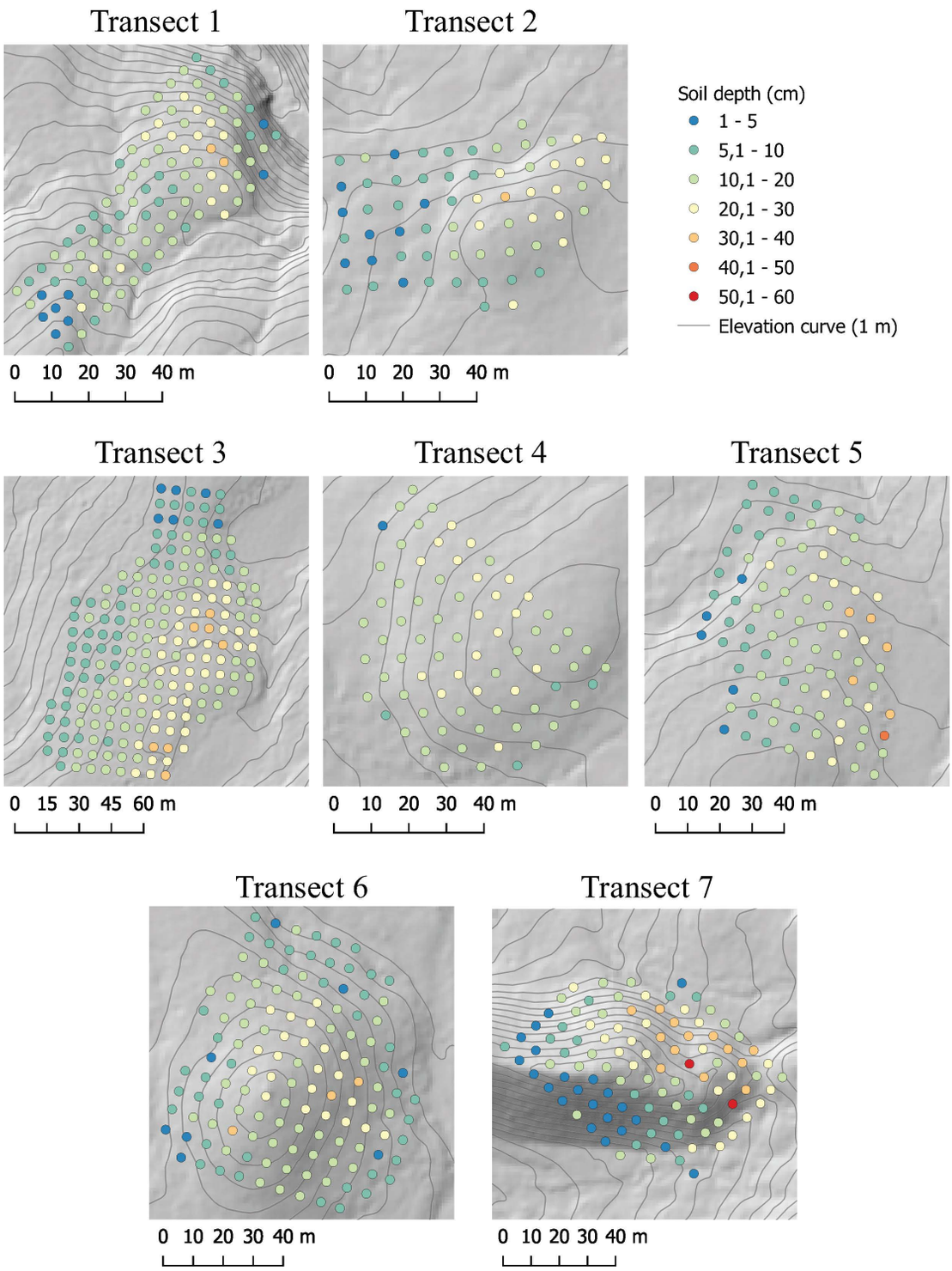

Figure 4.6: Soil depth measurements around each transect. The distance between each point is 7 meters. Equidistance curves with 1 meter intervals in the background, in addition to shadows portrayed by DEM (Digital Elevation Model). The top side of all figures faces north. Figure made in QGIS version 3.14.

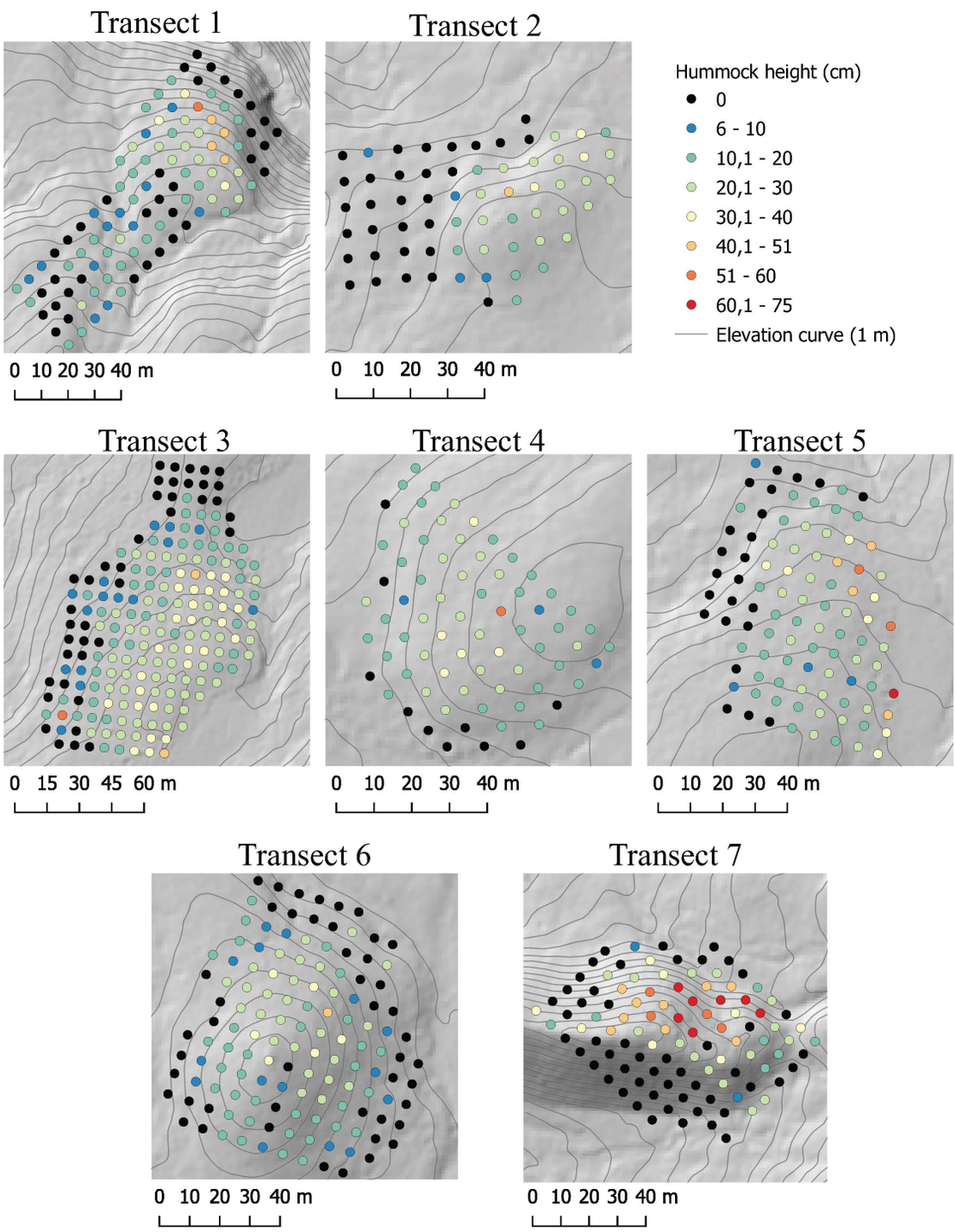

Figure 4.7: Maximum hummock height in a grid around each transect. The distance between each point is 7 meters. Equidistance curves with 1 meter intervals in the background, in addition to shadows portrayed by a DEM (Digital Elevation Model). The top side of all figures faces north. Figure made in QGIS version 3.14.

4.4 Land-cover mapping

Figure 4.8 and 4.9 show land-cover mapping around the transects. An overview of the nature types that were registered are shown in table 4.1. Additional nature types Peat forest (T4–C–21) and Peat heath (T3–C–15) were applied as to describe terrestrial peat accumulating nature types with and without tree-cover. Definition of these types can be found in section 3.1.1. Translations used for the NiN–system are described in the supplementary material for Halvorsen, Skarpaas, et al. (2020).

The land-cover mapping showed that all of the peat producing areas (T3–C–15)and (T4–C–21) were close to a forest or heath without peat accumulation. It also showed that many of the terrestrial peatlands, but not all, were within close proximity of nature types that have a relative high water supply, such as mires and fens.

Figure 4.8 show nature types surrounding transect 1, 2 and 3. Peat heath (T3–C–15) in transect 1 was located on a slope, angled towards a river. It was also close to an astatic spring. The terrestrial peatland around transect 2 contained both Peat heath and Peat forest (T4–C–21), and both were located close to a mire forest lawn. The terrestrial Peat heath in transect 3 had a gradual transition to a fen. In addition, both Peat forest and Peat heath in transect 3 were located close to a mire forest lawn, an astatic spring, and a fen.

Figure 4.9 show nature types surrounding transect 4, 5, 6 and 7. The terrestrial peatland around transect 4 consisted of Peat forest (T4–C–21) that relatively close to a fen and a mire forest lawn. Transect 5 had a gradual transition from Peat heath (T3–C–15) to a mire forest lawn. The area around transect 6 consisted of both Peat forest and Peat heath surrounded by forest. The area around transect 7 consisted of both Peat forest and Peat heath and was surrounded by forest. The majority of the Peat heath on transect 7 was placed in a concave formation on an esker, visible by evaluating the elevation curves in the map. The terrestrial peatlands around transect 7 located on the north side of the esker, while the south side of the esker had subxeric forest (T4–C–9) characterized by high risk of severe drought (UF) and shallow soil.

Table 4.1: List of nature types shown in figures 4.8 and 4.9. Nature types in *italic* are additional nature types used in this analysis and are not a part of the NiN–system. See description and definition of these in section 3.1.1

Type code	Name
L	Freshwater bottom systems (major type)
T3–C–1	Lime–poor alpine lee side
T3–C–2	Lime–poor alpine subxeric heath
T3–C–15	*"Peat heath"*
T4–C–1	Lime–poor submesic forest
T4–C–2	Intermediately lime–rich submesic forest
T4–C–5	Lime–poor submesic to subxeric forest
T4–C–9	Lime–poor subxeric forest
T4–C–21	*"Peat forest"*
T14–C–1	Lime–poor to intermediately lime–rich alpine ridge
T32–C–3	Intermediately lime–rich low–intensity managed semi–natural grassland
T32–C–9	Strongly lime–rich low–intensity managed semi–natural grassland
V1–C–6	Moderately lime–poor fen expanse carpet
V2–C–1	Lime–poor mire forest lawn
V4–C–1	Lime–poor astatic spring

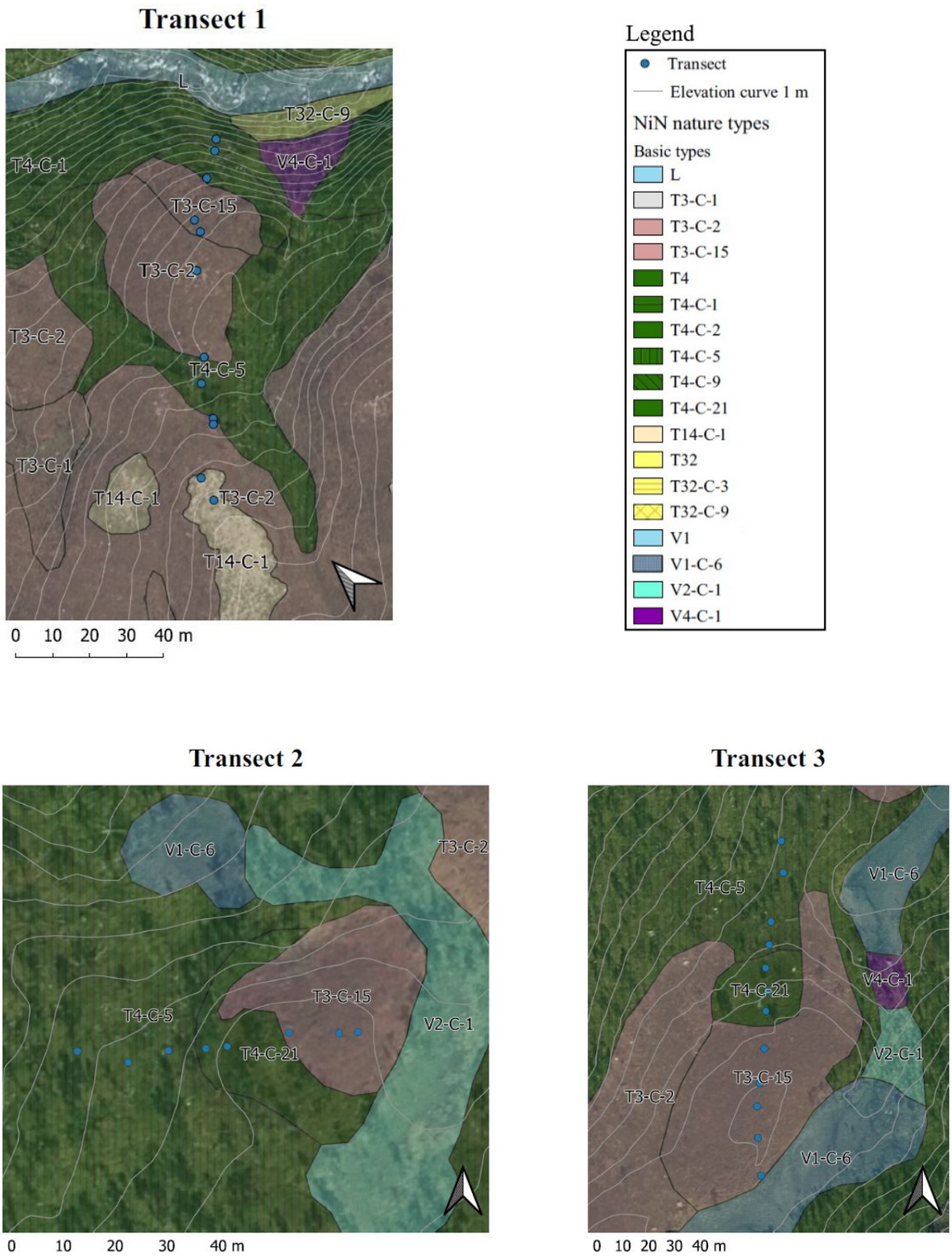

Figure 4.8: Land–cover mapping around transect 1, 2 and 3. Upper right corner shows legend for the registered nature types.

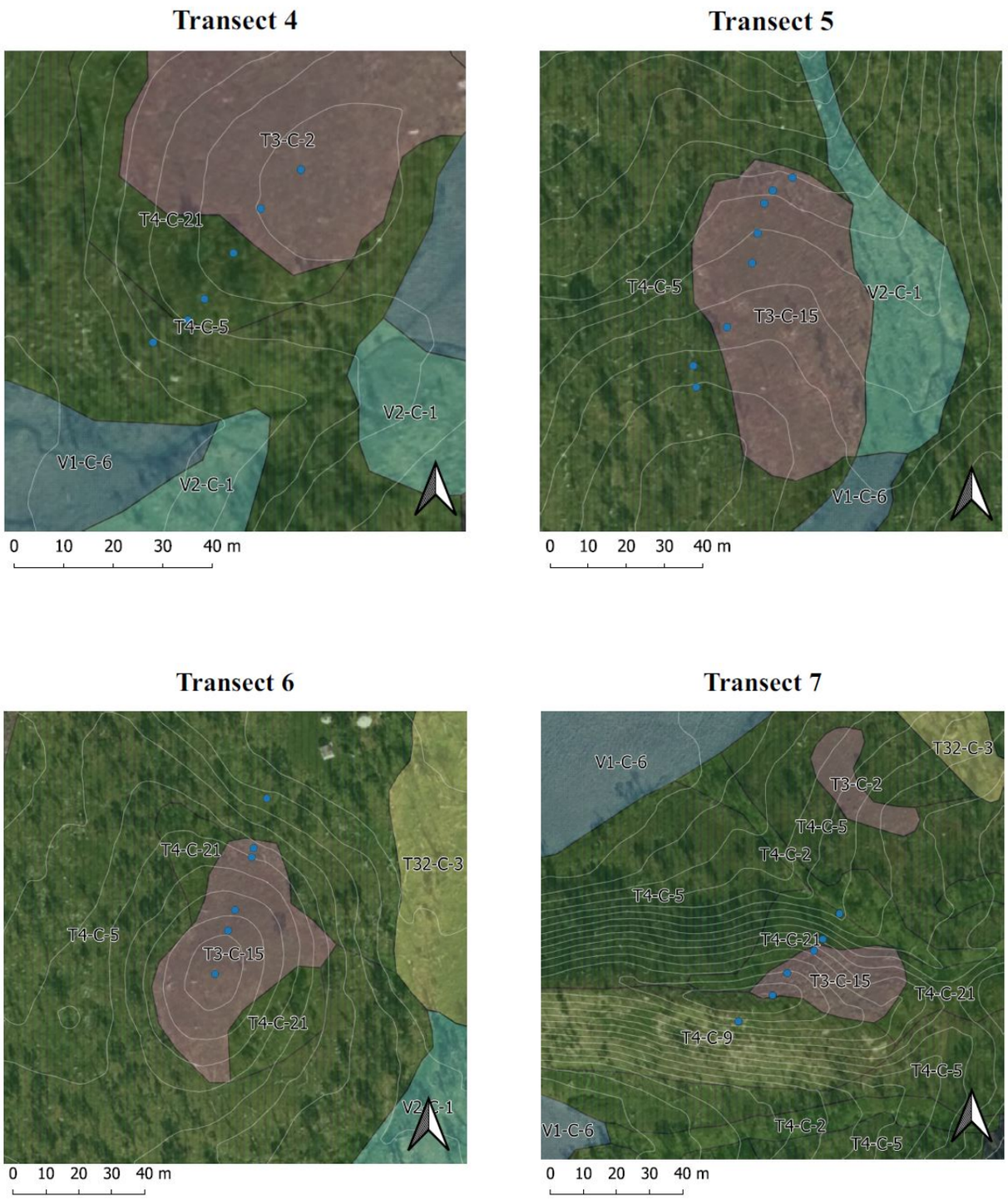

Figure 4.9: Land–cover mapping around transect 4, 5, 6 and 7. Legend for all registered nature types is displayed in figure 4.8.

4.5 Explanatory variables

An overview of Kendall's correlation coefficient τ between all continuous explanatory variables is shown in table 4.4. Table 4.2 shows Wilcoxon test statistic (V) between continuous variables and factor variables, and table 4.3 shows χ^2-test statistics between factor variables. An overview of the characteristics of the explanatory variables are shown in chp. 3. Appendix 5 contains untransformed values for all environmental variables and appendix 6 contains all transformed values for continuous variables.

Dead wood was related to the presence of alive trees (TreeDensAlive) and risk of severe drought (UF), reflecting a larger amount of deadwood in woodland areas. Mineral cover and wind-mediated disturbance intensity (VI) were related to each other, reflecting the exposure of stones and mineral in areas with high wind exposure. Mineral cover and VI were both related to a number of continuous variables that have distinct characteristic at exposed ridges, such as soil depth (which is low at exposed ridges), microtopography (which reflects a flat surface at exposed ridges) and pH (which is higher at exposed ridges where the soil is in close contact with the bedrock).

Several continuous environmental variables had weak correlations to each other ($\tau < 0.3$). The convexity variables (ConV and ConvH) did not correlate to any other continuous variables. Field layer was negatively related to alive tree cover (TreeDensAlive) ($\tau = -0.35$), reflecting a lower cover of vascular plants in woodland areas compared to open areas.

LOI was positively correlated to soil depth ($\tau = 0.3$) and negatively correlated to snow cover ($\tau = -0.32$), insinuating that areas with deep soil contain high amounts of organic matter and that areas with high amounts of organic matter has less snow cover. This reflects that the snow melts earlier in open peatland than in woodland plots, and attests to a thinner layer of snow on heath than in forest areas during the winter.

Total phosphorous content was positively correlated to total nitrogen content ($\tau = 0.43$) , reflecting a well-known property of nutrient variability in soil.

Density of dead trees and alive trees was positively correlated with each other ($\tau = 0.39$). They were both positively correlated with snow cover ($\tau_{TreeDensAlive} = 0.42$, $\tau_{TreeDensDead} = 0.51$) and negatively correlated with risk of severe drought (UF) ($\tau_{TreeDensAlive} = -0.47$, $\tau_{TreeDensDead} = -0.35$). This reflects that woodland areas consisted of a combination of dead and alive trees, and that woodland occurred in larges abundancies in areas with low risk of severe drought. The correlation to snow cover reflects that the snow last melts later in woodland areas than on heath and exposed ridges. Snow cover was negatively related

with UF (τ= –0.46) which reflects a well-known gradient from areas with long snow cover and less dry conditions, to areas with limited snow cover and high risk of severe drought (described in e.g. Økland & Bendiksen, 1985).

Microtopography in the vertical and horizontal direction (MicrotopoH, MicrotopoV) were positively correlated to each other (τ = 0.53) and to soil depth ($\tau_{MicrotopoH}$ =0.25, $\tau_{MicrotopoV}$ = 0.40). The correlation with soil depth reflects a larger variation in the surface vertical plane in areas with large soil depth, i.e. that hummock formation occur areas with high peat accumulation.

Table 4.2: Wilcoxon values (W) and corresponding p–values for factor variables against continuous variables. P≤0.05 is marked with bold.

	DroppingsRodent		DeadWood		Mineral		VI	
	W	p	W	p	W	p	W	p
Aspect	430.5	0.8763	179.5	0.3843	232	0.8773	106	0.4192
Slope	586	**0.0098**	156	0.1682	229	0.8284	83.5	0.9860
ConvH	510.5	0.0546	199.5	0.5457	245	0.8988	84	0.9616
ConvV	393	0.4913	211.5	0.7606	257	0.5708	79.5	0.8835
FieldLayer	410.5	0.8886	307.5	0.0631	266.5	0.5924	108	0.3799
BotLayer	473.5	0.4088	184.5	0.4451	314.5	0.1271	134.5	**0.0702**
pH	306.5	0.0766	227.5	0.8882	65.5	**0.0003**	0.5	**0.0040**
LOI	583	**0.0115**	266.5	0.3285	467	**<0.0001**	159	0.0076
TotP	410	0.8834	227	0.8992	126	**0.0178**	31	0.0734
TotN	488	0.2960	168	0.2691	161	0.1069	57	0.3801
DroppingsRangifer	287	**0.0380**	179.5	0.3814	213	0.5830	87.5	0.8737
SoilMoisture	374.5	0.4838	248	0.5620	420	**0.0002**	163	**0.0050**
TreeDensDead	298	**0.0475**	145.5	0.0935	203.5	0.4372	130.5	0.0804
TreeDensAlive	303.5	0.0634	61.5	**0.0005**	216	0.6188	136.5	0.0534
SoilDepth	566.5	**0.0230**	213	0.8804	388	**0.0024**	150	**0.0186**
MicrotopoH	499.5	0.2083	224.5	0.9387	359	**0.0125**	159	**0.0063**
MicrotopoV	479	0.3516	175	0.3227	374	**0.0049**	149	**0.0177**
Altitude	404.5	0.8154	200.5	0.6753	291	0.2985	88.5	0.8469
UF	571	**0.0114**	344.5	**0.0042**	168.5	0.1145	2	**0.0024**
SnowCover	257.5	**0.0065**	170.5	0.2510	242	0.9734	138	**0.0371**

Table 4.3: Pearson χ^2–test between factor variables with 1 degrees of freedom. P≤0.05 is marked with bold.

	DroppingsRangifer	DeadWood	Mineral	VI
DroppingsRangifer		0.9103	0.6400	1.000
DeadWood	0.0127		0.9604	1.000
Mineral	0.2188	0.0025		**0.0019**
VI	<0.0001	<0.0001	**9.6850**	

Table 4.4: Lower triangle shows Kendall's τ correlation coefficients for continuous explanatory variables, while upper triangle shows corresponding p–values. P≤0.05 is marked with bold.

	Aspect	Slope	ConvH	ConvV	Field Layer	Bot Layer	pH	LOI	TotP	TotN	Droppings Rangifer	Soil Moisture	TreeDens Dead	TreeDens Alive	Soil Depth	Micro topoH	Micro topoV	Altitude	UF	Snow Cover
Aspect		0.0885	0.8101	0.0795	**0.0145**	**0.0336**	0.9515	0.1710	0.0908	0.3685	0.5747	0.8510	0.7089	0.6434	0.5062	0.2932	0.9409	**0.0002**	0.5228	0.1131
Slope	-0.1578		0.1822	0.9282	0.3459	0.7513	0.6940	0.4592	0.5358	0.6185	0.6694	0.2058	0.4166	**0.0192**	0.0835	0.6606	**0.0161**	**0.0143**	0.3126	0.3077
ConvH	-0.0255	0.1444		0.9263	0.3365	0.5475	0.1519	0.2407	0.5001	0.7049	0.3429	0.7049	0.6213	0.5558	0.4652	0.7456	0.6630	0.2838	0.3166	0.7269
ConvV	0.1883	-0.0099	0.0117		0.2040	0.6526	0.5638	0.4790	0.9194	0.3869	0.4486	0.9552	0.8413	0.9263	0.7873	0.9910	0.5500	0.3282	0.3032	0.2910
Field Layer	**-0.2227**	-0.0875	0.1024	-0.1367		**0.0002**	0.2975	0.7935	0.7221	0.6147	0.1387	**0.0106**	0.3746	**0.0003**	0.4359	0.8556	0.8292	**0.0026**	0.6848	0.8217
Bot Layer	**0.1953**	-0.0297	0.0646	0.0489	-0.3406		**0.0401**	0.5587	0.0706	0.5232	0.2669	0.5319	0.7616	**0.0054**	0.4043	0.4580	0.9247	0.0665	0.1105	0.6997
pH	-0.0057	-0.0377	-0.1577	0.0642	**0.0983**	**-0.1953**		0.5700	0.2037	0.9353	0.7696	**0.0373**	0.4476	0.2395	0.1088	**0.0046**	0.2295	**0.0223**	0.1052	0.9708
LOI	0.1240	0.0683	0.1242	0.0757	-0.0238	-0.0535	-0.0532		**0.0027**	**0.0651**	0.3339	0.5505	**0.0519**	**0.0459**	**0.0008**	0.4670	0.2385	0.2246	0.1882	**0.0019**
TotP	0.1531	-0.0571	-0.0714	-0.0108	-0.0323	**-0.1655**	0.1192	**0.2704**		**<0.0001**	0.1876	0.7323	0.6624	0.8197	0.1292	0.5092	0.1513	**0.0369**	0.5084	0.3339
TotN	0.0814	0.0459	0.0401	-0.0925	-0.0457	-0.0584	0.0076	**0.1664**	**0.4338**		0.8978	0.6149	0.5080	0.4433	0.0987	0.6470	0.2227	0.1569	0.6521	0.9363
Droppings Rangifer	-0.0527	-0.0409	-0.1042	0.0841	-0.1394	0.1054	-0.0285	-0.0904	-0.1233	-0.0120		0.4451	0.3312	0.2131	0.9407	**0.0398**	0.2194	0.1786	0.6718	0.8093
Soil Moisture	0.0170	-0.1167	-0.0401	-0.0060	**0.2320**	-0.0572	**-0.1952**	-0.0538	-0.0309	-0.0454	-0.0715		0.7782	0.7247	0.5820	0.1150	0.1074	0.3373	**0.0059**	0.5085
TreeDens Dead	-0.0360	0.0798	0.0557	-0.0228	-0.0857	0.0296	0.0758	**-0.1866**	-0.0419	0.0635	0.0968	0.0270		0.0001	0.0977	0.8932	0.4409	0.3275	**0.0012**	**<0.0001**
TreeDens Alive	0.0439	**0.2265**	-0.0654	-0.0104	**-0.3464**	**0.2669**	-0.1156	**-0.1887**	-0.0215	0.0725	0.1222	-0.0333	**0.3859**		0.5114	0.4173	0.2583	0.8520	**<0.0001**	**0.0001**
SoilDepth	-0.0607	0.1609	0.0779	-0.0291	-0.0712	0.0769	-0.1515	**0.3038**	-0.1379	**-0.1501**	0.0070	0.0500	-0.1602	-0.0625		**0.0069**	**<0.0001**	0.8614	0.9102	0.2598
Micro topoH	0.0978	-0.0416	0.0353	0.0012	-0.0170	0.0698	**-0.2726**	0.0674	-0.0611	-0.0424	**-0.1976**	0.1460	0.0132	0.0788	**0.2523**		**<0.0001**	0.3998	0.5716	0.4225
Micro topoV	0.0069	**0.2283**	0.0475	0.0658	-0.0201	0.0089	-0.1159	0.1094	-0.1331	-0.1131	-0.1182	0.1494	0.0761	0.1099	**0.4033**	**0.5305**		0.2438	**0.0298**	**0.0449**
Altitude	**0.3363**	**-0.2265**	-0.1137	0.1048	**-0.2741**	0.1683	**-0.2147**	0.1098	**0.1886**	0.1280	0.1261	0.0867	-0.0942	0.0177	-0.0159	0.0782	-0.1084		0.3671	**0.0097**
UF	-0.0657	-0.1058	0.1206	-0.1253	0.0418	-0.1658	-0.1725	0.1353	0.0677	0.0462	-0.0450	**-0.2816**	**-0.3542**	**-0.4683**	0.0116	-0.0595	**-0.2289**	0.0925		**0.0001**
SnowCover	-0.1644	0.1079	-0.0425	-0.1298	0.0234	-0.0405	0.0039	**-0.3228**	-0.0999	-0.0083	0.0259	0.0683	**0.5067**	**0.4166**	-0.1173	0.0852	**0.2133**	**-0.2680**	**-0.4565**	

4.6 Ordinations

For the DCA ordinations, compositional turnover showed that higher order axes were longer than the subsequent ones, for all but DCA 4 (DCA4 = 1.1218 > DCA3 = 1.1662), see table 4.5. For GNMDS ordinations, the higher order axes were longer than the subsequent axes, see table 4.6.

Table 4.7 shows correlations between DCA and GNMDS axes. The first axes of GNMDS and DCA were strongly correlated ($\tau > 0.9$). The second axes show a weaker correlation ($\tau = 0.34$), but DCA2 shows a stronger correlation to GNMDS3 ($|\tau| > 0.4$). DCA4 shows a stronger correlation with GNMDS3 ($|\tau| = 0.5$) than DCA 2. DCA3 is not confirmed by any of the GNMDS axes.

Table 4.5: DCA axes characteristics and axis length in S.D. units.

	DCA 1	DCA 2	DCA 3	DCA 4
Eigenvalues	0.2632	0.0848	0.0459	0.0659
Axis length	2.8223	1.4406	1.1662	1.1218

Table 4.6: GNMDS axes characteristics in H.C. units.

	GNMDS 1	GNMDS 2	GNMDS 3
Gradient length	1.5846	0.9783	0.8225

Table 4.7: Correlation and corresponding p–values between DCA and GNMDS axes. P≥0.05 is marked in bold.

	DCA 1		DCA 2		DCA 3		DCA 4	
	τ	p	τ	p	τ	p	τ	p
GNMDS 1	**0.9383**	**0.0001**	−0.0780	0.3869	**0.2111**	**0.0192**	**0.1652**	**0.0671**
GNMDS 2	0.0369	0.6824	**0.3466**	**0.0001**	−0.1603	0.0755	−0.0200	0.8248
GNMDS 3	0.0200	0.8248	**−0.4277**	**0.0001**	0.0526	0.5595	**−0.5039**	**0.0001**

DCA and GNMDS ordinations in figure 4.10–4.13 show that plots are distributed in a similar pattern along the first axis, reflecting that the first axis of both ordination methods expresses the same gradient. The second and fourth DCA axes (figure 4.10 and 4.11) show a more dissimilar distribution of plots along the axes compared to GNMDS axes 2 and 3 (figure 4.12 and 4.13), reflecting how these axes express different variations in the data.

GNMDS ordinations of the transects (figure 4.12 and 4.13) show that variation between plots in the same transects is expressed to the same degree as variation of plots from different transects, reflecting a uniform species composition between transects.

GNMDS ordinations sorted by nature type (figure 4.14 and 4.15) show a separation of plots along the axes. A distinct separation of nature types along the first axis is identified, as it shows a variation from forest (T4) via Peat forest (T4–C–21), Arctic alpine heath (T3–C–2) and Peat heath (T3–C–15) to exposed ridges (T14–C–1). Plot nr 706 stands out from the other forest plots as it is placed much higher along the first axis. This plot was the only plot of minor type Lime-poor suxeric forest (T4–C–5) (see figure 4.9), reflecting conditions of high risk of severe drought (UF) and shallow soil. Plot distribution along GNMDS1 also show similar positioning for Peat heath (T3-C-15) and Arctic alpine heath (T3-C-2), reflecting a high similarity in species richness.

Distribution of plots according to nature types along GNMDS2 (figure 4.14) show that nature types with peat accumulation (T3-C-15 and T4-C-21) are placed along higher values of the axis, while plots with forest and exposed ridges are sorted towards the lower end of the axis.

Distributions along GNMDS3 according to nature types (figure 4.15) show a clumped distribution of Peat heat (T3-C-15) along higher values of the axis, while Peat forest plots (T4-C-21) are clumped along lower values of the axis, showing that the gradient expresses a separation in these nature types.

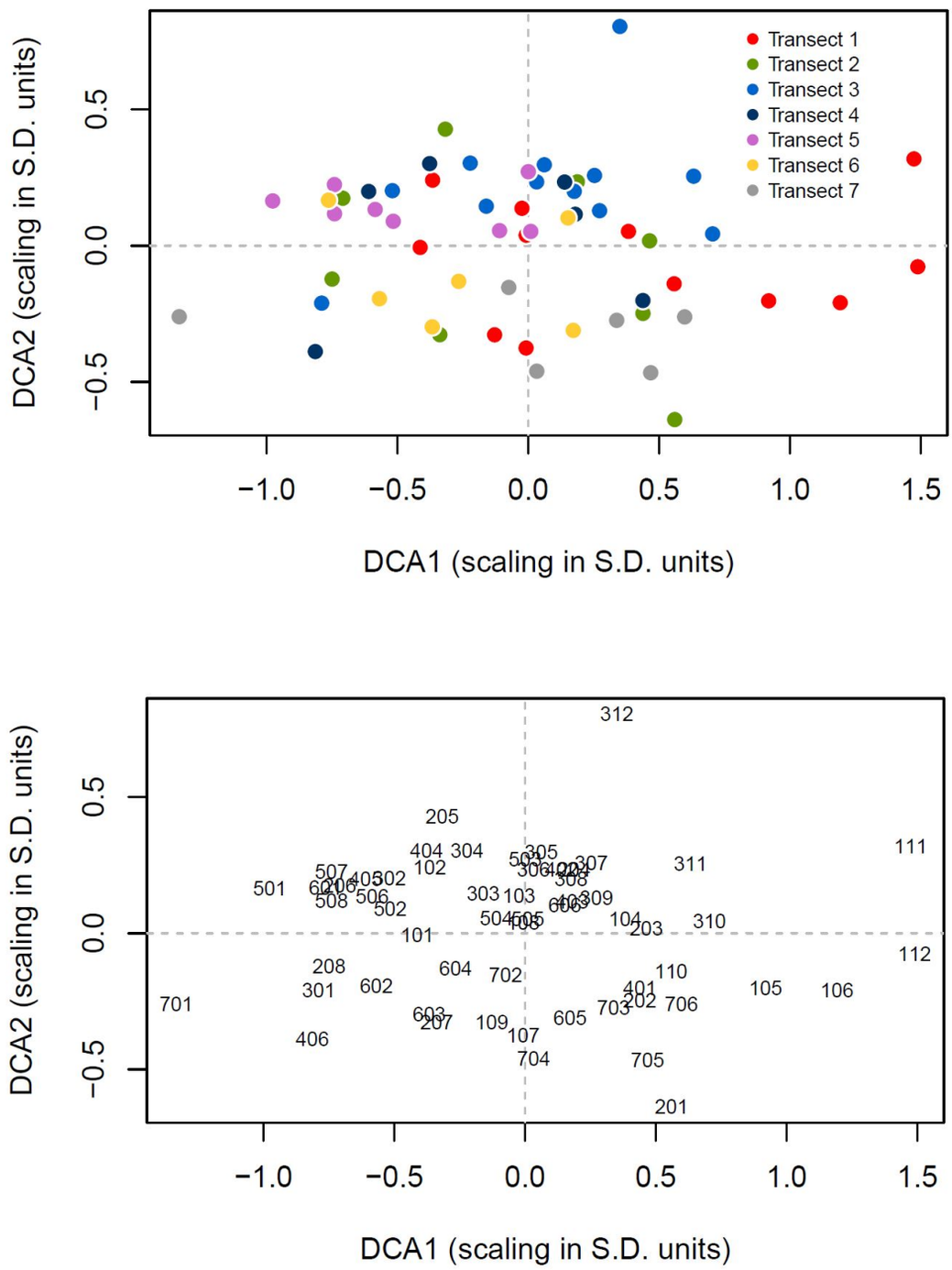

Figure 4.10: DCA ordinations of axis 1 and 2. In the upper figure the colors corresponds to a transect as described in the legend. The lower figure show positions represented by plot number.

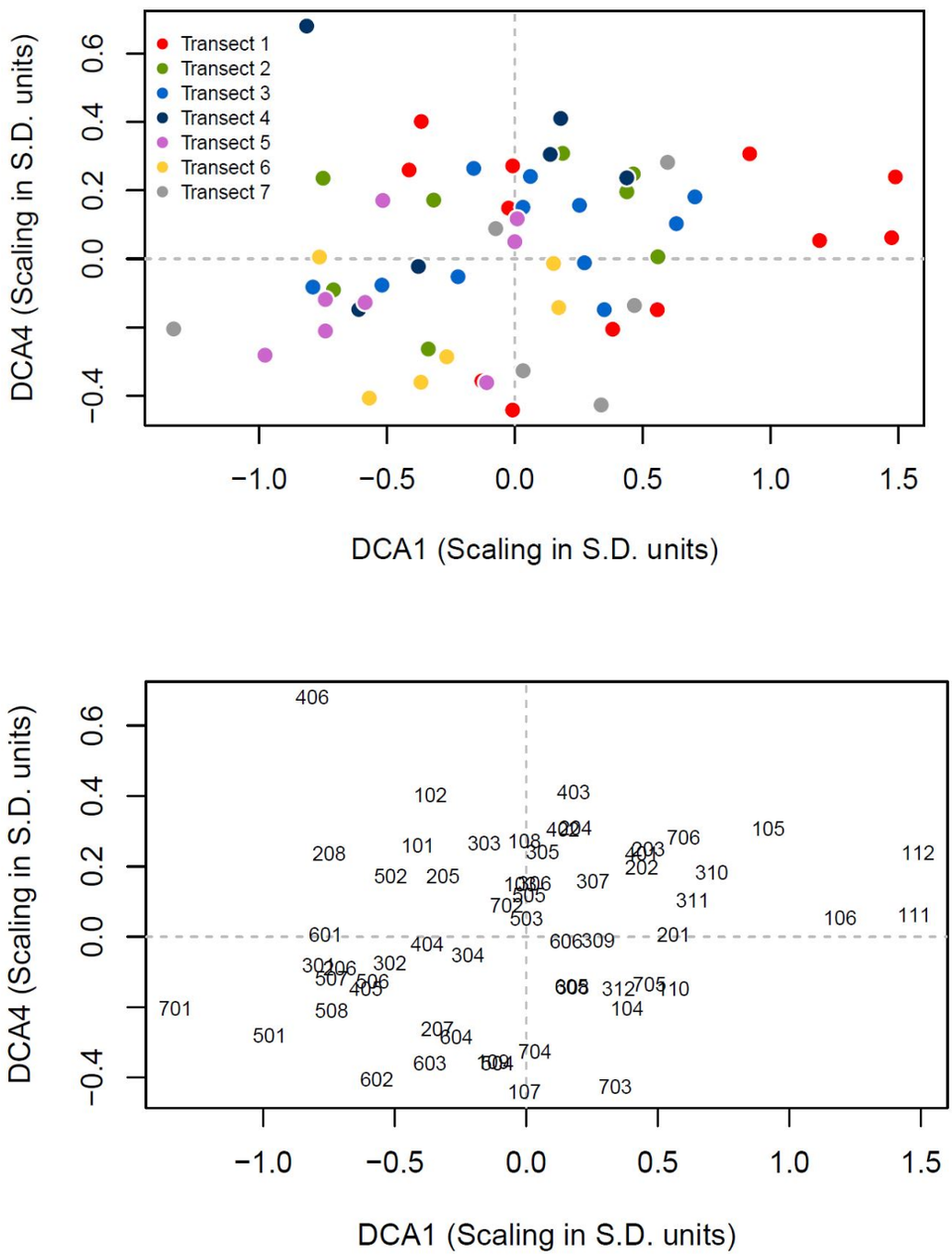

Figure 4.11: DCA ordinations of axis 1 and 4. In the upper figure the colors corresponds to a transect as described in the legend. The lower figure show positions represented by plot numbers.

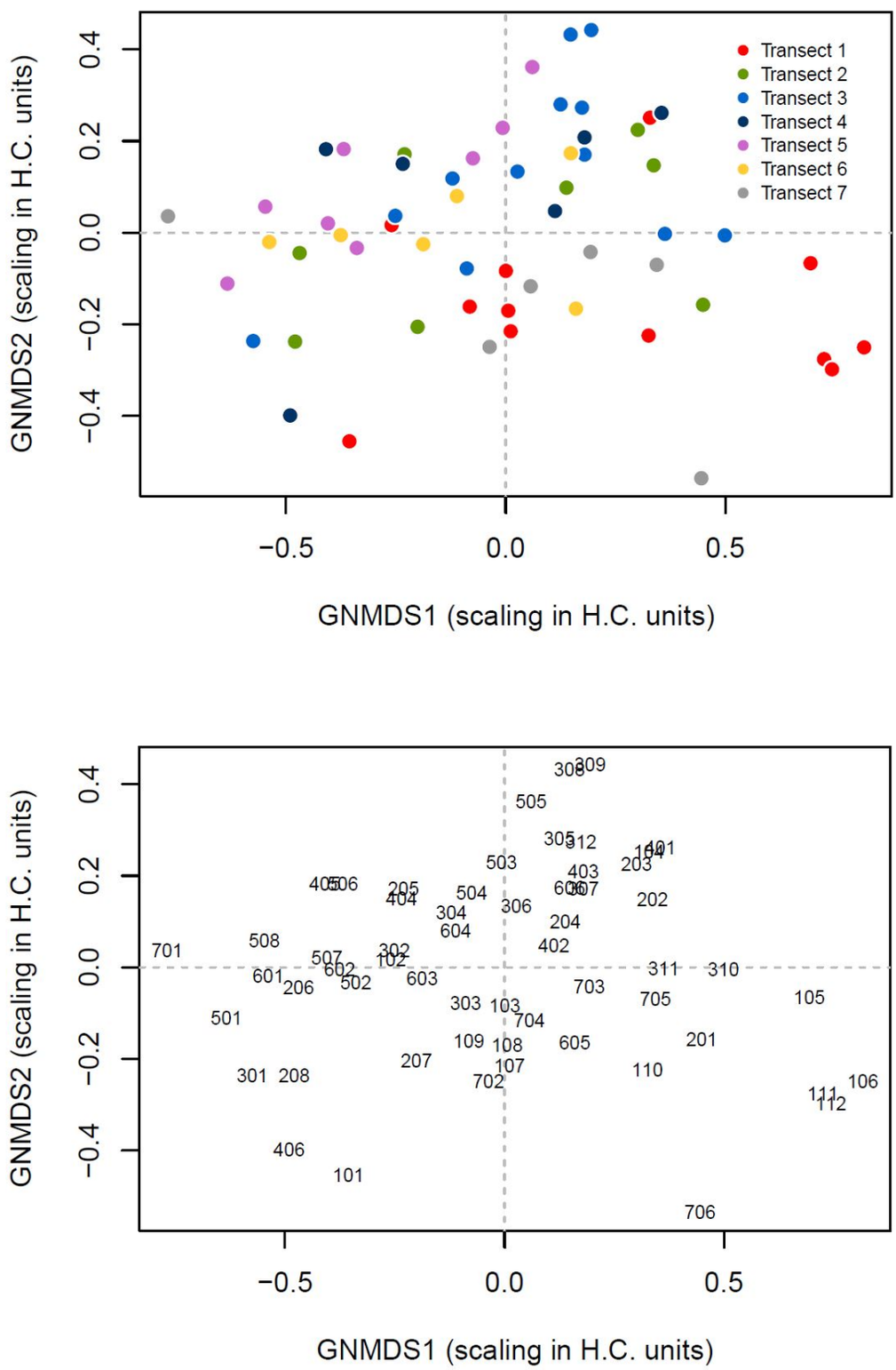

Figure 4.12: GNMDS ordinations for GNMDS axis 1 against axis 2. In the upper figure the colors corresponds to a transect as described in the legend. The lower figure show positions represented by plot number.

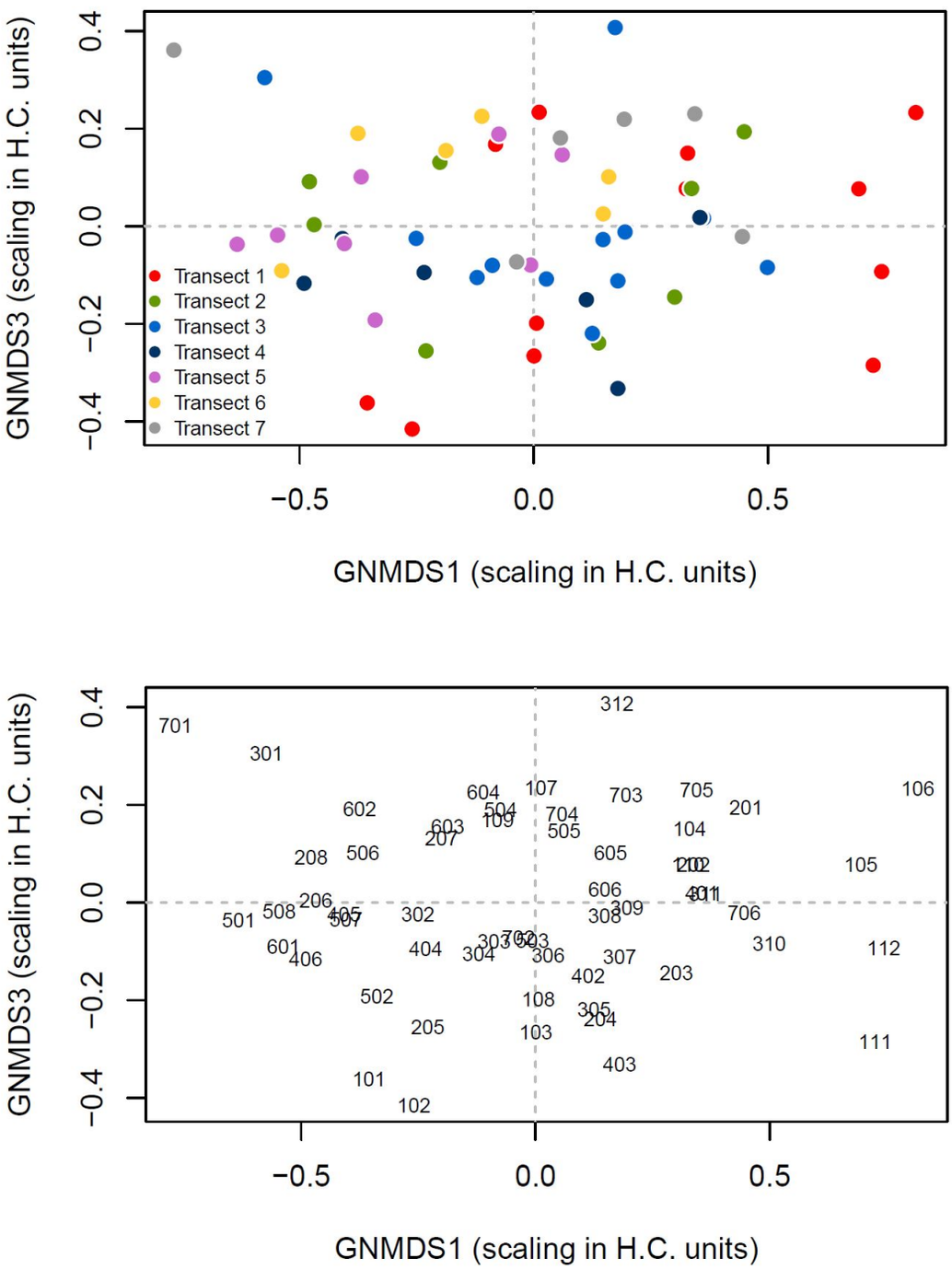

Figure 4.13: GNMDS ordinations of for GNMDS axis 1 against axis 3. In the upper figure the colors corresponds to a transect as described in the legend. The lower figure show positions represented by plot number.

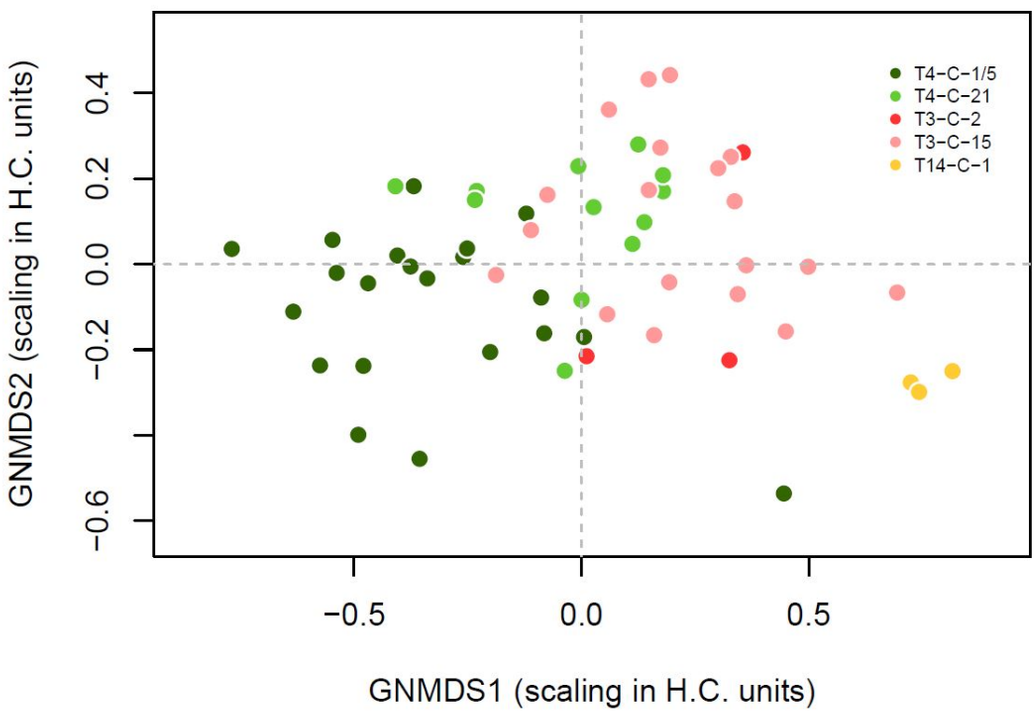

Figure 4.14: GNMDS ordinations for axis 1 and 2 with plots sorted by assigned nature type, as described in the legend. Colors correspond to figures 4.34 and 4.35.

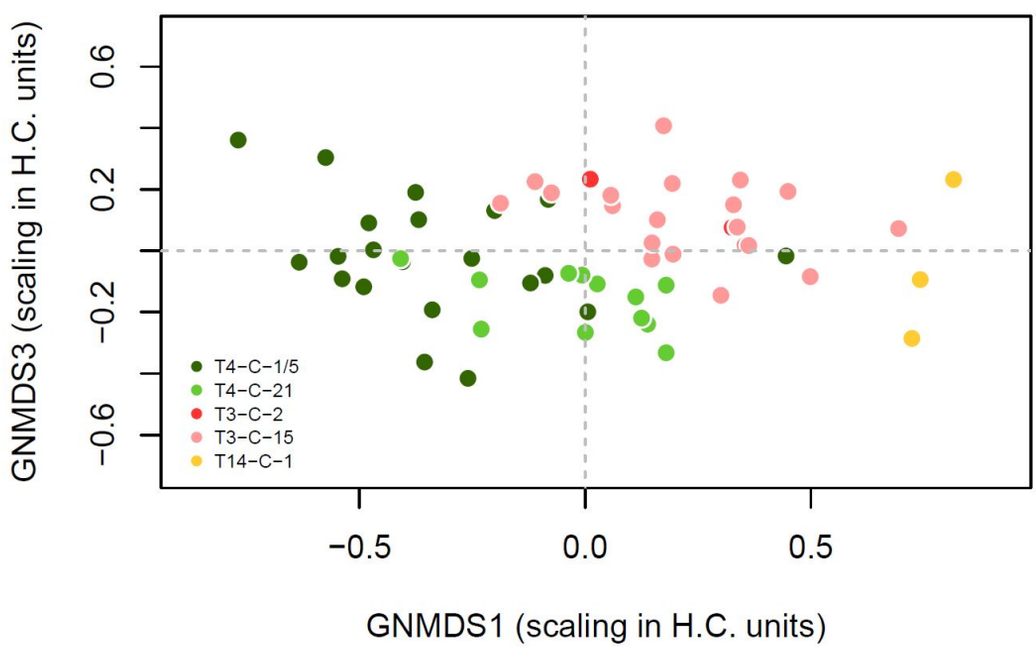

Figure 4.15: GNMDS ordinations for axis 1 and 3 plots sorted by assigned nature type, as described in the legend. Colors correspond to figures 4.34 and 4.35.

4.7 Correlation patterns

Table 4.8 contains correlations between continuous environmental variables and GNMDS axes. Table 4.9 contain Wilcoxon test statistics (V) showing relationships between GNMDS axes and factor variables. Figure 4.16 and 4.17 show biplots of GNMDS ordinations with vectors of maximum increase for the significant environmental variables related to the ordination axes.

Table 4.8 show that GNMDS1 was positively correlated with UF and LOI, and negatively correlated with TreeDensDead and TreeDensAlive and SoilMoisture. GNMDS2 was positively correlated with LOI, SoilMoisture, SoilDepth and Altitude, and negatively correlated with pH. GNMDS 3 was positively correlated with FieldLayer and SoilMoisture, and negatively correlated with Slope, BotLayer, DroppingsRangifer, TreeDensAlive and Altitude.

Moving from low to high scores along GNMDS1, the gradient is associated with increasing risk of severe drought (UF), decreasing snow cover (SnowCover), decreasing tree cover (TreeDensDead and TreeDensAlive). The gradient also has a weak association ($|\tau| < 0.3$) with increasing organic matter (LOI) and decreasing soil moisture (SoilMoisture). The significant factor variables wind-mediated disturbance intensity (VI), dead wood (DeadWood) and droppings from rodents (DroppingsRodent) show distinct points of optimum along the axis. VI has an optimum towards high scores along GNMDS1, while dead wood and droppings from rodents has their optimum at towards low scores along the axis.

Moving from low to high scores along GNMDS2, this gradient is associated with increasing organic matter (LOI) and decreasing pH, and has a weak association ($|\tau| < 0.3$) with increasing soil moisture, increasing soil depth (SoilDepth) and increasing altitudes (Altitude).

Moving from low to high scores along GNMDS 3 the gradient is It is most strongly associated with an increase in field layer (FieldLayer), τ=0.48, and is weakly associated ($|\tau| \geq 0.3$) with decreasing bottom layer (BotLayer), decreasing soil moisture, decreasing altitudes, decreasing droppings from *R. tarandus* (DroppingsRangifer) and decreasing alive tree cover.

Biplots with vectors of maximum increase along the GNMDS axes (figure 4.16 and 4.17) show the direction of maximum increase for the significant continuous variables correlated with the axes, marked with arrows. They also show points of optimum for the significant factor variables related to the axes. Figure 4.16 show how variation along the first GNMDS axis is strongly related to risk of severe drought (UF), treecover and snow cover, and that variation along the second axis is related to loss on ignition (LOI), pH and soil moisture

(SoilMoisture). Figure 4.17 show that variation along the third axis is largely explained by the FieldLayer variable.

Table 4.8: Kendall's τ correlations between continuous environmental variables and all three GNMDS axes. P≥0.05 is marked in bold.

	GNMDS 1		GNMDS 2		GNMDS 3	
	τ	p	τ	p	τ	p
Aspect	0.0462	0.6101	0.10088	0.2653	−0.12519	0.16686
Slope	−0.0906	0.3259	−0.04594	0.6185	**−0.2123**	**0.02136**
ConvH	−0.0127	0.9044	0.05572	0.59848	0.04008	0.70486
ConvV	0.0349	0.7445	0.1478	0.16693	−0.13338	0.21229
FieldLayer	0.0518	0.5684	−0.07369	0.41674	**0.48296**	**<0.0001**
BotLayer	−0.0794	0.3860	0.15808	0.08412	**−0.26141**	**0.00429**
pH	0.1001	0.2854	**−0.42338**	**<0.0001**	0.05451	0.5609
LOI	**0.2363**	**0.0089**	**0.39746**	**<0.0001**	0.13814	0.12612
TotP	0.0146	0.8720	−0.02801	0.75753	−0.06088	0.50212
TotN	−0.0702	0.4365	−0.05809	0.51959	−0.11498	0.20247
DroppingsRangifer	−0.0386	0.6802	−0.01201	0.89784	**−0.22068**	**0.01836**
SoilMoisture	**−0.2095**	**0.0203**	**0.25189**	**0.00526**	**0.22404**	**0.01306**
TreeDensDead	**−0.4718**	**<0.0001**	−0.16629	0.08318	−0.15817	0.09935
TreeDensAlive	**−0.5060**	**<0.0001**	−0.01632	0.86291	**−0.30753**	**0.00114**
SoilDepth	0.1646	0.0709	**0.26379**	**0.0038**	−0.03733	0.68207
MicrotopoH	−0.0836	0.3668	0.12354	0.18236	0.12853	0.16532
MicrotopoV	−0.0981	0.2902	0.12811	0.16729	0.07812	0.39976
Altitude	0.1049	0.2458	**0.29776**	**0.00099**	**−0.18617**	**0.03943**
UF	**0.5093**	**<0.0001**	0.00000	1.00000	0.11387	0.26603
SnowCover	**−0.5999**	**<0.0001**	−0.1344	0.1934	−0.0053	0.9594

Table 4.9: Wilcoxon test statistic and p-values showing relationships between GNMDS–axes and factor variables. P≥0.05 is marked in bold.

	GNMDS 1		GNMDS 2		GNMDS 3	
	W	p	W	p	W	p
DroppingsRodent	583	**0.0107**	476	0.3906	407	0.8470
DeadWood	350	**0.0042**	237	0.7355	237	0.7355
Mineral	229	0.8315	442	**<0.0001**	312	0.1429
VI	0	**0.0040**	156	**0.0104**	95	0.6735

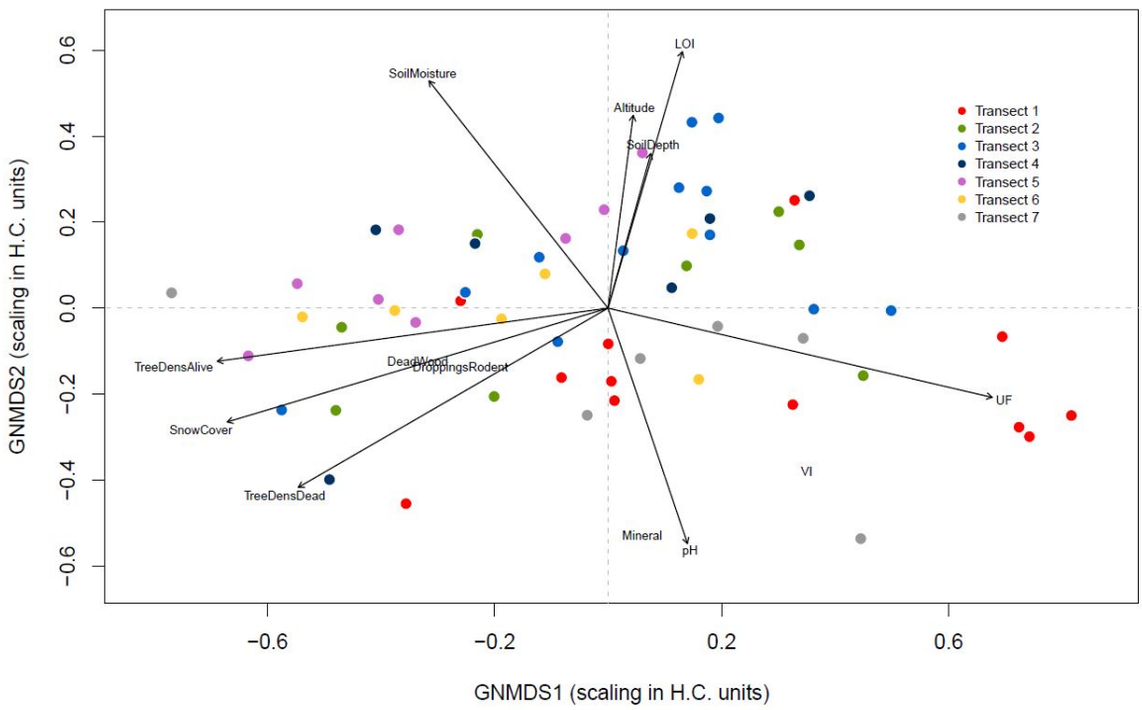

Figure 4.16: Biplot with ordinations of GNMDS1 and GNMDS2, vectors showing maximum increase for all significant continuous environmental variables and variable names showing point of optimum for significant factor variables.

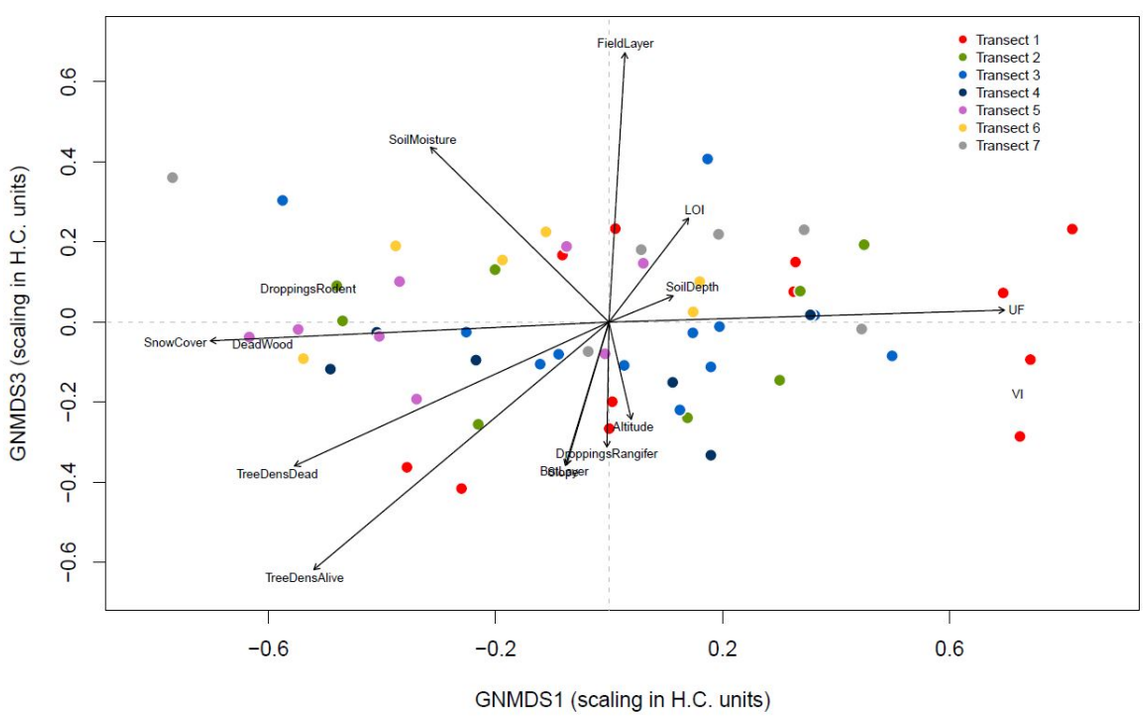

Figure 4.17: Biplot with ordinations of GNMDS1 and GNMDS3, vectors showing maximum increase for all significant continuous environmental variables and variable names showing point of optimum for significant factor variables. Variables “BotLayer” and “Slope” are overlapping in the figure.

Figures 4.18–4.29 show biplots with isoline diagrams for some of the significant environmental variables related to the GNMDS axes. Figures 4.27 and 4.29 show details on cover values for *E. nigrum* in the FieldLayer variable and for *P. juniperinum* in the BotLayer variable. Risk of severe drought (UF) (figure 4.18) shows a strong pattern along the first axis. pH (figure 4.19) show a pattern along the second axis. The variation within the variable expresses small changes in pH, ranging from 3.1 – 3.8. Soil depth (figure 4.20) show higher values towards high values of GNMDS2, but does not show a strong pattern related to the variation in the axis.

Snow cover (figure 4.21) explains a lot of the variation along the first axis, ranging from high snow cover to low snow cover along the axis. Loss on ignition (LOI) (figure 4.22) had very little variation within the variable, with most plots containing > 90% organic matter. It does however show a sorting of the variable along the second axis, and the highest LOI values (>95%) are contained in the plots situated in Peat heath (T3-C-14) at higher values of GNMDS2. Soil moisture (figure 4.23) show little variation within the soil samples as discussed in section 3.1.3, with most samples containing >72 % soil moisture. Comparing the variation in SoilMoisture variable to the LOI variable in figure 4.21, there are similarities in the variation, where plots with high LOI also have high soil moisture. Tree density of alive and dead trees (figure 4.24 and 4.25) show a very clear pattern with reference to variation explained by the first axis. Both variables vary from higher tree cover towards the lower values of GNMDS1 and decrease towards higher values along the axis. The two variables were measured on the same scale, and the isolines show that forest plots have more alive trees (ranging up to 182) than dead trees (ranging up to 81).

The field layer variable (figure 4.26) show variation related to GNMDS3. Values for the field layer variable expressed through cover values of *Empetrum nigrum* on a 0-10 scale along the axis show how the field layer variable varies with the cover of *Empetrum nigrum*. Higher values of GNMDS3 have a larger cover of *Empetrum nigrum*. This plot also shows how *Empetrum nigrum* varies from very low cover in forest plots towards low values of GNMDS1, to high cover and frequency towards higher ends of the gradient expressing areas without tree cover. The bottom layer variable (figure 4.28) does not have a strong variation along any of the axes, but shows tendencies of higher values towards lower parts of GNMDS3. Values for the bottom layer variable is expressed with cover values of *Polytrichum juniperinum* on a 0-10 scale along the axes in figure 4.29. It shows a tendency of higher cover values in areas with high values of the bottom layer variable. Comparing the cover of *P. juniperinum* in figure 4.29 to the cover of *Empetrum nigrum* in figure 4.27, one can see that there is a transition from areas of maximum cover of *P. juniperinum* to areas with maximum cover of *E. nigrum*.

4.7.1 Biplots for significant variables of GNMDS1 and GNMDS2

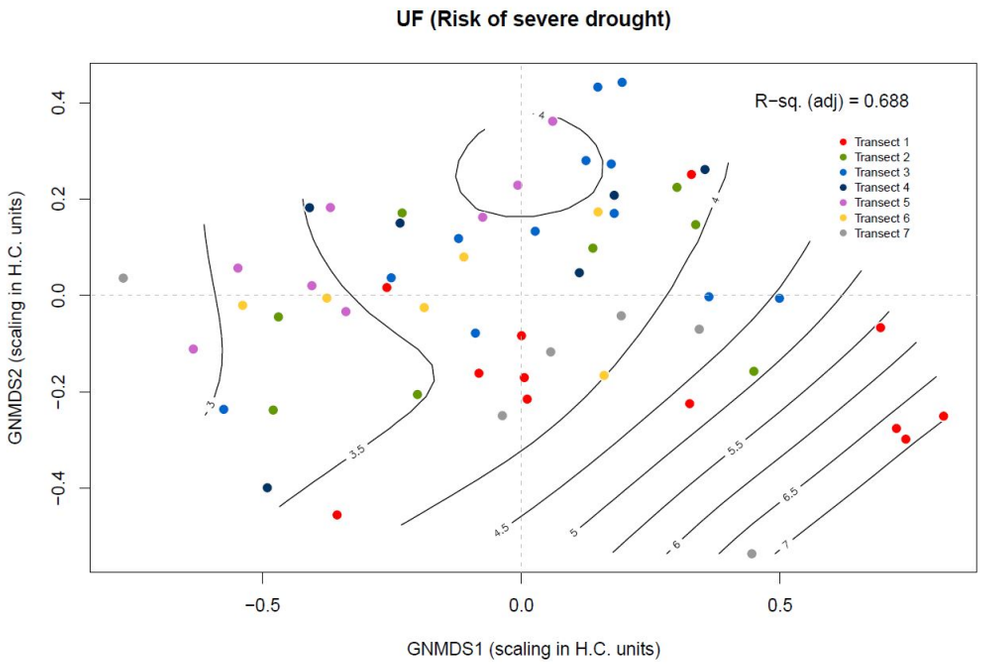

Figure 4.18: Biplot with ordinations of GNMDS1 and GNMDS2 and isolines representing UF (Risk of severe drought). Isoline values indicate UF on a 1–7 scale, increasing towards the higher end of GNMDS1

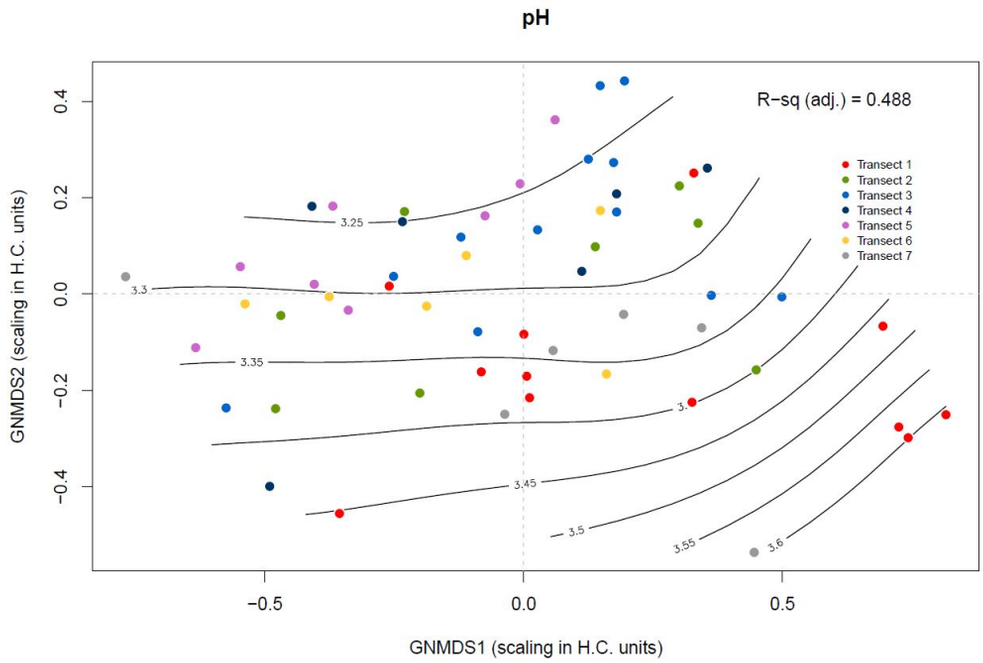

Figure 4.19: Biplot with ordinations of GNMDS1 and GNMDS2 and isolines representing pH. Isoline values indicate pH–value, increasing towards the lower end of GNMDS2.

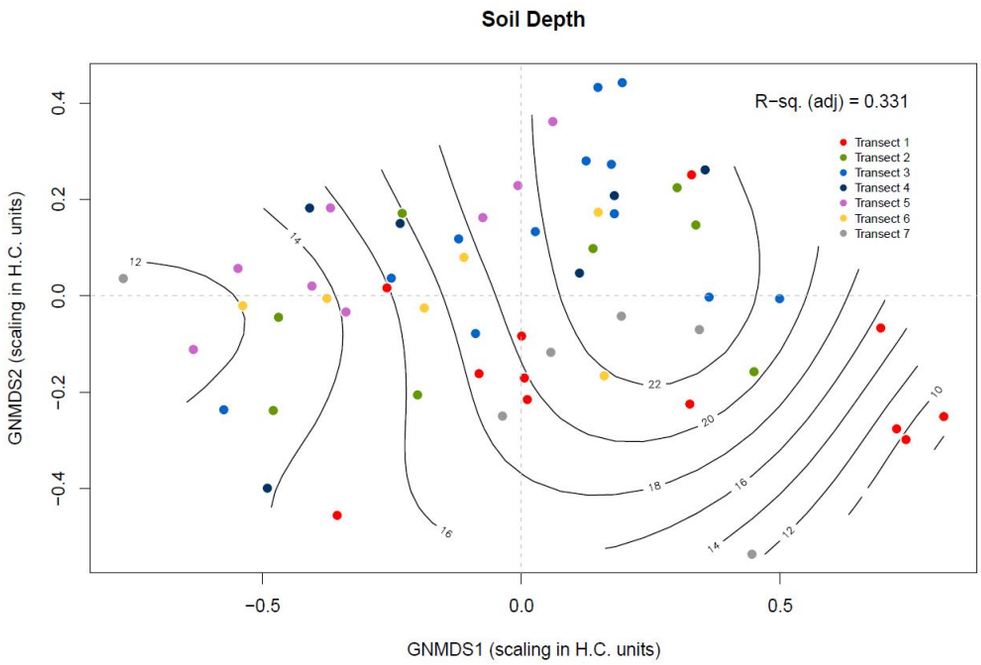

Figure 4.20: Biplot with ordinations of GNMDS1 and GNMDS2 and isolines representing soil depth. Isoline values indicate soil depth in cm, increasing towards the higher end of GNMDS2.

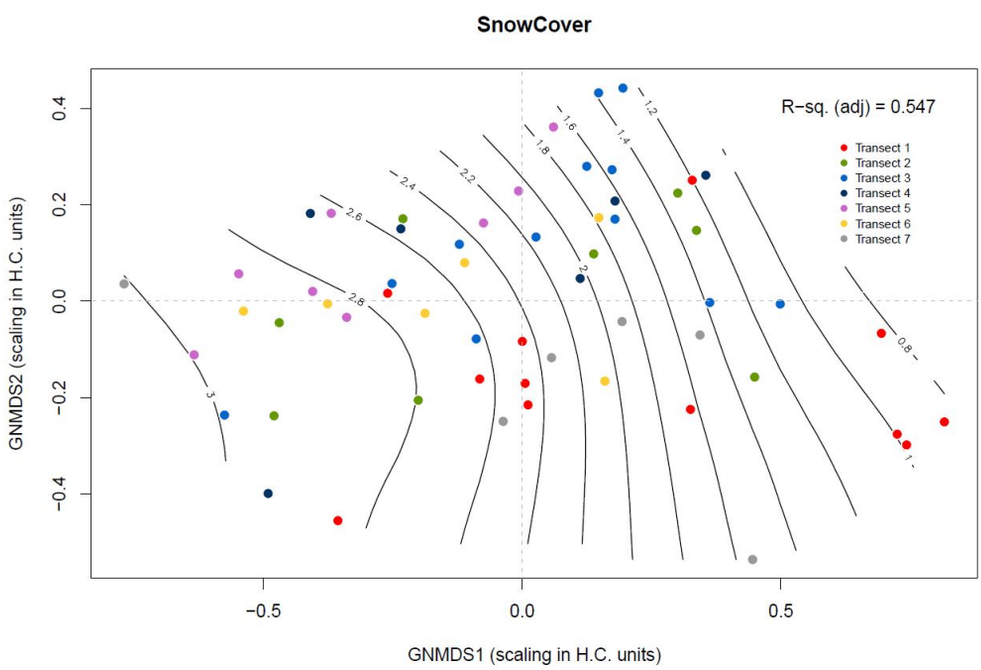

Figure 4.21: Biplot with ordinations of GNMDS1 and GNMDS2 and isolines of snow cover. Isoline values indicate snow cover on a 1–6 scale, increasing towards the lower end of GNMDS1 and higher end of GNMDS2.

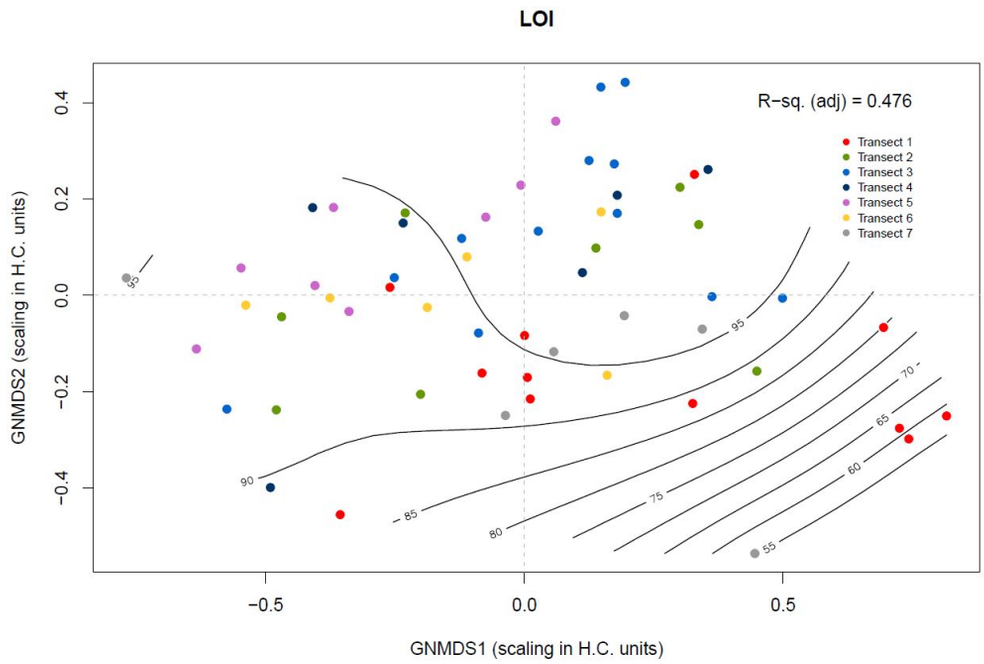

Figure 4.22: Biplot with ordinations of GNMDS1 and GNMDS2 and isolines representing LOI (Loss on ignition). Isoline values indicate LOI in percent, increasing towards the higher end of GNMDS1 and GNMDS2.

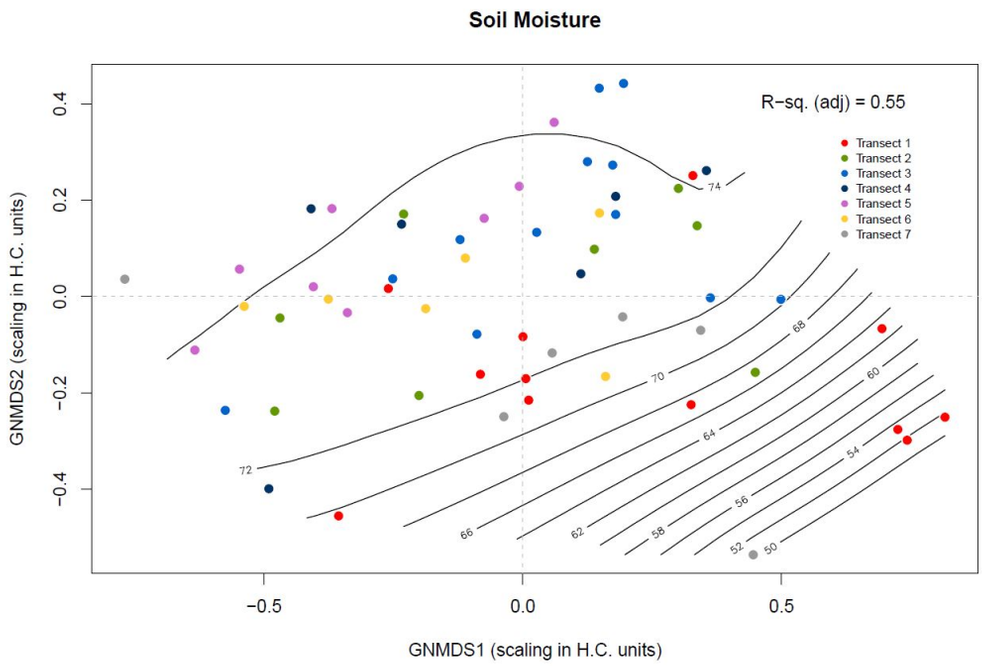

Figure 4.23: Biplot with ordinations of GNMDS1 and GNMDS2 and isolines of soil moisture. Isoline values show soil moisture in percent, increasing towards the lower end of GNMDS1 and higher end of GNMDS2.

4.7.2 Biplots for significant variables of GNMDS1 and GNMDS3

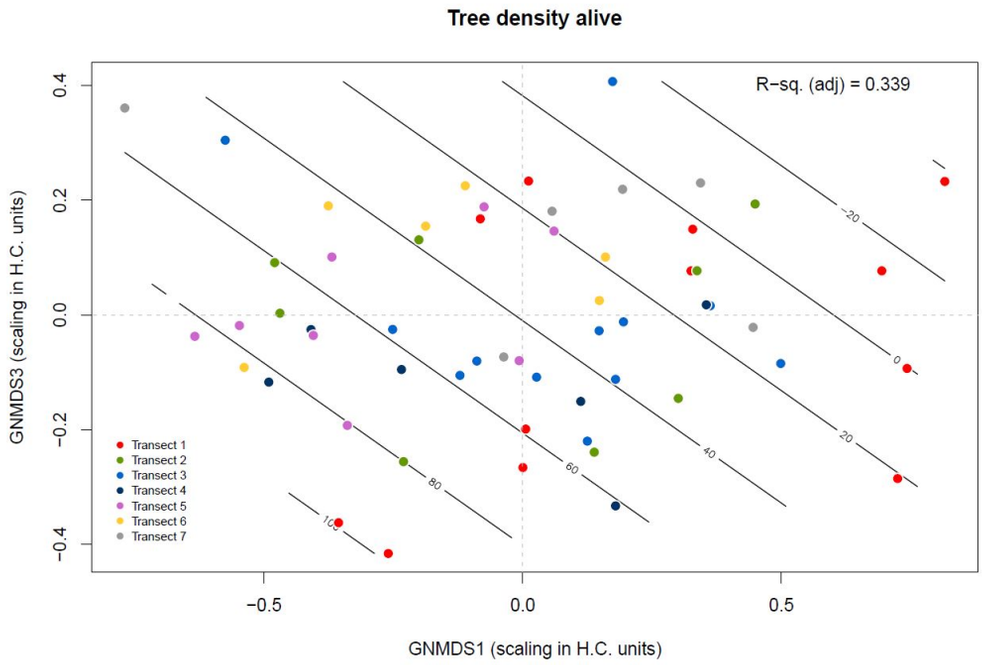

Figure 4.24: Biplot with ordinations of GNMDS1 and GNMDS3, and isolines representing tree cover density of alive tree branches. Isoline values indicate cover on a 0–96 scale, increasing towards the lower end of GNMDS1 and the lower end of GNMDS3

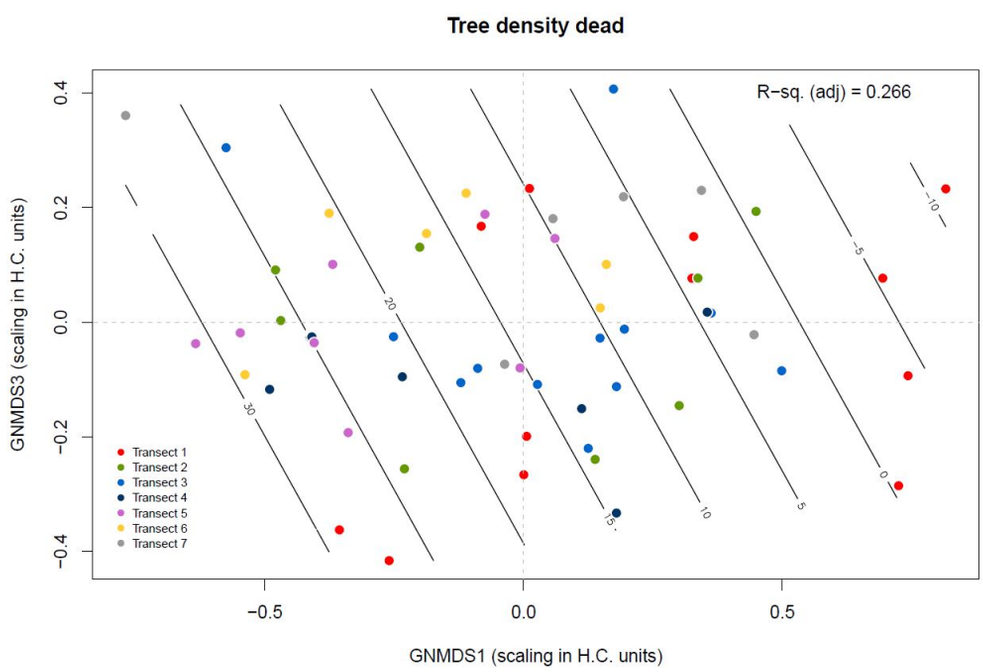

Figure 4.25: Biplot with ordinations of GNMDS1 and GNMDS3, and isolines representing tree cover density of dead tree branches. Isoline values indicate cover o a 0–96 scale, increasing towards the lower end of GNMDS1.

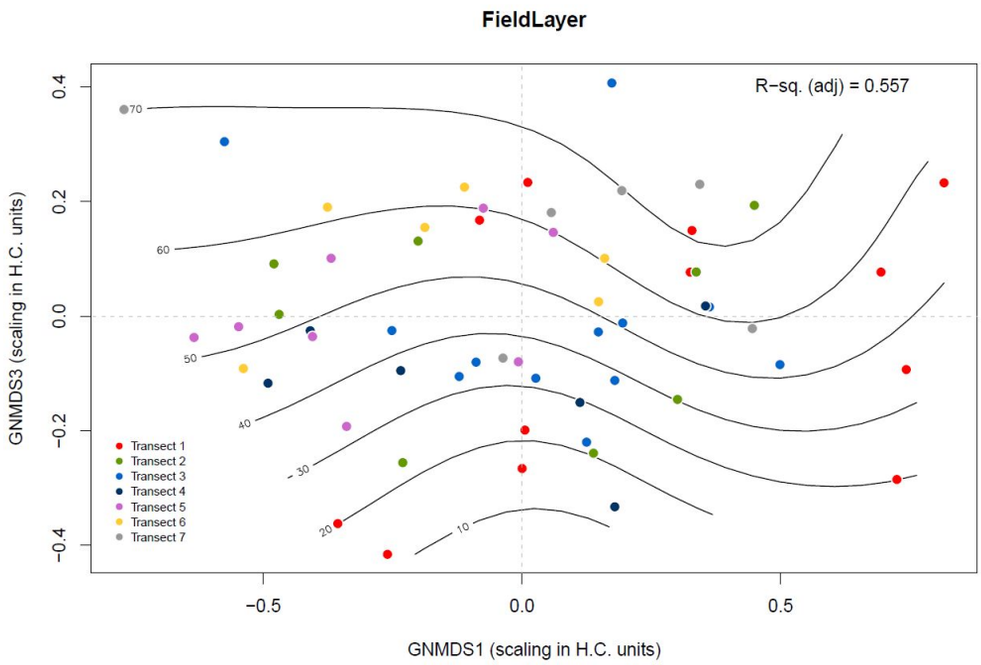

Figure 4.26: Biplot with ordinations of GNMDS1 and GNMDS3 and isolines representing Field layer. Isoline values indicate Field layer cover of vascular plants in a plot in percent, increasing towards the high end of GNMDS3.

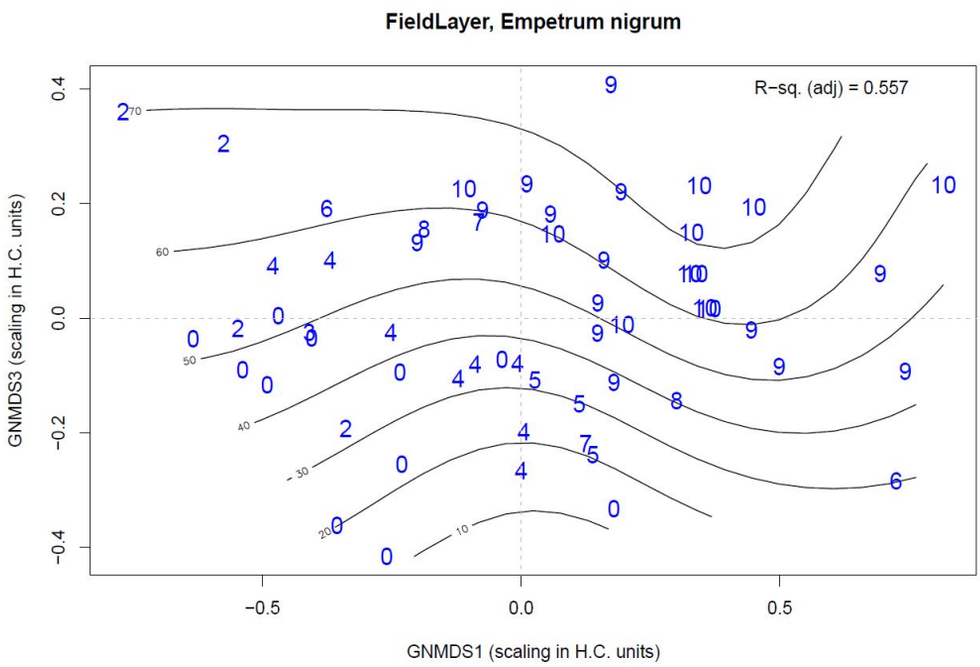

Figure 4.27: Isoline diagram with isolines representing FieldLayer and values for cover of *E. nigrum* in each plot for the ordination on a 0–10 scale. Increasing towards the high end of GNMDS3.

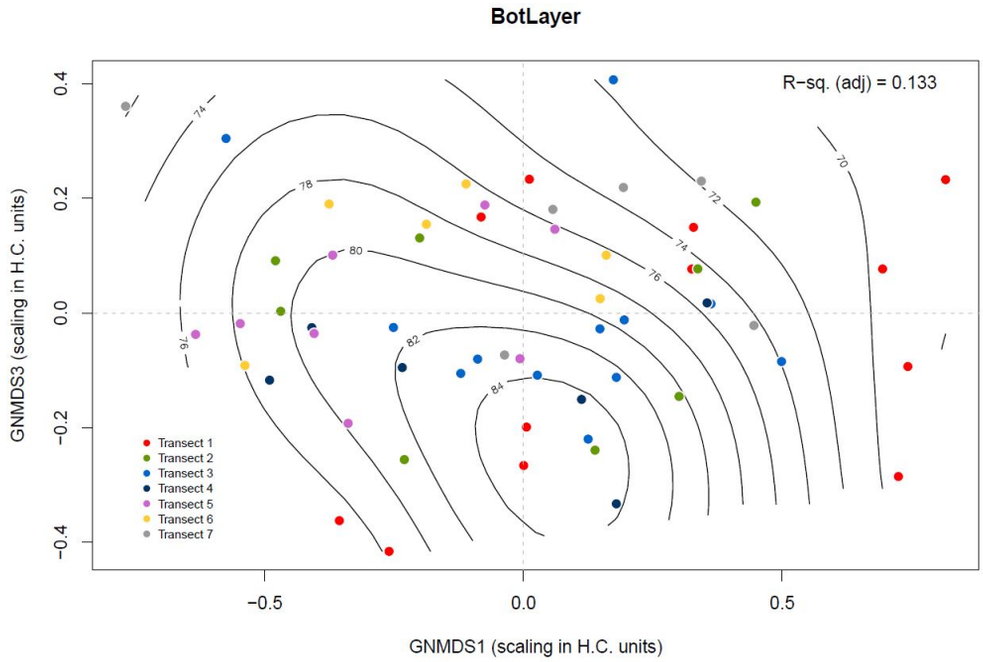

Figure 4.28: Biplot with ordinations of GNMDS1 and GNMDS3, and isolines representing Bottom layer cover. Isoline values indicate cover of bottom layer coverage of bryophytes and lichen in a plot in percent, decreasing towards the high end of GNMDS3.

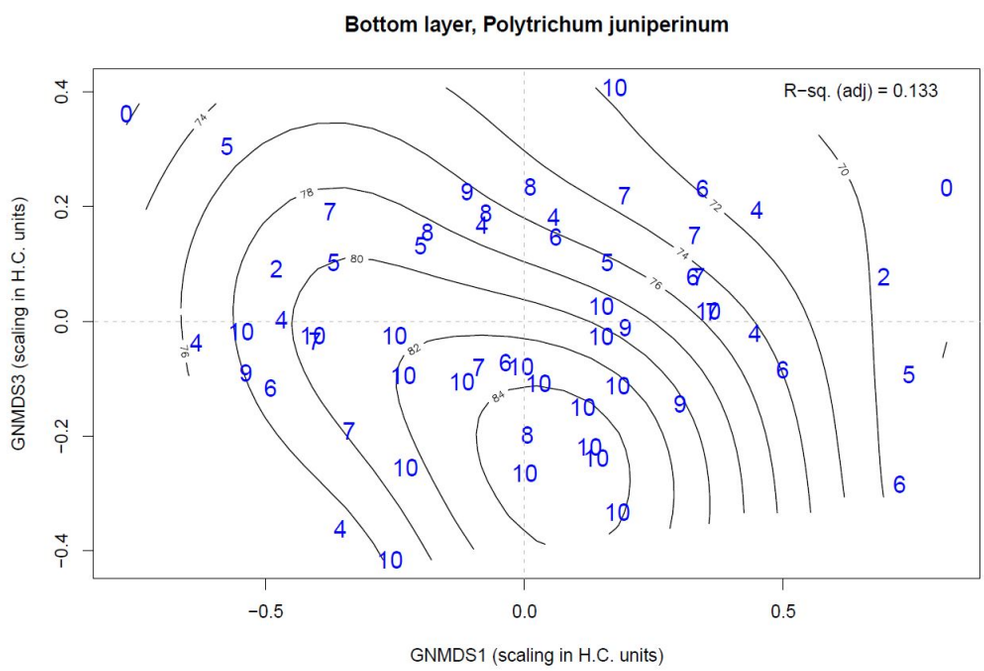

Figure 4.29: Isoline diagram with isolines representing BotLayer and values for cover of *P. juniperinum* in each plot for the ordination on a 0–10 scale. Decreasing towards the high end of GNMDS3

4.8 Standardized semivariograms

Standardized semivariograms for the three GNMDS axes and some of their significant environmental variables are included in figures 4.30–4.32. Semivariograms for all significant variables can be found in Appendix 13.

The semivariograms present variation within the GNMDS axes and environmental variables as a function of distance intervals, presented on a log2–scale. Starting distance for the semivariograms is set to 2 because of a lack of data at shorter distances, creating a large confidence interval at small distances. The vertical grey line distinguishes within-transect variation from between transect variation. The semivariance is the measure of spatial dependency of a variable between two plots. High semivariance suggest that the two observations have very different values, and low semivarance suggest that they have very similar values. We expect near objects to have similar values, i.e. low semivariance and further objects to have different values, i.e. high semivariance. If this is the case, we have spatiall dependence.

The semivariograms for the GNMDS axes how that the axes express variation on different spatial scales. GNMDS1 (figure 4.30) expresses spatially dependent variables within transects, while does not express spatial dependence at distances between transects. The second gradient (figure 4.31) expresses spatially dependent variation an an even smaller scale, expressing differences between plots at very short distances. GNMDS3 (figure 4.32) expresses spatially dependendent variation on a larger scale than the other axes.

5

Discussion

5.1 Interpretation of ordinations

5.1.1 Evaluation of ordination methods

The overall structure of the ordinations and the significant correlations between DCA and GNMDS axes indicate that the same underlying structure is captured in both methods for the first axes. The second GNMDS axis has a weak correlation with DCA2 ($|\tau| = 0.35$), but DCA2 has a stronger correlation to GNMDS3 ($|\tau| = 0.43$). The third GNMDS axis is also affirmed by DCA4. DCA3 is not affirmed by any of the GNMDS axes.

As DCA axes are extracted by decreasing amount of variation explained, it is interpreted as sign of weakness for the DCA ordination that variation explained by the fourth axis is confirmed by GNMDS, but the third axis is not. The DCA axes did not show a tongue effect (Minchin, 1987), a common cause of the detrending effect in the DCA process causing a distortion of the data. The distinct correlations of GNMDS2 and GNMDS3 to DCA4 make it clear that all three GNMDS axes express variation that is affirmed by DCA. For these reasons, a three–dimensional GNMDS was used as the basis for interpretation.

5.1.2 Identification and interpretation of gradients

Based on patterns and strong correlations in the ordinations, three distinct gradients were identified. These patterns point to an underlying structure in the dataset that is associated with a selection of the recorded environmental variables.

1) Main gradient: from forest to exposed ridges

GNMDS1 represents the main coenocline in the ordination of the dataset and expresses the variation from plots in woodland, via open heath to exposed ridges. This axis describes a well-known complex-gradient in the NiN-system, expressing variation from forest plots with less risk of severe drought (F) and longer lasting snow cover, and the transition towards the end point of the LEC risk of severe drought (UF) where wind-mediated disturbance intensity (VI) takes over in treeless areas on exposed ridges that are free of snow during large parts of the year. Terrestrial peatland plots are placed at the middle of this axis, with Peat forest plots placed slightly farther to the lower part of the axis due to tree cover.

This complex-gradient is known in Fennoscandian literature as one of the two determining gradients determining variation in forest and alpine vegetation, in addition to lime-richness (KA) (Økland & Bendiksen, 1985). The correlation to snow cover is related to the variational pattern that an uneven snow cover has on vegetation (Økland & Bendiksen, 1985). The duration of snow cover affects reduction of soil moisture through transpiration as affected by winds. A stable snow cover during winter has an insulating effect making extreme cold and freeze thawing events in the soil less likely to occur (Økland & Bendiksen, 1985). The snow cover also directly affects the vegetation by shortening the growing season, where extreme variations exist in snow beds (T7) (Økland & Bendiksen, 1985).

Evaluating the spatial structure of GNMDS1 and its significantly correlated environmental variables, there is a strong fine–scale (within transect) spatial structure for pH, TreeDensDead and TreeDensAlive. The spatial structure for TreeDensAlive is stronger than that for TreeDensDead at fine scales.

2) Second gradient: peat producing ability

The second gradient expresses the variation from areas with no peat accumulation to areas with a peat producing ability. A large and complex set of environmental variables are responsible for peat accumulation, encompass-

ing soil acidity (pH), peat depth, soil moisture and amount of organic matter, among other factors. The peat accumulating areas investigated reflected a very acidic environment, which is related to precipitation from rainwater and decomposition of organic matter (Joosten et al., 2017). Although there was no correlation between LOI and pH in this study, as one might assume as the decomposition of organic matter results in an acidic environment (Joosten et al., 2017). A possible cause for this is that both variables showed a small variation between samples.

This gradient in species composition may be due to a variation in species abundances in depressions between hummocks, and livermosses such as *L. ventricosa* and *C. neesiana* dominated. In addition, *E. nigrum* and *P. juniperinum* dominated to a large extent in the peat producing areas compared to plots in forest and on exposed ridges. Evaluating figure 4.8 that sorts plots along GNMDS2 according to nature type, there is no clear differentiation between plots of heath with peat accumulation (T3–C–21) and plots of heath without peat accumulation (T3–C–2) along the axis. The gradient does however express an increase in soil depth. The lack of distinction between these nature types is likely caused by there only being three plots with heath without peat accumulation. The data are not sufficient to make concluding remarks about the differentiation in species composition between heath with and without peat accumulation. The data does however indicate that the studied heath with peat accumulation has a species composition that is similar to heath without peat accumulation on soil with low calcium levels (KA b).

On bog (V3) there is a large fine–scale variation in dominating species, mainly livermosses, lichen and *Sphagnum* spp. The main difference in species richness on our peat accumulating areas and on bogs, was the lack of *Sphagnum* spp. and other species requiring high amount of moisture. In bogs, *Sphagnum* spp. produces the organic material that accumulates in an area. This attest to the fact that this gradient expresses terrestrial peat accumulation.

The distribution of *P. juniperinum* is affected by microtopography, moisture and light access, preferring flat areas, slopes and micro depressions (Shafigullina & Karzhavkina, 2018). It is adapted to open, dry and sandy environments, and grow on a variety of peatlands and especially on drained habitats (Lappalainen, Huttunen, Suokanerva, & Lakkala, 2010). In general, *Polytrichum* spp. inhabit exposed and disturbed areas to a larger degree than other moss species (Mäkipää & Heikkinen, 2003). According to (Groeneveld, Massé, & Rochefort, 2007) *P. juniperinum* can act as a nurse plant and cause a promotion of vascular plant seed growth.

Table 3.1 shows the ranges of the altitude variable for each transect. The Altitude variable is unevenly distributed and has higher values towards transects 1–5,

which are located at altitudes 20–30 meters higher than transect 6 and 7. However, within each transect forest plots were located at lower altitudes than the plots with peat accumulation. This is likely the reason why this variable is correlated with the axis. The TE gradient is defined as:

3) Third gradient: a gradient in *Empetrum nigrum* dominance

The third gradient expresses variation in species composition in relation to the presence of *E. nigrum*. The FieldLayer variable expresses the total cover of vascular plants in each plot in percent. In figure 4.20, isolines for field layer is plotted with sub–plot frequency and cover values for *E. nigrum* for each plot. This figure shows a tendency of less *E. nigrum* along lower parts of GNMDS3 where FieldLayer values are low, and more at higher values of the axis. It is evident from the data that high sub–plot frequency and cover values for *E. nigrum* relate to high values of the FieldLayer variable. *E. nigrum* was not present in forest areas, likely due a regime shift as a response to geometrid moth outbreaks. In these areas *A. flexuosa* dominated and contributed to high Field Layer values in some plots, as explained in section 2.2.2.

The ability of *E. nigrum* to act as a niche constructor has been thoroughly documented (e.g. K. Bråthen, González, & Yoccoz, 2017; K. A. Bråthen, Fodstad, & Gallet, 2010; González et al., 2015). Its allelopathic effects impact the surrounding vegetation specifically by producing and releasing phytotoxic biochemicals that inhibit growth and establishments of other vascular plants (González et al., 2019). Humus from tundra dominated by *E. nigrum* has been shown to be infertile for seedlings of several herbaceous plants (K. A. Bråthen et al., 2010). In addition, withered leaves affect soil decomposition rates and habitability for other plants, and have been found to be as bioactive as green leaves (Pilsbacher, Lindgård, Reiersen, González, & Bråthen, 2021). During soil sample analyses for this study, the presence of *E. nigrum* leaves and roots were observed in many of the soil samples, some that were collected up to 15 cm below the surface (pers. obs. E.K. Plathe). This indicates that *E. nigrum* leaves may directly impact the soil biota below the surface.

E. nigrum is a key species in arctic alpine heath ecosystems. It also seems to be a key species in the studied peat producing systems, as it has traits that promote peat accumulation (K. Bråthen et al., 2017; K. A. Bråthen et al., 2010; Pilsbacher et al., 2021). Wardle, Bonner, and Barker (2002) found that *E. nigrum* has a negative impact on soil biota and soil microbial activity, causing decreased decomposition rates. This supports the theories on peat accumulation on heath discussed in Edvardsen et al. (1988), which concluded that *E. nigrum* is a causal factor of peat accumulation.

The bottom layer variable expresses the total cover of bryophytes and lichen in a plot in percent and is negatively correlated with this gradient. *E. nigrum* has a tendency to form dense mats (González, Lindgård, Reiersen, Hagen, & Bråthen, 2021), making it difficult for other species to establish among it. *E. nigrum* has also been shown to be resilient to strong winter damage (González et al., 2019) making it an even stronger competitor to other plants. During field work for this study, it became clear that areas with dense mats of *E. nigrum* lacked a bottom layer (pers. obs. E.K. Plathe), likely due to a combination of biochemicals and light deprivation.

Grazing by *R. tarandus* on *E. nigrum* is not common, although they have been shown to forage on new shoots in spring and early summer and sometimes feed on the berries (Iversen et al., 2014). According to K. A. Bråthen et al. (2010), *E. nigrum* thrives with some but not too much fertilization by *R. tarandus*. In cases of over–grazing, the plant can be destroyed by trampling (K. A. Bråthen et al., 2010). It is likely that the correlation of droppings from *R. tarandus* to GNMDS3 is a cause of randomness. The correlation is caused by a result of randomness and does not reflect a causal effect.

Variation in tree cover (TreeDensAlive) is described by GNMDS1 and may be a variable associated with this third axis due to the geometrid moth regime shift, causing forest plots to be almost completely lacking *E. nigrum*. The correlation to this axis could also be as a result of randomness.

5.1.3 Other possible gradients

Several variables were significantly correlated with the ordination axes, but some with low correlation values (τ <0.3). Of the 26 recorded environmental variables, some did not explain variation along any of the ordination axes, e.g. convexity (ConvV and ConvH), TotP and TotN.

There is also a chance that important explanatory variables that could potentially explain a lot of the underlying structure in the species data are lacking in the analysis.

5.2 Possible causes for peat accumulation and hummock formation

This study shows that several environmental factors contribute to terrestrial peat accumulation, and many of these factors are the same that contribute

to peat accumulation on wetland. The factors that cause and facilitate terrestrial peat accumulation are a part of a complex set of self-reinforcing processes.

Peat accumulation in the investigated systems is likely a slow process that has occurred over time and is still occurring. The low pH, high LOI combined with the presence of species such as *P. juniperinum* and *E. nigrum* that decrease rates of decomposition, attest to a slow decomposition rate. As described in Joosten et al. (2017) among others, environmental factors such as pH and soil moisture are important processes in peat accumulation. Soil moisture in the terrestrial peatland comes from rainwater, and our study shows that it can also be affected by horizontal water transport from nearby nature types. Registered hummock sizes and soil depths around the investigated transects, shows that hummock size increases towards transition zones to wetland. In addition, the large hummock sizes in the concave formation on the esker is likely due to higher soil moisture. The high acidity in the peatland is probably a result of several factors, including the supply of bases from rainwater and a poor bedrock and accumulation of acid production as a result of the decomposition of organic matter, which are all known factors that influence acidity in ombrotrophic bog. Rainwater is characterized by somewhat acidic properties due to the dissolution of CO_2 in the water (Joosten et al., 2017). Low pH influences the solubility and availability of nutrients, resulting in a poor species richness, as was observed on the terrestrial peatland and hummocks.

The intrinsic abilities of peat are important factors in the terrestrial peatland. According to (Joosten et al., 2017), peat has an insulating capability that enables the upper layer of hummocks and peat to be dry whilst maintaining a moist conditions further in. On a slope, water can be lost trough lateral waterflow, however the peat has an ability to retain waterflow, and peat accumulation therefore enlarges the water retention of the landscape (Joosten et al., 2017). This may be a contributing factor to the observed terrestrial peat accumulation formation on slopes in this study. The stratigraphy of terrestrial peatland and hummocks was not studied in detail in this study, however soil analyses revealed that the upper peat layer consists of *Polytrichum juniperinum*, *Empetrum nigrum* and likely other species that grow on the peat.

The hummocks investigated in this study lacked a prescence of *Sphagnum* spp., which have been attributed a central contributor to peat accumulation on wetland (Joosten et al., 2017). *Sphagnum* spp. has intrinsic slow decomposition rates, acting as a key species in hummock formation on bog and in mire (Joosten et al., 2017). The terrestrial peatland dominated of *P. juniperinum* seems to attest to the qualities of this moss as a peat accumulating species (e.g. Fenton, 1980).

Frost processes and hummock formation

Frost processes are likely a central part of the formation of hummocks on terrestrial peatland. Cracks in the peat similar to ice-wedges (see figure 4.5) and the occurrence of a palsa mire close to the study area suggest that there is localized, sporadic permafrost in Laggu. According to Turetsky, Wieder, Vitt, Evans, and Scott (2007) permafrost in Northern ecosystems can enhance internal drainage or result in increased saturation of soil layers. Deep seasonal freezing is enough to cause frost heave, mass wasting and frost sorting, causing the presence of phenomena that occur due to permafrost, such as patterned ground (Seppala, 1997). The signs of frost formation in the terrestrial peatland, suggest that sporadic permafrost or seasonal deep freezing have at some point affected the terrestrial peatland, and may still be affecting it.

I suggest that the formation hummocks is initiated by the process that is similar to what causes ice-wedges, as described in Kokelj et al. (2014). During winter, frost processes cause cracks in the peatland where snowmelt accumulate and refreeze in the spring, causing the cracks to largen. If the ground is frozen due to localized permafrost, the water is prevented from training into the terrain. A repeated refreezing and accumulation of water in these cracks will cause polygonal formations in the peat. This is a known frost affection than strengthens a hummock–depression structure through cryoturbation in mires (Joosten et al., 2017).

A series of self-reinforcing processes are proposed to be causing terrestrial accumulation peat in the hummocks. The depressions between hummocks make for a natural place for plant debris and other falloffs to accumulate. This causes limited light access for the plants growing in the depressions, which has a negative impact on bryophyte growth. The terrestrial peat accumulation that is dominated by *P. juniperinum* will be slower in depressions because of a slower bryophytes growth rates. Over time, this self-reinforcing process of decreasing decomposition rates and distribution of light access cause the hummocks to grow relative to the depressions. In addition, larger hummocks will accumulate more soil moisture due to the water retaining properties of peat, which cause an increase in peat accumulation rates. In addition, cold climate also facilitates slow decomposition rates (Joosten et al., 2017).

Snow cover has several functions when interacting with peatland. During the winter, a snow cover will function as an insulator prohibiting evapotranspiration from wind. During the snowmelt season, a thin or lacking snow cover will enable frost processes to occur in the soil. According to Seppala (1997), palsa formation on mire happens ideally with less than 20 cm snow cover, and not more than 80 cm of snow. This balance might also be a factor in terrestrial hummock formation. The snow cover variable (SnowCover) shows that most

of the Peat heath areas are free from snow in early spring, exposing them to rapid freezing and melting at these high latitudes. However, the areas in Peat forest and the Peat heath areas on transect 7 were still covered in snow.

Many characteristics identified in the investigated terrestrial peatland show similarities with ombrotrophic bog. Their water supply comes from rainwater, as is the case with bog. The large hummock formations in the southern end of transect 3 are likely a cause of a greater water supply from the nearby mire. The concave formation along transect 7 also indicate the importance of moisture conditions, where a larger accumulation of moisture might occur.

Special transect Transect 7 was situated on the north side of an esker with different sediment, with a steeper slope, larger hummock sizes and soil depths (see figure 4.31 and 4.32) than the other transects. The largest hummocks and deepest soil occurred in a concave landform on the esker.

The peat accumulation around transect 7 is likely a complex case caused by a combination of factors, such as its landform, sediment, moisture conditions, dominating wind direction, and snow cover which may be located here longer than in the other peat accumulating areas (supported by the SnowCover variable). Moisture conditions are likely larger in the concave formation of the esker as the landform can cause runoff from water to accumulate here. In addition, longer lasting snow cover will protect against loss of moisture trough evapotranspiration. It is likely that the concave formation on the esker accumulates higher soil moisture, which slows decomposition rates and causes more peat accumulation. In addition, the concave landform protects against erosion, which can be have eroding effect on peat (Joosten et al., 2017). High snow depth during winter increases insulation, as snow acts as a good insulator.

A self–reinforcing system: feedback mechanisms

Peat forest Although the identified gradients in this study showed that *Empetrum nigrum* has an important role in inducing peat accumulation, the species data from this study show that Peat forest has a low frequency of this evergreen shrub. It is unknown whether *E. nigrum* has never been present in these forest systems. One possibility is that the reoccurring mass outbreaks of geometrid moths in the 2000s and 2010s has caused *E. nigrum* to die out in woodland areas. If this is the case, bryophytes such as *Polytrichum juniperinum* might have enjoyed a growth boost as a result of greater access to light, causing an increased dominance in the Peat forest plots. Another possibility is that the peat accumulation in Peat forest systems has occurred without the presence of *E. nigrum*. In this case, the slow decomposition rates of *P. juniperinum* may have played the key part in slowing decomposition rates further. Comparing

soil depth and hummock size in Peat forest and Peat heath, both are higher in Peat heath plots where *E. nigrum* is present. Fenton (1980) investigated moss banks consisting of *P. alpestre* in Antarctica, a subspecies of *P. juniperinum* (Artsdatabanken, 2015), concluding that the intrinsic slow decomposition rates of *P. alpestre* was a contributing factor to the accumulation.

Holocene: Initial peat occurrence This study does not have the means to decide how peat accumulation initially occurred. However, several theories on peat accumulation have been proposed to have occurred after the last great ice age, during a cooling period after Holocene.

Localized permafrost are caused by permafrost maintained since the Little Ice Age (ca. 1600 to 1900), that have preserved by the insulative nature of dry surface peat (Turetsky et al., 2007).

A form of normal variation?
There is a possibility that peat accumulation is a normal phenomenon in nature at high latitudes. The reason they have not been discussed before is because the species composition resembles a lot like normal variation in the mountain, i.e. Arctic alpine heath and lee side (T3). The reason the areas in Laggu were discovered in the first place, was the hummock occurrence and extreme peat accumulation on convex landforms below the tree line.

Since this project was started, terrestrial peat accumulating areas has been observed in several areas in Finnmark. In addition to the locations in Laggu, a team of experts reviewing nature types in the NiN system observed many areas with peat accumulation and hummock formation in Finnmark in the summer of 2020 (Halvorsen, Arnesen, Eidesen, & Storeng, 2020). Ground hummock formation was also observed in the area around Skaidi in Repparfjord, Finnmark, in summer 2020 (pers. obs. G. Arnesen, E.K. Plathe). This points to the hypothesis that this phenomenon is not as uncommon as initially thought.

5.3 Comparisons with other studies

The peat accumulating areas in Laggu shares many traits with the terrestrial peatland *Empetrum*-heath investigated in Edvardsen et al. (1988).They observed heath build up on convex landforms at 5 to 100 meters above the sea that had low pH, high LOI (84–97 %) and a dominance of *E. nigrum*, similar to the terrestrial Peat heath studied here. Comparing species occurrences to those found on Peat heath in this study, there were several similarities, with both areas reflecting a poor species richness with a dominance of dwarf shrubs and high frequency of lichens. The studied areas in Edvardsen et al. (1988) did

not have hummock formation. In addition, there was only a few occurrences of *P. juniperinum*, and the peat was accumulated by a one or several other species.

Edvardsen et al. (1988) suggested that the terrestrial peat accumulation was a result of a cold and wet climate, retarded metabolism of the carbon supply through the main roots into the soil and possibly the allelopathic properties of *E. nigrum*. The identified environmental gradients in this study supports these claims. In addition, Edvardsen et al. (1988) hypothesizes that the lack of *Betula pubescens* is a cause of sea spray and wind caused by close proximities to the ocean. This is not the case in the studied terrestrial peatland in this area, as peat accumulation in woodland were identified, and the area is not affected by sea spray.

5.4 Implications for NiN

The results from this study indicate that further versions of NiN should recognize a Peat accumulating LEC in terrestrial systems similar to TE in wetland. This terrestrial peat-accumulating gradient is affected a complex set of environmental variables acting in a self-reinforcing manner. Factors that affect this terrestrial gradient are a cold climate, the intrinsic moisture retaining abilities of peat, species that affect decomposition rates such as the bryophyte *Polytrichum juniperinum*. This gradient is likely also affected by frost processes, possibly caused by locally sporadic permafrost. A gradient identifying the allelopathic dwarf shrub *Empetrum nigrum* was also identified. More research is needed to determine the environmental variables determining this complex-gradient and how it differs from TE in wetland.

A separation between heath with and without peat accumulation based on vegetational patterns was not identified in this study. The criteria for creating a separate major type in NiN were not fulfilled. Although the species composition does not call for a creation of a separate nature type, there are many factors that is separate the terrestrial peatlands ecologically from non-peat accumulating areas, and these traits should be captured by the NiN system.

If further research show that hummock formation causes an increase in species richness, a variable in the attribute table to describe degree of hummock formation might be a good way of describing this, that might call for the creating of a subordinate LEC (uLEC) that captures observable variation within a major type. It is associated with gradient length between 1 and 2 EDU within a major type (Halvorsen et al., 2016). In addition, it is necessary to determine whether terrestrial peatland with tree cover should be differentiated from terrestrial peat heath, as tree cover is an important structuring process in ecosystems.

5.5 Future studies

More research is needed to gain an understanding of the processes that account peat accumulation in terrestrial systems. Studies should focus on monitoring snow cover variation during the winter and recording soil moisture levels in throughout the year. Snow cover monitoring should ideally be conducted over several years to account for seasonal variation and may be recorded for example by the use of cameras. Detailed information on frost processes is needed to determine how frost processes affect terrestrial hummock formation and peat accumulation. Temperature recording of surface temperatures over a period of more than one year is suggested to evaluate the existence of permafrost.

A detailed study of the stratigraphy of the hummock is suggested to establish whether they can have an ice core similar to palsas, or if they freeze during winter months. In addition, a comparative study of terrestrial peatland in several locations in Finnmark and Troms county is suggested to cover regional variation within the systems.

6

Conclusion

Investigations of terrestrial peatland with and without tree-cover identified three distinct gradients. The main gradient was related to the variation from forest to exposed ridges. The second gradient was related to peat producing ability, moving from areas of low soil depth, LOI, soil moisture and high pH. The second gradient was a gradient based on the degree of *Empetrum nigrum*, reflecting its allelopathic effects and its documented effects on lowering decomposition rates.

The study indicates that there exists a peat producing mechanism in terrestrial ecosystems in the sub-arctic zone. The accumulation process is reinforced by species that affect decomposition rates, in particular the bryophyte *P. juniperinum* and the dwarf shrub *E. nigrum*.

Regarding the NiN system, this study concludes that a local environmental complex-gradient (LEC) describing terrestrial peat accumulation similar to the existing LEC Peat accumulating ability (TE) in wetland systems should be recognized. More research is required to identify the environmental variables that cause peat accumulation and hummock formation. Ideally, the studies should be conducted in several locations with terrestrial peat accumulation in Finnmark and Troms. Detailed investigations of frost processes and permafrost is be crucial to explain this process.

References

Ammunét, T., Kaukoranta, T., Saikkonen, K., Repo, T., & Klemola, T. (2012). Invading and resident defoliators in a changing climate: cold tolerance and predictions concerning extreme winter cold as a range-limiting factor. *Ecological Entomology*, *37*(3), 212–220. doi: 10.1111/j.1365-2311.2012.01358.x

Artsdatabanken. (2015). *Artsnavnebasen; norsk taksonomisk database.* Retrieved 01.02.2021, from http://www.artsportalen.artsdatabanken.no/

Barristi, C., Poeta, G., & Fanellu, G. (2016). *An introduction to disturbance evology* (U. Förstner, W. H. Rulkens, & W. Salomons, Eds.). Springer.

Bråthen, K., González, V., & Yoccoz, N. (2017). Gatekeepers to the effects of climate warming? niche construction restricts plant community changes along a temperature gradient. *Perspectives in Plant Ecology, Evolution and Systematics*, *30*, 71–81. doi: 10.1016/j.ppees.2017.06.005

Bråthen, K. A., Fodstad, C. H., & Gallet, C. (2010). Ecosystem disturbance reduces the allelopathic effects of empetrum hermaphroditum humus on tundra plants. *Journal of Vegetation Science*, *21*(4), 786–795. Retrieved from http://www.jstor.org/stable/40925532

Bryn, A., Halvorsen, R., & Ullerud, H. A. (2018). *Hovedveileder for kartlegging av terrestrisk naturvariasjon etter nin (2.2.0): Report.*

Edvardsen, H., Elvebakk, A., Øvstedal, D. O., Prøsch-Danielsen, L., Schwenke, J. T., & Sveistrup, T. (1988). A peat-producing empetrum heath in coastal north norway. *Arctic and Alpine Research*, *20*(3), 299–309. Retrieved from http://www.jstor.org/stable/1551262 doi: 10.2307/1551262

European Space Agency (ESA). (2021). *The copernicus open access hub.* Retrieved 26.02.2021, from https://scihub.copernicus.eu/

Fenton, J. H. C. (1980). The rate of peat accumulation in antarctic moss banks. *Journal of Ecology*, *68*(1), 211–228. Retrieved from http://www.jstor.org/stable/2259252

Førland, E. J. (1993). *Nedbørnormaler. normalperiode 1961-1990: Report.*

Gisnås, K., Etzelmüller, B., Lussana, C., Hjort, J., Sannel, A. B. K., Isaksen, K., ... Åkerman, J. (2017). Permafrost map for norway, sweden and finland. *Permafrost and Periglacial Processes*, *28*(2), 359-378. Retrieved from https://onlinelibrary.wiley.com/doi/abs/10.1002/ppp.1922 doi: https://doi.org/10.1002/ppp.1922

Givens, D. I., de Boever, J. L., & Deaville, E. R. (1997). The principles, practices and some future applications of near infrared spectroscopy for predicting the nutritive value of foods for animals and humans. *Nutrition research reviews*, *10*(1), 83–114. doi: 10.1079/NRR19970006

González, V. T., Junttila, O., Lindgård, B., Reiersen, R., Trost, K., & Bråthen, K. A. (2015). Batatasin–iii and the allelopathic capacity of empetrum nigrum. *Nordic Journal of Botany*, *33*(2).

González, V. T., Lindgård, B., Reiersen, R., Hagen, S. B., & Bråthen, K. A.

(2021). Niche construction mediates climate effects on recovery of tundra heathlands after extreme event. *PLoS One*, *16*(2), e0245929. doi: 10.1371/journal.pone.0245929

González, V. T., Moriana-Armendariz, M., Hagen, S. B., Lindgård, B., Reiersen, R., & Bråthen, K. A. (2019). High resistance to climatic variability in a dominant tundra shrub species. *PeerJ*, *7*, e6967. doi: 10.7717/peerj.6967

Grime, J. (1979). Plant strategies and vegetation processes. , *68*.

Groeneveld, E. V. G., Massé, A., & Rochefort, L. (2007). Polytrichum strictum as a nurse-plant in peatland restoration. *Restoration Ecology*, *15*(4), 709-719. Retrieved from https://onlinelibrary.wiley.com/doi/abs/10.1111/j.1526-100X.2007.00283.x doi: https://doi.org/10.1111/j.1526-100X.2007.00283.x

Halvorsen, R. (2012). A gradient analytic perspective on distribution modelling. *Sommerfeltia*, *35*, 1-165. doi: 10.2478/v10208-011-0015-3

Halvorsen, R. (2016). Nin - typeinndeling og beskrivelsessystem for natursystemnivået. - natur i norge, article 3 (versjon 2.1.0). , 1–528.

Halvorsen, R., Andersen, T., Blom, H., Elvebakk, A., Elven, R., Erikstad, L., ... Ødegaard, F. (2009). Naturtyper i norge - teoretisk grunnlag, prinsipper for inndeling og definisjoner. *Naturtyper i Norge, version 1.0, article*, *1*, 1-210.

Halvorsen, R., Arnesen, G., Eidesen, P. B., & Storeng, A. B. (2020). Ninnot196: referat av observasjoner og diskusjoner på ekskursjonen til nins arktiske faggruppe til øst-finnmark 24.–30. august 2020. *not published*.

Halvorsen, R., Bryn, A., & Erikstad, L. (2016). Nin systemkjerne - teori, prinsipper og inndelingskriterier. versjon 2.2. *Systemdokumentasjon 1*, 1–292.

Halvorsen, R., Økland, T., & Rydgren, K. (2001, 01). Vegetation-environment relationships of boreal spruce swamp forests in Østmarka nature reserve, se norway. *Sommerfeltia*, *29*, 1-190.

Halvorsen, R., Skarpaas, O., Bryn, A., Bratli, H., Erikstad, L., Simensen, T., & Lieungh, E. (2020). Towards a systematics of ecodiversity: The ecosyst framework. *Global Ecology and Biogeography*, *29*, 0–190.

Halvorsen, R., Wollan, A., Bryn, A., Bratli, H., & Horvath, P. (2021). Naturtypekart etter nin for området omkring veia (nedre eiker og Øvre eiker, buskerud). *NHM Rapport 100*, 1–120.

Hill, M. O. (1979). Decorana – a fortran program for detrended correspondance analysis and reciprocal averaging.

Hill, M. O., & Gauch, H. G. (1980). Detrended correspondence analysis: An improved ordination technique. *Vegetatio*, *42*(1/3), 47–58. Retrieved from http://www.jstor.org/stable/20145789

Horvath, P., Nilsen, A.-B., & Bryn, A. (2019). *Oppsett og tilrettelegging av qgis for nin naturtypekartlegging: Report*.

Iversen, M., Fauchald, P., Langeland, K., Ims, R. A., Yoccoz, N. G., & Bråthen, K. A. (2014). Phenology and cover of plant growth forms predict herbivore

habitat selection in a high latitude ecosystem. *PLoS One*, *9*(6), e100780. doi: 10.1371/journal.pone.0100780

Jensen, C. (2012). *Fortellinger fra langfjorden i gamvik kommune*. [Nervei]: C. Jensen.

Jepsen, J., Biuw, M., Ims, R. A., Kapari, L., Schott, T., Vindstad, O. P. L., & Hagen, S. B. (2013). Ecosystem impacts of a range expanding forest defoliator at the forest-tundra ecotone. *Ecosystems*, *16*(4), 561–575. doi: 10.1007/s10021-012-9629-9

Jepsen, J., Hagen, S., Høgda, K., Ims, R., Karlsen, S., Tømmervik, H., & Yoccoz, N. (2009). Monitoring the spatio-temporal dynamics of geometrid moth outbreaks in birch forest using modis-ndvi data. *Remote Sensing of Environment*, *113*, 1939–1947. doi: 10.1016/j.rse.2009.05.006

Johansen, K. S., Tandstad, H. R., Arnesen, G., & Finne, E. A. (2020). *Basiskartlegging av utvalgte verneområder i troms og finnmark: Report.*

Joosten, H., Tanneberger, F., & Moen, A. (Eds.). (2017). *Mires and peatlands of europe: Status, distribution and conservation*. Stuttgart, Germany: Schweizerbart Science Publishers.

Karlsen, S. R., Jepsen, J. U., A., O., Ims, R. A., & Elvebakk, A. (2013). Outbreaks by canopy-feeding geometrid moth cause state-dependent shifts in understorey plant communities. *Oecologica*(173), 859–870. doi: 10.1007/s00442-013-2648-1

Kartverket. (2021). *Høydedata*. Retrieved from `https://www.kartverket.no/`, `https://hoydedata.no/LaserInnsyn/` (Accessed: 2021-03-20)

Økland, R. H. (1990). Vegetation ecology: theory, methods and application with reference to fennoscandia. *Nordic Journal of Botany*, *11*(4), 458-458. Retrieved from `https://onlinelibrary.wiley.com/doi/abs/10.1111/j.1756-1051.1991.tb01247.x` doi: https://doi.org/10.1111/j.1756-1051.1991.tb01247.x

Kokelj, S. V., Lantz, T. C., Wolfe, S. A., Kanigan, J. C., Morse, P. D., Coutts, R., ... Burn, C. R. (2014). Distribution and activity of ice wedges across the forest-tundra transition, western arctic canada. *Journal of Geophysical Research: Earth Surface*, *119*(9), 2032-2047. Retrieved from `https://agupubs.onlinelibrary.wiley.com/doi/abs/10.1002/2014JF003085` doi: https://doi.org/10.1002/2014JF003085

Køste, R. (2006). *En søring nordpå: fra gjenreisingstida og brakkeliv i telegrafverket*. Kongsvinger: Norsk Telemuseum.

Kristiansen, J. N. (2006). Myrer og våtmarksundersøkelser - vurdering av langfjorddalen - gamvik kommune. *RAPPORT, Fylkesmannen i Finnmark, Miljøvernavdelingen*, *4*, 1–22.

Kruskal, J. B. (1964a). Multidimensional scaling by optimizing goodness of fit to a nonmetric hypothesis. *Psychometrika*, *29*(1), 1–27. doi: 10.1007/BF02289565

Kruskal, J. B. (1964b). Nonmetric multidimensional scaling: A numerical method. *Psychometrika*, *29*(2), 115–129. doi: 10.1007/BF02289694

Lappalainen, N. M., Huttunen, S., Suokanerva, H., & Lakkala, K. (2010). Seasonal acclimation of the moss polytrichum juniperinum hedw. to natural and enhanced ultraviolet radiation. *Environmental Pollution*, *158*(3), 891-900. Retrieved from https://www.sciencedirect.com/science/article/pii/S0269749109004680 doi: https://doi.org/10.1016/j.envpol.2009.09.017

Lemmon, P. E. (1956). *A sperical densiometer for estimating forest overstory density: Report.*

Lilleøren, K. S., Etzelmüller, B., Schuler, T. V., Gisnås, K., & Humlum, O. (2012). The relative age of mountain permafrost — estimation of holocene permafrost limits in norway. *Global and Planetary Change*, *92-93*, 209-223. Retrieved from https://www.sciencedirect.com/science/article/pii/S0921818112000999 doi: https://doi.org/10.1016/j.gloplacha.2012.05.016

Lovdata. (2007). *Forskrift om verneplan for rik løvskog i finnmark. vedlegg 9. fredning av langfjorddalen/laggu naturreservat, gamvik og lebesby kommuner, finnmark.*

Minchin, P. (1987). An evaluation of the relative robustness of techniques for ecological ordination. *Plant Ecology*, *69*, 89–107. doi: 10.1007/BF00038690

Mäkipää, R., & Heikkinen, J. (2003, 08). Large-scale changes in abundance of terricolous bryophytes and macrolichens in finland. *Journal of Vegetation Science*, *14*, 497 - 508. doi: 10.1111/j.1654-1103.2003.tb02176.x

Moen, A. (1999). *National atlas of norway: Vegetation*. Hønefoss: Statens kartverk.

Murguzur, F. J. A., Bison, M., Smis, A., Böhner, H., Struyf, E., Meire, P., & Bråthen, K. A. (2019). Towards a global arctic-alpine model for near-infrared reflectance spectroscopy (nirs) predictions of foliar nitrogen, phosphorus and carbon content. *Scientific Reports*, *9*(1), 8259. doi: 10.1038/s41598-019-44558-9

NGU. (2017a). *Berggrunnskart: Nasjonal berggrunnsdatabase.* Norsk Geologisk Undersøkelse: Norsk Geologisk Undersøkelse, NGU. Retrieved 07.05.2021, from http://geo.ngu.no/kart/berggrunn/

NGU. (2017b). *Løsmasser: Nasjonal løsmassedatabase.* Norsk Geologisk Undersøkelse: Norsk Geologisk Undersøkelse, NGU. Retrieved 07.05.2021, from http://geo.ngu.no/kart/losmasse/

NIBIO. (2020). *Kilden - arealinformasjon: Reindrift: Årstidsbeite.* Kilden: NIBIO, Norsk institutt for bioøkonomi. Retrieved 19.01.2021, from https://kilden.nibio.no

Norsk klimaservicesenter. (2020). *Observasjoner og værstatistikk: Nedbørsnormaler.* Retrieved 17.02.21, from https://seklima.met.no/observations/

Økland, R. H., & Bendiksen, E. (1985). The vegetation of the forest-alpine transition in grunningsdalen, s. norway. *Sommerfeltia*, *2*, 224.

Oksanen, J., Kindt, R., Legendre, P., O'Hara, B., Simpson, G. L., Solymos, P., ... Wagner, H. (2020, 11). vegan: Community ecology package [Computer software manual]. Retrieved from http://cran.r-project.org/, https://github.com/vegandevs/vegan (R package version 2.5-7)

Oksanen, P. (2006). Holocene development of the vaisjeäggi palsa mire, finnish lapland. *Boreas*, *35*(1), 81-95. doi: https://doi.org/10.1111/j.1502-3885.2006.tb01114.x

Olofsson, J., Ericson, L., Torp, M., Stark, S., & Baxter, R. (2011). Carbon balance of arctic tundra under increased snow cover mediated by a plant pathogen. *Nature Climate Change*, *1*(4), 220–223. doi: 10.1038/nclimate1142

Petit Bon, M., Böhner, H., Kaino, S., Moe, T., & Bråthen, K. A. (2020). One leaf for all: Chemical traits of single leaves measured at the leaf surface using near-infrared reflectance spectroscopy. *Methods in Ecology and Evolution*, *11*(9), 1061-1071. Retrieved from https://besjournals.onlinelibrary.wiley.com/doi/abs/10.1111/2041-210X.13432 doi: https://doi.org/10.1111/2041-210X.13432

Pilsbacher, A. K., Lindgård, B., Reiersen, R., González, V. T., & Bråthen, K. A. (2021). Interfering with neighbouring communities: Allelopathy astray in the tundra delays seedling development. *Functional Ecology*, *35*(1), 266–276. doi: 10.1111/1365-2435.13694

QGIS Development Team. (2021). Qgis geographic information system [Computer software manual]. Retrieved from http://qgis.osgeo.org

RCoreTeam. (2021). R: A language and environment for statistical computing [Computer software manual]. Vienna, Austria. Retrieved from https://www.R-project.org/

Seppala, M. (1997, 12). Distribution of permafrost in finland. *Bulletin of the Geological Society of Finland*, *69*, 87-96. doi: 10.17741/bgsf/69.1-2.007

Seppala, M. (2006, 01). Palsa mires in finland. *The Finnish Environment*, *23*.

Shafigullina, N., & Karzhavkina, E. (2018, 01). Productivity of polytrichum juniperinum hedw. in forest ecosystem of tatarstan. *IOP Conference Series: Earth and Environmental Science*, *107*, 012092. doi: 10.1088/1755-1315/107/1/012092

Sigmond, E. M., Bryhni, I., & Jorde, K. (2013). *Norsk geologisk ordbok*. Fagbokforlaget.

Sousa, W. P. (1984). The role of disturbance in natural communities. *Annual Review of Ecology and Systematics*, *15*(1), 353–391. doi: 10.1146/annurev.es.15.110184.002033

Tarnocai, C., & Zoltai, S. C. (1978). Earth hummocks of the canadian arctic and subarctic. *Arctic and Alpine Research*, *10*(3), 581–594. Retrieved from http://www.jstor.org/stable/1550681

Turetsky, M., Wieder, R., Vitt, D., Evans, R., & Scott, K. (2007, 09). The disappearance of relict permafrost in boreal north america: Effects on peatland carbon storage and fluxes. *Global Change Biology*, *13*, 1922 - 1934. doi: 10.1111/j.1365-2486.2007.01381.x

van Son, T. C., & Halvorsen, R. (2014). Multiple parallel ordinations: the importance of choice of ordination method and weighting of species abundance data. *Sommerfeltia*, *37*, 1 - 37.

Vitt, D., Halsey, L., & Zoltai, S. (1994, 02). The bog landforms of continental western canada in relation to climate and permafrost patterns. *Arctic and Alpine Research*, *26*, 1-13. doi: 10.2307/1551870

Vliet-Lanoë, B., & Seppala, M. (2002, 03). Stratigraphy, age and formation of peaty earth hummocks (pounus), finnish lapland. *Holocene*, *12*, 187-199. doi: 10.1191/0959683602hl534rp

Wardle, D., Bonner, K., & Barker, G. (2002). Linkages between plant litter decomposition, litter quality, and vegetation responses to herbivores. *Functional Ecology*, *16*, 585–595. doi: 10.1046/j.1365-2435.2002.00659.x

White, P. S. (1979). Pattern, process, and natural disturbance in vegetation. *The Botanical Review*, *45*(3), 229–299. doi: 10.1007/BF02860857

Appendix 1

Translations of NiN–terms used in this thesis. Translations for the NiN–system are described in Appendix Support information of Halvorsen R., et al (2020). For further details on terms see Halvorsen (2016) and Halvorsen et. al. (2016).

Norwegian term	English translation
Kalkinnhold (KA)	Lime Richness (KA)
Uttørkingsfare (UF)	Risk of severe drought (UF)
Vindutsatthet (VI)	Wind–mediated disturbance intensity (VI)
Lokal kompleks miljøvariabel (LKM)	Local environmental complex–variable (LEC)
Økologisk avstandsenhet (ØAE)	Ecological distance unit (EDU)
Basistrinn	Elementary segment
Tresatt areal	Woodland
Hovedtypegruppe	Major–type group
Hovedtype	Major type
Grunntype	Minor type
Landskapstype	Landscape type
Natursystem	Ecosystem level
Livsmedium	Microhabitat
T4 Fastmarkskogsmark	T4 Forest
T3 Fjellhei, leside og tundra	T3 Arctic–alpine heath and lee side
T14 Rabbe	T14 Exposed ridge
“Tueskog”	“Peat forest”
“Tuehei”	“Peat heath”
T7 Snøleie	T7 Snowbed
Mark	Ground
Torvproduserende evne (TE)	Peat producing ability (TE)
Vanntilførsel (VT)	Categories of prevaling water supply (VT)
Tørrleggingsvarighet (TV)	Duration of period without inundation (TV)
Myrflatepreg (MF)	Mire expanse character (MF)
Våtmarkssystem (V)	Wetland system (V)
Terrestrisk system(T)	Terrestrial system (T)
Hevdintensitet (HI)	Management intensity (HI)

References: Halvorsen, R., Skarpaas, O., Bryn a., et al. Towards a systematics of ecodiversity: The EcoSyst framework. Global Ecol Biogeogr. 2020; 1–20. https://doi.org/10.1111/geb.13164. Appendix Support information.

Halvorsen, R. (2016). NiN – typeinndeling og beskrivelsessystem for natursystemnivået. Natur i Norge, Article 3 (v 2.1.0), 1–528. Trondheim: Norwegian

Biodiversity Information Centre.

Halvorsen, R., Bryn, A., & Erikstad, L. (2016). NiNs systemkjerne: Teori, prinsipper og inndelingskriterier. Natur i Norge, Article 1 (v 2.1.0), 1–328. Trondheim: Norwegian Biodiversity Information Centre

Appendix 2 Details on recording of explanatory variables.

Variable	Abbreviation	Description
Aspect	Aspect	Aspect was measured from the middle of the plot and recorded in the direction of the dominant aspect. A Silva Compass Ranger was used. Aspect was expressed on a 0–360°scale.
Altitude	Altitude	Altitude data was extracted post fieldwork using plot coordinates from the NN2000 system, using hoydedata.com (2020).
Bottom layer	BotLayer	Percentage cover of mosses (bryophytes) and lichen.
Convexity (horizontal)	ConvH	A measure to describe the topography of a plot. A subjective unit estimated by observer. The scale used ranged from –2 to +2, where –2 corresponded to strongly concave and +2 corresponded to strongly convex topography, applied in the horizontal direction. Convexity was evaluated 1 m out from each side of a plot.
Convexity (vertical)	ConvV	Same scale as Convexity (horizontal) ranging from –2 to +2, applied in the vertical direction.
Dead Wood	DeadWood	presence/absence of dead wood (trees), e.g. broken tree stems or large branches.
Droppings reindeer	DroppingsRangifer	Frequency of droppings form reindeer (Rangifer tarandus) in each of the 16 subplots.
Droppings rodent	DroppingsRodent	Frequency of droppings from small rodents in each of the 16 subplots.
Field layer	FieldLayer	Percentage cover of vascular plants.
Lime richness	KA	Based on elementary segments in the LEC KA in the NiN–system. Two steps were registered: b and c. As 57 plots were registered as KA b and one plot KA c, the variable was not used in analyses. Uncertainty: subjective decisions.
Loss on ignition	LOI	Analyzed from soil samples to represent percentage of organic matter in the soil. Details on method can be found in Materials and methods, chp.. 3.1.3.
Microtopography (horizontal)	MirotopoH	Average horizontal microtopography. Detailed description in Materials and methods, chapter 3.1.3.
Microtopography (vertical)	MicrotopoV	Average vertical microtopography. Detailed description in Materials and methods, chapter 3.1.3.
Mineral cover	Mineral	Percent cover of loose rocks with a diameter > 6 cm in the plot.
pH	pH	Soil pH measured in distilled water. Detailed description in Materials and methods, chapter 3.1.3.
Risk of severe drought	UF	Based on elementary segments in the LEC UF in the NiN–system. Five steps were registered: c, d, e, f, g. In statical analyses they correspond to steps 3–6. Uncertainty: subjective decisions.
Slope incline	Slope	A BCA Slope Meter 20/21 clinometer was used to estimate inclination inside plots. A rod was placed along the slope and the clinometer was placed on it to measure average inclination.
Snow cover from the snow melting season of 2020.	SnowCover	Measure of snow cover on a 1–6 scale, based on Sentinel–2 satellite images
Soil depth	SoilDepth	A soil rod (jordbor) was used to measure soil depth in five positions in each plot. See description in Materials and Method chp.. 3.1.3.
Soil moisture	SoilMoisture	Percentage (%) of moisture in soil analyzed from soil moisture samples. See description in Materials and Method chp.. 3.1.3.
Total nitrogen	TotN	Total nitrogen analyzed from soil samples. See description in Materials and Method chp.. 3.1.3.
Total phosphorous	TotP	Total phosphorous analyzed from soil samples. See description in Materials and Method chp.. 3.1.3.
Tree cover density (alive trees)	TreeDensAlive	Density of living tree branches covering the area above a plot. Measured with a densitometer of 92 small quadrats measured facing east, west, north and south. See description in Materials and Method chp.. 3.1.3.
Tree cover density (dead trees)	TreeDensDead	Density of dead tree branches covering the area above a plot. Measured with a densitometer of 92 small quadrats measured facing east, west, north and south. See description in Materials and Method chp.. 3.1.3.
Wind–mediated disturbance intensity	VU	Based on elementary segments in the LEC VU in the NiN–system. Four steps were registered: 0, a, b, c. In statical analyses they correspond to steps 0–3. Uncertainty: subjective decisions.

Appendix 3 Formulas used for calculations of chemical soil analyses.

a) Percent loss on ignition:

$$LOI = \frac{\Delta Weight_{drymatter}}{Weight_{initial}} = \frac{W_S \tilde{} W_C}{W_S \tilde{} W_A} \times 100$$

where W_C is weight of cubicle, W_S is weight of cubicle and soil sample after drying, W_A is weight of cubicle and ash after combustion.

Calculations of total nitrogen and phosphorous:

b) Total nitrogen: $\frac{TotN}{LOI} \times 100$

c) Total phosphorous: $\frac{TotP}{LOI} \times 100$

where TotN and TotP is expressed in g/kg and LOI is expressed in percent.

d) Percent soil moisture: $Soilmoisture\% = S_w \tilde{} S_d \times 100$

where S_w is soil weight in g before drying and S_d is weight in g after drying.

Appendix 4 Details on soil depth and heap size measurements.

Grid:
• A grid was created with the corresponding transect as basis, choosing one of the plots as starting point.
• Perpendicular lines were measured using a compass 90°to each side of the transect.
• Each grid extended one measuring point further than the plots along the transect.

Soil depth:
• Soil depth was measured at 4 points surrounding each grid point.
• Two 2–meterstics were laid out in a cross to indicate point of measurements 1 meter from the center.

Maximum heap size:
• The largest heap within <2 meters of the measure point was measured.
• Only heaps ≥ 6 cm were recorded.
• A meterstick was kept at a 90°angle from the top of a heap to the lowest point beside it. The height difference was recorded.

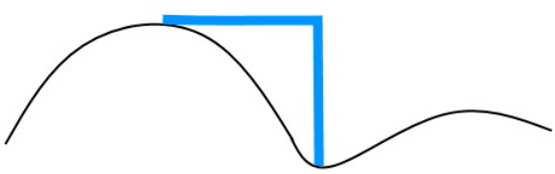

Illustration of heap size measurement. Red line illustrates a meterstick at 90 °angle.

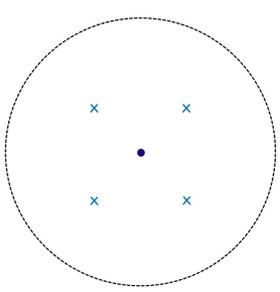

Figure illustrating peat depth and maximum hummock size measuring. Blue dot indicates point of measurement, blue crosses show positions of peat depth measurements 1 meter from center. Black circle shows 2–metre circle, within which the largest hummock was recorded.

Appendix 5 Untransformed values for all explanatory variables in all plots.

Plot	UTM E	UTM N	Main type	KA	UF	VI	Aspect	Slope	Altitude	ConvH	ConvV	FieldLayer	BotLayer	Mineral	Droppings Rangifer
101	27.4023	70.56715	T4	b	c	0	50	23	83.5	0	0	16	24	1	10
102	27.40219	70.56727	T4	b	c	0	30	28	85	0	0	29	86	2	10
103	27.40205	70.5671	T4	b	d	0	18	9	87.8	0	0	11	98	0	13
104	27.40174	70.56702	T3-C-15	b	d	0	15	11	89.2	0	0	85	39	0	4
105	27.40177	70.56705	T3-C-15	b	e	0	11	5	89.9	0	0	67	82	0	5
106	27.40152	70.56696	T3	b	f	a	30	4	90.8	0	0	61	53	6	14
107	27.40111	70.5668	T3	b	d	0	312	14	91.3	0	0	48	78	0	0
108	27.40096	70.56676	T4	b	c	0	29	9	91.2	-0.5	0	32	85	0	6
109	27.40084	70.56668	T4	b	c	0	25	1	92.5	-0.5	0	66	62	0	5
110	27.40081	70.56667	T3	b	d	0	30	3	92.5	0	-0.5	68	85	0	4
111	27.40047	70.5666	T14	b	h	c	20	8	94.5	0	0	14	79	7	2
112	27.40042	70.56654	T14	b	h	c	35	12	95.4	0	0	35	55	15	2
201	27.39641	70.56586	T3-C-15	b	d	0	39	1	92.7	0	0	59	86	0	5
202	27.39631	70.56589	T3-C-15	b	d	0	59	5	93.3	0	0	89	86	0	7
203	27.39605	70.56586	T3-C-15	b	d	0	51	7	93.9	0	0	60	82	0	11
204	27.39573	70.56582	T4-C-21	b	c	0	282	15	93.5	0	0	8	91	0	2
205	27.3956	70.56587	T4-C-21	b	c	0	272	16	92.1	0	0	4	97	0	2
206	27.39542	70.56583	T4	b	c	0	310	7	91.4	0.5	0	65	89	0	7
207	27.39521	70.56581	T4	b	c	0	70	1	91.2	0	0	75	89	6	4
208	27.39495	70.56583	T4	b	c	0	265	6	90.80	0	0	71	86	6	2
301	27.38896	70.56297	T4	b	c	0	318	2	101.1	0	0	47	83	0	0
302	27.38898	70.56286	T4	b	c	0	272	4	101.2	0	0	47	74	0	5
303	27.38885	70.56269	T4	b	d	0	65	3	101.5	0	0	37	75	5	9
304	27.38883	70.56261	T4-C-21	b	d	0	355	2	102	0	0	38	92	0	4
305	27.38879	70.56253	T4-C-21	b	d	0	355	4	102.6	0	0.5	29	85	0	6
306	27.38881	70.56245	T4-C-21	b	d	0	347	6	103.1	0	0	19	79	0	5
307	27.38879	70.56238	T3-C-15	b	d	0	335	9	103.4	0	0	41	93	0	12
308	27.38877	70.56225	T3-C-15	b	d	0	331	13	104.4	0	0	48	81	0	7
309	27.38872	70.56213	T3-C-15	b	d	0	300	7	105	0	0	61	72	0	0
310	27.38869	70.56205	T3-C-15	b	d	0	149	10	105.2	0	0	54	75	0	4
311	27.3887	70.56194	T3-C-15	b	d	0	157	3	105.2	0	0	57	81	0	9
312	27.38873	70.56181	T3-C-15	b	d	0	156	1	104.8	0	0	45	89	0	3
401	27.387	70.56156	T3	b	d	0	318	9	105.5	0	0	57	87	0	4
402	27.38678	70.56149	T3	b	d	0	191	9	105	0	0.5	19	92	0	10
403	27.38663	70.56141	T4-C-21	b	d	0	190	7	104.5	0	0	5	88	0	2
404	27.38644	70.56113	T4-C-21	b	d	0	181	9	104	0	0	11	98	0	2
405	27.38638	70.56129	T4-C-21	b	d	0	187	8	103	0	0	8	95	0	12
406	27.38619	70.56125	T4	b	e	0	182	5	102	0	-0.5	26	86	5	8
501	27.39006	70.56381	T4	b	b	0	18	12	95.2	0	0	71	74	0	11
502	27.38992	70.56378	T4	b	c	0	16	16	95.7	0	0	68	86	0	12
503	27.38986	70.56375	T4	b	d	0	10	10	96.6	0.5	0	7	98	0	13
504	27.38981	70.56368	T3-C-15	b	d	0	355	1	97.2	-0.5	0	58	46	0	7
505	27.38977	70.56361	T3-C-15	b	d	0	10	7	97.6	0	0	69	49	0	2
506	27.38959	70.56346	T3-C-15	b	d	0	4	5	98.6	-0.5	-0.5	61	74	0	12
507	27.38935	70.56337	T4	b	d	0	15	12	100	0	0	51	82	0	6
508	27.38937	70.56332	T4	b	d	0	21	7	100	0	0	41	79	0	4
601	27.3903	70.56989	T4	b	c	0	14	18	62.1	0	0	54	79	0	0
602	27.39004	70.56969	T4	b	d	0	11	11	66.4	0	0	74	72	0	2
603	27.39001	70.56969	T3-C-15	b	d	0	10	8	66.5	0	0	58	71	0	2
604	27.38994	70.56955	T3-C-15	b	e	0	7	15	69	0.5	0	89	79	0	1
605	27.38985	70.56949	T3-C-15	b	e	0	14	7	70.2	0.5	-0.5	66	71	0	4
606	27.38977	70.56941	T3-C-15	b	d	0	166	1	70.8	0.5	0	64	88	0	0
701	27.40854	70.57233	T4	b	b	0	24	23	61.6	0.5	0	76	62	0	2
702	27.40833	70.57234	T4	b	c	0	27	34	66	0	0	16	90	0	14
703	27.40833	70.57223	T3-C-15	b	d	0	28	23	67.8	-0.5	-1	62	88	0	0
704	27.40811	70.57217	T3-C-15	b	d	0	23	4	70.2	-0.5	0.5	59	79	0	7
705	27.40799	70.57211	T3-C-15	b	e	0	92	11	71.8	2	0	85	60	0	5
706	27.40771	70.57204	T4	b	g	0	184	25	69.5	0	0	68	38	12	3

Appendix 5, cont.

Plot	Droppings Rodent	TreeDens Dead	TreeDens Alive	Dead Wood	Snow Cover	Soil Moisture	Soil Depth	Micro topoH	Micro topoV	pH	LOI	TotP (raw)	TotP	TotN (raw)	TotN
101	0	30	152	1	3	67.13	28	2	6	3.50	86.75	0.75	0.8681	13.43	15.4762
102	2	32	92	0	3	67.76	22	0	1	3.43	54.03	0.28	0.5193	3.65	6.7627
103	7	25	7	0	2	73.07	17.5	1	5	3.33	97.22	0.38	0.3941	9.01	9.2722
104	1	0	0	0	1	75.57	36	0	2	3.37	97.59	0.76	0.7740	13.74	14.0813
105	1	0	0	0	1	71.67	9.5	1	0	3.30	96.44	0.37	0.3861	10.48	10.8628
106	2	0	0	0	1	60.75	3.5	0	1	3.60	89.89	0.51	0.5666	5.90	6.5676
107	0	5	14	0	2	73.27	21	4	5	3.37	98.24	0.60	0.6060	13.60	13.8435
108	4	58	49	0	3	72.47	19	1	2	3.50	96.65	0.45	0.4612	13.84	14.3152
109	1	14	9	0	2	75.62	11.5	1	1	3.53	95.88	0.49	0.5091	9.79	10.2113
110	0	5	0	0	2	72.09	18	2	1	3.40	97.49	0.66	0.6751	16.48	16.9025
111	0	0	0	0	1	21.34	11.5	0	0	3.83	23.96	1.30	5.4074	5.26	21.9509
112	0	0	0	0	1	57.16	6	0	0	3.70	31.54	1.16	3.6646	7.31	23.1703
201	0	0	0	0	1	75.07	33	5	3	3.30	97.80	0.63	0.6461	15.44	15.7854
202	0	0	0	0	1	71.76	28	2	1	3.40	97.77	0.35	0.3619	12.72	13.0125
203	0	0	8	0	1	70.83	15	2	1	3.30	95.93	0.23	0.2415	12.70	13.2394
204	0	0	102	0	2	70.84	21.5	3	4	3.30	97.73	0.51	0.5176	15.25	15.6039
205	0	1	118	0	2	73.77	20.5	4	5	3.27	97.66	0.71	0.7259	15.13	15.4939
206	4	2	18	0	3	75.57	8.5	2	1	3.27	95.06	0.53	0.5532	13.69	14.3979
207	3	7	12	0	3	71.09	5	3	1	3.37	67.90	0.87	1.2801	16.57	24.3968
208	7	13	164	0	3	75.17	6	2	2	3.53	93.68	0.71	0.7565	11.79	12.5840
301	2	43	79	1	3	73.55	8.5	2	2	3.50	93.39	0.53	0.5624	10.12	10.8313
302	2	47	7	1	3	73.80	12	1	1	3.50	97.01	0.66	0.6849	15.33	15.8003
303	2	9	63	0	3	71.21	9	1	1	3.37	95.15	0.56	0.5851	15.54	16.3296
304	3	81	11	0	3	72.72	16	2	2	3.33	97.46	0.64	0.6581	15.65	16.0554
305	2	4	19	0	3	71.56	17.5	2	3	3.27	97.54	0.52	0.5299	13.56	13.9035
306	3	19	77	0	3	73.15	18	4	2	3.23	97.27	0.95	0.9813	15.16	15.5907
307	0	7	24	1	2	72.25	18.5	4	3	3.23	97.21	0.46	0.4746	13.44	13.8208
308	0	0	0	0	1	76.25	23	2	3	3.23	97.99	0.66	0.6744	14.65	14.9561
309	0	0	0	0	1	75.61	23.5	3	3	3.30	98.28	0.76	0.7775	14.31	14.5648
310	0	0	0	0	1	73.64	21	4	3	3.23	97.39	0.43	0.4423	12.49	12.8272
311	2	0	0	0	1	74.29	25	4	3	3.40	97.96	0.60	0.6166	14.47	14.7681
312	0	0	0	0	1	74.20	31	5	3	3.33	97.89	0.62	0.6295	12.98	13.2638
401	0	0	0	0	1	74.07	11.5	0	0	3.20	97.69	0.59	0.6076	14.08	14.4127
402	0	0	17	0	1	71.98	16.5	1	1	3.20	97.76	0.70	0.7211	14.62	14.9579
403	2	3	182	0	1	73.24	27	5	2	3.17	97.68	0.61	0.6225	11.97	12.2537
404	0	0	143	1	1	71.82	21	2	2	3.17	97.61	0.67	0.6822	15.54	15.9252
405	0	11	119	1	1	73.89	17.5	2	1	3.13	97.63	0.61	0.6214	15.88	16.2641
406	4	56	40	0	2	72.06	12	4	0	3.20	94.65	0.40	0.4211	14.70	15.5334
501	4	41	27	0	3	78.02	17	2	2	3.33	97.23	0.99	1.0164	16.88	17.3581
502	0	49	70	0	3	74.41	13	1	2	3.27	96.99	0.49	0.5086	14.55	14.9996
503	0	54	29	0	3	72.16	39	2	3	3.23	97.16	0.35	0.3621	10.30	10.5966
504	2	0	0	0	3	75.62	18	3	5	3.23	97.77	0.61	0.6272	13.33	13.6305
505	4	0	0	0	2	73.71	17.5	5	5	3.23	97.39	0.65	0.6628	11.73	12.0458
506	1	0	114	0	3	77.20	10.5	1	1	3.23	97.13	0.71	0.7352	16.16	16.6363
507	2	15	146	1	3	71.65	10.5	2	1	3.23	96.95	0.72	0.7433	15.52	16.0093
508	2	8	18	0	3	68.51	10	2	2	3.30	76.56	0.72	0.9348	11.05	14.4266
601	0	27	29	0	4	74.38	9.5	5	2	3.30	89.48	0.30	0.3334	10.55	11.7907
602	0	62	25	0	3	75.88	15.5	7	5	3.20	96.81	0.39	0.4036	13.07	13.5006
603	0	31	4	0	3	73.11	22	5	5	3.23	97.47	0.62	0.6335	14.81	15.1932
604	0	0	0	0	3	73.83	24	4	3	3.23	97.60	0.26	0.2712	14.46	14.8177
605	0	0	0	0	3	72.28	29	1	1	3.13	97.96	0.58	0.5890	12.47	12.7269
606	0	0	0	0	1	74.29	13.5	1	1	3.27	97.73	0.50	0.5127	12.25	12.5338
701	3	33	86	1	3	75.33	19.5	1	5	3.33	97.03	0.34	0.3475	15.24	15.7067
702	6	0	178	1	3	71.54	29.5	4	6	3.33	96.81	0.16	0.1634	12.31	12.7128
703	0	0	10	0	3	69.20	31	2	5	3.30	96.92	0.48	0.4905	11.10	11.4560
704	2	0	0	0	2	73.57	25	2	1	3.33	97.09	0.39	0.3981	10.96	11.2873
705	0	8	0	0	1	69.03	28	10	5	3.30	98.01	0.66	0.6713	14.79	15.0938
706	0	3	0	0	1	48.26	3.5	0	0	3.60	51.09	0.59	1.1631	9.96	19.5034

Appendix 6 Transformed values for 22 continuous explanatory variables in all 58 plots.

Plot	UF	VI	Aspect	Slope	Altitude	ConvH	ConvV	Field Layer	Bot Layer	Droppings Rangifer	TreeDens Dead	TreeDens Alive	Snow Cover	Soil Moisture	Soil Depth	Micro topoH	Micro topoV	pH	LOI	TotP	TotN
101	0.4111	0.0000	0.5037	0.8416	0.2047	0.3810	0.5529	0.0934	0.0000	0.8174	0.8677	0.9658	0.6055	0.1717	0.7524	0.3535	1.0000	0.7550	0.0001	0.6326	0.5681
102	0.5811	0.0000	0.3823	0.9206	0.2314	0.3810	0.5529	0.2087	0.6009	0.8174	0.8763	0.8707	0.6055	0.1899	0.5988	0.0000	0.2213	0.6840	0.0000	0.4811	0.0146
103	0.5811	0.6717	0.2678	0.4944	0.2885	0.3810	0.5529	0.0530	1.0000	0.9581	0.8434	0.4017	0.2757	0.4485	0.4729	0.1710	0.8752	0.5499	0.4184	0.3874	0.1921
104	0.7340	0.6717	0.2291	0.5636	0.3209	0.3810	0.5529	0.9305	0.0459	0.4295	0.0000	0.0000	0.0000	0.6725	0.9363	0.0925	0.4552	0.5993	0.5681	0.6011	0.4902
105	0.5811	0.6717	0.1667	0.3121	0.3383	0.3810	0.5529	0.6511	0.5048	0.5087	0.0000	0.0000	0.0000	0.3577	0.2203	0.2994	0.1200	0.4942	0.2190	0.3801	0.2963
106	0.8728	0.8757	0.3823	0.2520	0.3616	0.3810	0.5529	0.5690	0.1218	1.0000	0.0000	0.0000	0.0000	0.0611	0.0000	0.0000	0.2213	0.8438	0.0010	0.5088	0.0000
107	0.7340	0.6717	0.9666	0.6508	0.3752	0.3810	0.5529	0.4080	0.4227	0.0000	0.6297	0.5221	0.2757	0.4635	0.5717	0.6265	0.9406	0.5993	0.9722	0.5295	0.4765
108	0.5811	0.0000	0.3744	0.4944	0.3724	0.0000	0.5529	0.2376	0.5755	0.5807	0.9555	0.7522	0.6055	0.4073	0.5160	0.2994	0.5176	0.7550	0.2618	0.4420	0.5035
109	0.5811	0.0000	0.3405	0.0000	0.4095	0.0000	0.5529	0.6371	0.1980	0.5087	0.7662	0.4445	0.2757	0.6781	0.2874	0.1710	0.2213	0.7867	0.1380	0.4746	0.2544
110	0.5811	0.6717	0.3823	0.1827	0.4095	0.3810	0.2313	0.6653	0.5755	0.4295	0.6297	0.0000	0.2757	0.3827	0.4874	0.4024	0.3089	0.6437	0.5225	0.5618	0.6445
111	1.0000	1.0000	0.2907	0.4553	0.4725	0.3810	0.5529	0.0770	0.4420	0.2432	0.0000	0.0000	0.0000	0.0000	0.2874	0.0000	0.0000	1.0000	0.0000	1.0000	0.8915
112	1.0000	1.0000	0.4183	0.5946	0.5036	0.3810	0.5529	0.2674	0.1364	0.2432	0.0000	0.0000	0.0000	0.0341	0.0956	0.0000	0.0000	0.9176	0.0000	0.9392	0.9464
201	0.7340	0.6717	0.4440	0.0000	0.4154	0.3810	0.5529	0.5428	0.6009	0.5087	0.0000	0.0000	0.0000	0.6204	0.8698	0.6839	0.7206	0.4942	0.6741	0.5488	0.5850
202	0.5811	0.6717	0.5442	0.3121	0.4338	0.3810	0.5529	1.0000	0.6009	0.6467	0.0000	0.0000	0.0000	0.3633	0.7524	0.3535	0.3861	0.6437	0.6583	0.3565	0.4281
203	0.7340	0.6717	0.5086	0.4124	0.4528	0.3810	0.5529	0.5559	0.5048	0.8671	0.0000	0.4243	0.0000	0.3124	0.3982	0.3535	0.3861	0.4942	0.1438	0.1933	0.4414
204	0.5811	0.0000	0.9405	0.6765	0.4400	0.3810	0.5529	0.0298	0.7446	0.2432	0.0000	0.8902	0.2757	0.3130	0.5853	0.5620	0.8025	0.4942	0.6360	0.4800	0.5751
205	0.5811	0.0000	0.9312	0.7008	0.3977	0.3810	0.5529	0.0000	0.9591	0.2432	0.4197	0.9178	0.2757	0.5026	0.5580	0.6265	0.8752	0.4304	0.6008	0.5829	0.5691
206	0.4111	0.0000	0.9649	0.4124	0.3779	0.6080	0.5529	0.6232	0.6837	0.6467	0.5093	0.5673	0.6055	0.6727	0.1857	0.4024	0.3861	0.4304	0.0703	0.5012	0.5082
207	0.4111	0.0000	0.5864	0.0000	0.3724	0.3810	0.5529	0.7688	0.6837	0.4295	0.6742	0.4947	0.6055	0.3257	0.0581	0.5620	0.3861	0.5993	0.0000	0.7304	1.0000
208	0.4111	0.0000	0.9244	0.3651	0.3616	0.3810	0.5529	0.7087	0.6009	0.2432	0.7564	0.9802	0.6055	0.6307	0.0956	0.4024	0.4552	0.7867	0.0224	0.5946	0.4026
301	0.4111	0.0000	0.9715	0.1006	0.7456	0.3810	0.5529	0.3965	0.5274	0.0000	0.9156	0.8420	0.6055	0.4853	0.1857	0.4471	0.4552	0.7550	0.0176	0.5064	0.2943
302	0.4111	0.0000	0.9312	0.2520	0.7506	0.3810	0.5529	0.3965	0.3526	0.5087	0.9275	0.4017	0.6055	0.5048	0.3037	0.2994	0.3861	0.7550	0.3523	0.5661	0.5858
303	0.5811	0.0000	0.5680	0.1827	0.7660	0.3810	0.5529	0.2878	0.3691	0.7645	0.7076	0.7994	0.6055	0.3320	0.2031	0.2994	0.3089	0.5993	0.0752	0.5187	0.6142
304	0.5811	0.0000	1.0000	0.1006	0.7922	0.3810	0.5529	0.2982	0.7769	0.4295	1.0000	0.4794	0.6055	0.4243	0.4285	0.4024	0.5176	0.5499	0.5086	0.5543	0.5996
305	0.5811	0.0000	1.0000	0.2520	0.8247	0.3810	1.0000	0.2087	0.5755	0.5807	0.6002	0.5771	0.6055	0.3515	0.4729	0.4471	0.6270	0.4304	0.5433	0.4876	0.4800
306	0.5811	0.6717	0.9941	0.3651	0.8527	0.3810	0.5529	0.1186	0.4420	0.5087	0.8069	0.8371	0.6055	0.4549	0.4874	0.6560	0.4552	0.3558	0.4350	0.6649	0.5744
307	0.5811	0.6717	0.9850	0.4944	0.8700	0.3810	0.5529	0.3299	0.8105	0.9139	0.6742	0.6197	0.2757	0.3929	0.5018	0.6265	0.6755	0.3558	0.4149	0.4516	0.4752
308	0.5811	0.6717	0.9819	0.6236	0.9298	0.3810	0.5529	0.4080	0.4830	0.6467	0.0000	0.0000	0.0000	0.7503	0.6255	0.4024	0.6270	0.3558	0.7874	0.5615	0.5395
309	0.5811	0.6717	0.9565	0.4124	0.9675	0.3810	0.5529	0.5690	0.3215	0.0000	0.0000	0.0000	0.0000	0.6766	0.6387	0.4883	0.6755	0.4942	1.0000	0.6023	0.5176
310	0.5811	0.8757	0.7767	0.5303	0.9804	0.3810	0.5529	0.4796	0.3691	0.4295	0.0000	0.0000	0.0000	0.4920	0.5717	0.6560	0.6270	0.3558	0.4827	0.4277	0.4171
311	0.7340	0.6717	0.7900	0.1827	0.9804	0.3810	0.5529	0.5171	0.4830	0.7645	0.0000	0.0000	0.0000	0.5471	0.6775	0.6560	0.7206	0.6437	0.7734	0.5348	0.5290
312	0.7340	0.8757	0.7884	0.0000	0.9548	0.3810	0.5529	0.3738	0.6837	0.3418	0.0000	0.0000	0.0000	0.5392	0.8239	0.7104	0.6270	0.5499	0.7262	0.5410	0.4429
401	0.5811	0.6717	0.9715	0.4944	1.0000	0.3810	0.5529	0.5171	0.6275	0.4295	0.0000	0.0000	0.0000	0.5273	0.2874	0.0000	0.0000	0.2659	0.6157	0.5303	0.5090
402	0.5811	0.6717	0.8402	0.4944	0.9675	0.3810	1.0000	0.1186	0.7769	0.8174	0.0000	0.5569	0.0000	0.3765	0.4434	0.2392	0.3089	0.2659	0.6534	0.5810	0.5396
403	0.5811	0.0000	0.8389	0.4124	0.9360	0.3810	0.5529	0.0073	0.6550	0.2432	0.5624	1.0000	0.0000	0.4615	0.7279	0.6839	0.5176	0.1528	0.6130	0.5377	0.3826
404	0.5811	0.0000	0.8264	0.4944	0.9054	0.3810	0.5529	0.0530	1.0000	0.2432	0.0000	0.9542	0.0000	0.3665	0.5717	0.4471	0.4552	0.1528	0.5748	0.5649	0.5925
405	0.5811	0.0000	0.8348	0.4553	0.8470	0.3810	0.5529	0.0298	0.8819	0.9139	0.7342	0.9194	0.0000	0.5123	0.4729	0.3535	0.2213	0.0000	0.5890	0.5371	0.6107
406	0.7340	0.0000	0.8278	0.3121	0.7922	0.3810	0.2313	0.1807	0.6009	0.7077	0.9508	0.7143	0.2757	0.3809	0.3037	0.5953	0.1200	0.2659	0.0500	0.4108	0.5713
501	0.2195	0.0000	0.2678	0.5946	0.4965	0.3810	0.5529	0.7087	0.3526	0.8671	0.9093	0.6414	0.6055	1.0000	0.4582	0.4024	0.4552	0.5499	0.4197	0.6739	0.6683
502	0.4111	0.0000	0.2427	0.7008	0.5143	0.3810	0.5529	0.6653	0.6009	0.9139	0.9330	0.8192	0.6055	0.5577	0.3359	0.2994	0.5176	0.4304	0.3469	0.4744	0.5419
503	0.5811	0.0000	0.1485	0.5303	0.5477	0.6080	0.5529	0.0223	1.0000	0.9581	0.9460	0.6546	0.6055	0.3872	1.0000	0.3535	0.6270	0.3558	0.3975	0.3567	0.2793
504	0.5811	0.6717	1.0000	0.0000	0.5710	0.0000	0.5529	0.5299	0.0786	0.6467	0.0000	0.0000	0.6055	0.6782	0.4874	0.5620	0.8752	0.3558	0.6587	0.5399	0.4642
505	0.5811	0.6717	0.1485	0.4124	0.5871	0.3810	0.5529	0.6796	0.0957	0.2432	0.0000	0.0000	0.2757	0.4976	0.4729	0.7104	0.8752	0.3558	0.4821	0.5564	0.3700
506	0.4111	0.6717	0.0000	0.3121	0.6289	0.0000	0.2313	0.5690	0.3526	0.9139	0.0000	0.9113	0.6055	0.8752	0.2542	0.2994	0.3089	0.3558	0.3867	0.5865	0.6305
507	0.4111	0.0000	0.2291	0.5946	0.6920	0.3810	0.5529	0.4432	0.5048	0.5807	0.7754	0.9582	0.6055	0.3569	0.2542	0.3535	0.3861	0.3558	0.3338	0.5896	0.5971
508	0.4111	0.0000	0.3014	0.4124	0.6920	0.3810	0.5529	0.3299	0.4420	0.4295	0.6919	0.5673	0.6055	0.2146	0.2374	0.4471	0.4552	0.4942	0.0000	0.6522	0.5098
601	0.4111	0.0000	0.2149	0.7457	0.0022	0.3810	0.5529	0.4796	0.4420	0.0000	0.8536	0.6546	1.0000	0.5551	0.2203	0.7356	0.5746	0.4942	0.0007	0.3257	0.3544
602	0.5811	0.0000	0.1667	0.5636	0.0247	0.3810	0.5529	0.7535	0.3215	0.2432	0.9644	0.6272	0.6055	0.7066	0.4135	0.8656	0.9406	0.2659	0.2975	0.3959	0.4567
603	0.5811	0.6717	0.1485	0.4553	0.0253	0.3810	0.5529	0.5299	0.3068	0.2432	0.8720	0.3116	0.6055	0.4515	0.5988	0.6839	0.9087	0.3558	0.5144	0.5430	0.5526
604	0.5811	0.6717	0.0846	0.6765	0.0414	0.6080	0.5529	1.0000	0.4420	0.1308	0.0000	0.0000	0.6055	0.5073	0.6517	0.5953	0.6755	0.3558	0.5733	0.2432	0.5318
605	0.7340	0.6717	0.2149	0.4124	0.0501	0.6080	0.2313	0.6371	0.3068	0.4295	0.0000	0.0000	0.6055	0.3948	0.7766	0.2392	0.3089	0.0000	0.7709	0.5208	0.4111
606	0.5811	0.6717	0.8043	0.0000	0.0547	0.6080	0.5529	0.6094	0.6550	0.0000	0.0000	0.0000	0.0000	0.5468	0.3517	0.2994	0.3089	0.4304	0.6371	0.4770	0.3995
701	0.0000	0.0000	0.3312	0.8416	0.0000	0.6080	0.5529	0.7842	0.1980	0.2432	0.8804	0.8580	0.6055	0.6471	0.5301	0.2392	0.8752	0.5499	0.3567	0.3413	0.5807
702	0.4111	0.0000	0.3580	1.0000	0.0223	0.3810	0.5529	0.0934	0.7136	1.0000	0.0000	0.9958	0.6055	0.3504	0.7886	0.6560	0.9710	0.5499	0.2975	0.0000	0.4103
703	0.4111	0.6717	0.3663	0.8416	0.0334	0.0000	0.0000	0.5824	0.6550	0.0000	0.0000	0.4627	0.6055	0.2399	0.8239	0.4471	0.9087	0.4942	0.3251	0.4625	0.3336
704	0.4111	0.6717	0.3217	0.2520	0.0501	0.0000	1.0000	0.5428	0.4420	0.6467	0.0000	0.0000	0.2757	0.4867	0.6775	0.4024	0.3861	0.5499	0.3758	0.3910	0.3231
705	0.7340	0.6717	0.6546	0.5636	0.0627	1.0000	0.5529	0.9305	0.1786	0.5087	0.6919	0.0000	0.0000	0.2333	0.7524	1.0000	0.9087	0.4942	0.8025	0.5602	0.5471
706	1.0000	0.8757	0.8306	0.8749	0.0450	0.3810	0.5529	0.6653	0.0419	0.3418	0.5624	0.0000	0.0000	0.0080	0.0000	0.0925	0.0000	0.8438	0.0000	0.7075	0.7760

Appendix 7 Species lists of sub–plot–frequencies for all species in all 58 plots.

	101	102	103	104	105	106	107	108	109	110	111	112	201	202	203	204	205	206	207	208
Betula nana	0	0	0	0	5	0	0	0	0	2	0	0	5	4	6	0	0	0	0	0
Betula pubescens	0	0	0	1	0	0	0	1	0	0	0	0	0	0	0	0	0	1	0	0
Sorbus aucuparia	0	0	0	0	0	0	0	0	0	0	0	0	0	0	0	0	0	0	0	0
Juniperus communis	0	0	0	0	0	0	0	0	0	0	0	0	0	0	0	0	0	0	0	0
Empetrum nigrum	0	0	4	10	9	10	9	4	7	10	6	9	10	10	8	5	0	0	9	4
Loiseleuria procumbens	0	0	0	0	0	0	0	0	0	0	5	0	0	0	0	0	0	0	0	0
Phyllodoce caerulea	0	0	0	0	0	0	0	0	0	0	0	0	0	0	0	0	0	0	0	0
Vaccinium myrtillus	0	0	5	2	0	0	4	0	0	4	0	0	0	0	0	2	0	6	3	4
Vaccinium uliginosum	0	0	0	4	0	4	5	0	4	0	0	0	6	0	0	0	0	0	0	0
Vaccinium vitis-idaea	0	3	6	6	5	6	7	5	6	6	6	6	6	6	6	6	6	6	6	6
Kalmia procumbens	0	0	0	0	0	0	0	0	0	0	0	0	0	0	0	0	0	0	0	0
Chamaepericlymenum suecicum	0	0	2	0	0	0	6	4	6	0	0	0	0	0	0	0	0	6	6	3
Dryopteris expansa	1	0	0	0	0	0	0	0	0	0	0	0	0	0	0	0	0	0	0	0
Rubus chamaemorus	0	0	0	4	0	0	0	0	0	3	0	0	0	1	0	0	0	0	0	0
Lysimachia europaea	5	6	5	0	0	0	0	0	0	0	0	0	0	0	0	5	5	6	5	6
Listera cordata	0	0	0	0	0	0	0	0	0	0	0	0	0	0	0	0	0	0	0	1
Lycopodium annotinum	0	0	0	0	0	0	0	0	2	0	0	0	0	0	0	0	0	0	1	0
Avenella flexuosa	8	8	3	1	0	0	5	6	7	3	0	0	0	0	0	0	5	8	6	9
Juncus trifidus	0	0	0	0	0	0	0	0	0	0	4	3	0	0	0	0	0	0	0	0
Nardus stricta	0	0	0	0	0	0	0	0	0	0	0	0	0	0	0	0	0	0	2	0
Carex brunnescens	0	0	0	0	0	0	0	0	0	0	0	0	0	0	0	0	0	0	0	0
Dicranum fuscescens	8	6	6	5	8	7	7	6	7	6	5	7	7	5	5	7	5	5	5	5
Dicranum scoparium	0	0	0	0	0	0	0	0	0	0	0	0	4	4	0	0	0	0	0	0
Dicranum undulatum	0	0	0	0	0	0	0	0	0	0	0	0	0	0	0	0	4	0	0	0
Pohlia nutans agg.	2	3	4	2	5	0	5	6	5	5	4	4	5	4	6	5	4	6	3	5
Plagiothecium laetum agg.	1	0	0	0	0	0	0	0	0	0	0	0	0	1	0	0	0	0	0	4
Pleurozium schreberi	4	0	0	0	0	0	7	6	5	4	0	0	3	3	0	0	6	6	6	7
Polytrichastrum alpinum	0	0	0	0	0	0	0	0	0	0	0	0	0	0	0	0	0	0	0	0
Polytrichum longisetum	0	0	0	0	0	0	0	0	0	0	0	0	0	0	0	0	0	0	0	0
Polytrichum juniperinum agg. [inkl. P.strictum]	4	10	10	7	2	0	8	8	4	6	6	5	4	7	9	10	10	4	5	2
Polytrichum piliferum	0	0	0	0	0	0	0	0	0	0	0	5	0	0	0	0	0	0	0	0
Sanionia uncinata	0	0	0	0	0	0	0	0	0	0	0	0	0	0	0	0	0	0	0	4
Tetraphis pellucida	0	0	0	0	0	0	0	0	0	0	0	0	0	1	0	0	0	0	0	0
Hylocomium splendens	0	0	0	0	0	0	0	0	0	0	0	0	0	0	0	0	1	0	0	0
Anastrophyllum minutum	1	0	0	4	5	4	0	0	0	1	0	4	4	4	3	3	0	2	1	3
Barbilophozia floerkei	1	4	4	4	0	1	0	3	5	4	0	1	4	4	4	3	5	7	5	6
Barbilophozia lycopodioides	2	0	1	0	0	0	1	0	3	0	0	0	0	0	0	0	3	4	5	4
Calypogeia neesiana	1	1	1	4	0	0	1	0	2	1	0	0	0	3	3	6	3	4	0	0
Cephalozia agg.	2	4	0	5	3	3	1	0	3	0	0	0	0	5	2	5	3	4	3	3
Cephaloziella spp.	0	0	0	0	0	0	0	0	0	0	0	0	0	0	0	0	0	0	0	0
Lophozia incisa	0	0	0	0	0	0	0	0	1	0	0	0	0	0	0	0	0	0	0	0
Lophozia ventricosa agg.	4	5	3	1	5	1	4	4	3	3	0	1	6	5	3	5	0	0	1	1
Mylia anomala	0	0	0	0	0	0	0	0	0	0	0	0	0	0	0	0	0	0	0	1
Ptilidium ciliare	0	0	0	0	4	5	0	0	2	4	4	5	5	5	0	0	0	0	0	0
Tetralophozia setiformis	0	0	0	0	0	0	0	0	0	0	0	3	0	0	0	0	0	0	0	0
Cladonia arbuscula	1	0	0	1	0	3	1	0	0	0	0	0	3	4	5	4	0	0	0	0
Cladonia bellidiflora	1	0	0	0	2	3	0	1	1	0	0	0	0	0	0	0	0	0	0	0
Cladonia carneola	0	1	0	0	0	0	0	1	0	0	0	0	0	0	0	0	0	0	0	0
Cladonia chlorophaea agg.	4	5	4	1	4	5	5	5	4	5	5	5	5	4	4	5	4	5	5	5
Cladonia coccifera agg.	2	1	4	1	4	6	3	4	2	2	3	3	3	0	1	4	0	0	4	0
Cladonia coniocraea	1	0	1	1	0	0	0	0	0	0	0	0	0	0	0	0	0	0	0	4
Cladonia crispata	0	0	0	0	0	0	0	0	0	0	0	0	0	0	3	0	0	0	0	0
Cladonia digitata	0	0	0	0	0	0	0	1	0	0	0	0	0	0	0	0	0	0	0	0
Cladonia fimbriata	0	0	0	0	1	0	0	0	1	0	0	0	0	0	0	1	0	0	1	0
Cladonia gracilis	0	0	1	2	2	0	3	5	0	0	4	0	0	3	4	5	6	0	3	0
Cladonia pleurota	0	0	1	0	1	0	0	0	0	0	0	0	0	0	0	0	0	0	0	0
Cladonia rangiferina	1	0	4	5	5	5	5	1	4	6	5	5	5	4	0	1	0	0	0	0
Cladonia squamosa	3	5	1	3	1	0	0	5	3	0	0	5	5	3	4	5	2	3	5	3
Cladonia straminea	0	0	0	0	1	0	0	0	0	0	0	0	0	0	0	0	0	0	0	0
Cladonia subulata	0	0	0	0	0	0	0	0	0	0	0	0	0	0	0	0	0	0	0	0
Cladonia sulphurina	0	0	1	0	1	0	1	0	1	0	0	0	0	0	1	0	0	0	0	0
Cladonia uncialis	1	2	5	5	6	6	0	5	1	5	6	5	5	4	5	4	5	0	0	0
Cetraria aculeata	0	0	0	0	0	0	0	0	0	0	5	5	0	0	0	0	0	0	0	0
Cetraria islandica	0	0	0	0	4	3	0	0	0	3	4	3	0	0	0	0	0	0	0	0
Flavocetraria nivalis	0	0	0	0	0	3	0	0	0	0	0	2	0	0	0	0	0	0	0	0
Icmadophila ericetorum	0	0	0	0	2	0	0	0	0	0	0	0	0	0	0	2	0	0	0	0
Lichenomphalia hudsoniana	0	0	0	0	0	0	0	2	0	0	0	0	0	0	0	0	0	0	0	0
Nephroma arcticum	0	0	0	0	0	0	3	0	0	4	0	0	3	0	0	0	0	0	4	0
Ochrolechia spp.	1	0	0	0	0	6	0	0	0	0	6	9	0	0	0	1	0	0	0	0
Sphaerophorus globosus	0	0	0	0	0	1	0	0	0	3	4	5	0	0	0	0	0	0	0	0

Appendix 7, cont.

	301	302	303	304	305	306	307	308	309	310	311	312	401	402	403	404	405	406	501
Betula nana	0	0	0	0	0	0	0	4	2	0	0	1	2	0	0	0	0	0	0
Betula pubescens	2	2	0	1	4	0	0	2	0	0	2	0	0	0	0	2	1	0	0
Sorbus aucuparia	0	0	0	0	1	0	0	0	0	0	0	0	0	0	0	0	0	0	0
Juniperus communis	0	0	0	0	0	0	0	0	0	0	0	0	0	0	0	0	0	1	0
Empetrum nigrum	2	4	4	4	7	5	9	9	10	9	10	9	10	5	0	0	3	0	0
Loiseleuria procumbens	0	0	0	0	0	0	0	0	0	0	0	0	0	0	0	0	0	0	0
Phyllodoce caerulea	0	0	0	0	0	0	0	0	0	0	0	0	0	0	0	0	0	0	0
Vaccinium myrtillus	3	5	6	3	1	4	3	0	1	0	3	6	0	6	0	5	2	5	7
Vaccinium uliginosum	0	0	0	0	0	0	0	0	0	0	2	0	0	0	0	0	0	0	0
Vaccinium vitis-idaea	6	6	6	6	4	6	6	6	6	5	6	5	6	6	6	6	6	0	0
Kalmia procumbens	0	0	0	0	0	0	0	0	0	0	2	3	0	0	0	0	0	0	0
Chamaepericlymenum suecicum	2	6	5	4	0	0	0	0	0	0	0	4	0	0	0	3	4	5	8
Dryopteris expansa	0	0	0	0	0	0	0	0	0	0	0	0	0	0	0	0	0	0	2
Rubus chamaemorus	0	0	0	0	0	0	1	4	2	0	0	5	0	0	0	0	0	0	0
Lysimachia europaea	6	5	5	0	0	0	0	0	0	0	0	0	0	0	0	6	6	6	6
Listera cordata	0	0	0	0	0	0	0	0	0	0	0	0	0	0	0	0	0	0	0
Lycopodium annotinum	3	0	0	2	0	0	0	0	0	0	0	0	0	0	0	0	0	0	0
Avenella flexuosa	10	8	7	7	4	5	0	0	0	0	4	0	0	4	0	2	4	6	10
Juncus trifidus	0	0	0	0	0	0	0	0	0	0	0	0	0	0	0	0	0	0	0
Nardus stricta	0	0	0	0	0	0	0	0	0	0	0	0	0	0	0	0	0	0	0
Carex brunnescens	0	0	0	0	0	0	0	0	0	0	0	0	1	0	0	0	0	1	0
Dicranum fuscescens	4	5	7	6	6	6	6	5	4	8	7	10	6	6	6	6	3	7	6
Dicranum scoparium	3	0	0	0	0	0	0	1	0	0	0	0	0	0	4	0	0	4	2
Dicranum undulatum	0	0	0	0	0	0	0	0	0	0	0	2	0	0	0	0	0	0	0
Pohlia nutans agg.	4	5	6	5	6	6	5	3	3	2	3	3	4	5	6	5	4	7	4
Plagiothecium laetum agg.	0	0	0	0	0	0	0	0	0	0	0	0	0	0	0	0	0	0	0
Pleurozium schreberi	1	4	4	2	0	0	0	1	1	0	1	5	2	0	0	5	6	5	6
Polytrichastrum alpinum	0	0	0	0	0	0	0	0	0	0	0	0	0	0	0	0	0	0	1
Polytrichum longisetum	0	0	0	0	0	0	0	0	0	0	0	0	0	0	0	0	0	5	0
Polytrichum juniperinum agg. [inkl. P. strictum]	5	10	7	10	10	10	10	10	9	6	7	10	10	10	10	10	10	6	4
Polytrichum piliferum	0	0	0	0	0	0	0	0	0	0	0	0	0	0	0	0	0	0	0
Sanionia uncinata	4	0	0	0	0	0	0	0	0	0	0	0	0	0	0	0	0	0	0
Tetraphis pellucida	0	0	0	0	0	0	0	0	0	0	0	0	0	0	0	0	0	0	0
Hylocomium splendens	0	0	0	0	0	0	0	2	0	0	0	0	0	0	0	0	0	0	0
Anastrophyllum minutum	0	0	2	0	0	0	0	0	0	3	3	0	5	3	0	0	0	0	0
Barbilophozia floerkei	2	6	6	6	5	6	6	6	5	5	5	6	4	5	5	5	6	4	7
Barbilophozia lycopodioides	8	4	1	1	0	0	0	2	0	0	0	0	0	0	0	0	2	3	3
Calypogeia neesiana	0	3	0	5	3	5	5	5	5	2	4	3	2	2	5	5	1	0	3
Cephalozia agg.	4	4	4	6	5	5	5	6	5	0	4	5	4	5	4	5	5	0	4
Cephaloziella spp.	0	0	0	0	0	0	0	0	0	0	0	0	0	0	0	0	0	0	0
Lophozia incisa	0	0	0	0	0	0	0	0	0	0	0	0	0	0	0	0	0	0	0
Lophozia ventricosa agg.	4	4	5	5	1	2	4	3	3	3	2	0	1	2	3	5	5	2	4
Mylia anomala	0	0	0	0	0	0	0	0	0	0	4	5	0	0	0	0	0	0	0
Ptilidium ciliare	1	0	0	0	0	0	0	0	1	1	7	0	5	0	0	0	0	0	0
Tetralophozia setiformis	0	0	0	0	0	0	0	0	0	0	0	0	0	0	0	0	0	0	0
Cladonia arbuscula	0	0	5	0	2	2	5	5	6	2	4	4	0	0	2	1	0	0	0
Cladonia bellidiflora	0	0	0	0	0	0	0	0	0	0	3	0	0	1	0	0	0	0	1
Cladonia carneola	0	0	0	1	0	0	0	0	0	0	0	0	0	3	2	0	0	0	0
Cladonia chlorophaea agg.	0	4	5	5	1	5	5	1	2	5	4	5	1	5	5	5	2	6	4
Cladonia coccifera agg.	5	0	3	1	4	1	2	0	0	3	4	0	0	2	0	0	0	4	0
Cladonia coniocraea	0	0	0	0	0	0	0	0	0	0	0	0	1	0	0	0	0	4	1
Cladonia crispata	0	0	0	0	0	2	0	0	4	4	0	0	0	1	4	0	0	0	0
Cladonia digitata	0	0	4	0	4	0	0	0	0	0	0	0	0	0	0	0	0	0	0
Cladonia fimbriata	0	0	0	0	0	0	0	0	0	0	0	0	0	0	0	0	0	0	0
Cladonia gracilis	1	2	6	3	5	5	6	5	4	5	5	0	3	3	4	0	0	1	1
Cladonia pleurota	0	0	0	5	0	0	0	0	0	2	0	3	0	0	0	0	0	0	0
Cladonia rangiferina	0	0	3	0	2	4	1	0	0	5	5	5	4	4	4	5	0	0	0
Cladonia squamosa	0	3	5	4	4	3	5	4	4	0	4	0	5	4	6	1	0	5	0
Cladonia straminea	0	0	0	0	0	0	1	0	0	0	0	0	0	0	0	0	0	0	0
Cladonia subulata	0	0	3	0	0	0	0	0	0	0	0	0	0	0	0	0	0	0	0
Cladonia sulphurina	0	0	0	0	0	0	0	0	0	0	0	0	0	0	0	0	0	0	0
Cladonia uncialis	0	3	5	5	4	2	6	3	0	5	5	5	1	5	6	1	0	0	0
Cetraria aculeata	0	0	0	0	0	0	0	0	0	0	0	0	0	0	0	0	0	0	0
Cetraria islandica	0	0	0	0	0	0	0	0	0	0	0	0	0	0	1	0	0	0	0
Flavocetraria nivalis	0	0	0	0	0	0	0	0	0	0	1	0	0	0	0	0	0	0	0
Icmadophila ericetorum	0	0	0	0	0	0	0	0	0	0	0	3	0	0	0	0	0	0	0
Lichenomphalia hudsoniana	0	0	0	0	0	0	0	0	0	0	0	0	0	0	0	0	0	0	0
Nephroma arcticum	0	0	0	0	0	0	0	0	0	0	0	0	1	0	0	0	0	0	0
Ochrolechia spp.	0	0	0	0	0	0	0	0	0	4	4	4	0	0	0	0	0	0	0
Sphaerophorus globosus	0	0	0	0	0	0	0	0	0	0	3	0	0	0	0	0	0	0	0

Appendix 7, cont.

	502	503	504	505	506	507	508	601	602	603	604	605	606	701	702	703	704	705	706
Betula nana	0	0	0	5	0	0	0	0	0	0	0	0	0	0	0	0	0	0	0
Betula pubescens	0	0	0	0	1	0	1	1	0	1	0	0	0	0	0	0	0	0	0
Sorbus aucuparia	0	0	0	0	1	2	0	0	0	0	0	0	0	0	0	0	0	0	0
Juniperus communis	0	0	0	0	0	0	0	0	0	0	0	0	0	0	0	0	0	0	0
Empetrum nigrum	2	4	9	10	4	0	2	0	6	8	10	9	9	2	0	9	9	10	9
Loiseleuria procumbens	0	0	0	0	0	0	0	0	0	0	0	0	0	0	0	0	0	0	0
Phyllodoce caerulea	0	0	0	0	0	0	0	0	0	0	0	0	0	6	0	0	0	0	0
Vaccinium myrtillus	4	0	0	6	0	4	4	5	6	5	4	0	0	3	4	0	4	0	0
Vaccinium uliginosum	0	0	2	0	0	0	3	0	7	6	0	5	0	0	0	6	6	3	0
Vaccinium vitis-idaea	1	6	6	6	6	5	0	0	5	6	6	6	6	3	6	6	6	6	0
Kalmia procumbens	0	0	0	0	0	0	0	0	0	0	0	0	0	0	0	0	0	0	0
Chamaepericlymenum suecicum	0	4	5	0	5	5	4	5	6	6	4	0	0	5	0	4	5	0	0
Dryopteris expansa	0	0	0	0	0	0	0	0	0	0	0	0	0	1	0	0	0	0	0
Rubus chamaemorus	0	0	4	0	0	0	0	0	0	0	0	0	0	0	0	4	0	0	0
Lysimachia europaea	0	0	4	0	2	6	6	6	6	6	0	1	1	2	0	0	0	0	0
Listera cordata	0	0	0	0	0	0	0	0	0	0	0	0	0	0	0	0	0	0	0
Lycopodium annotinum	0	0	0	0	0	0	0	0	0	0	0	0	0	0	0	0	0	0	0
Avenella flexuosa	10	1	4	3	10	10	9	9	8	7	4	0	4	8	5	4	6	0	4
Juncus trifidus	0	0	0	0	0	0	0	0	0	0	0	0	0	0	0	0	0	0	0
Nardus stricta	0	0	0	0	0	0	0	0	0	0	0	0	0	0	0	0	0	0	0
Carex brunnescens	0	0	0	0	0	0	0	0	0	0	0	0	0	0	0	0	0	0	0
Dicranum fuscescens	6	5	2	6	6	6	5	5	4	4	7	8	6	2	7	5	8	4	5
Dicranum scoparium	0	0	0	0	0	0	0	4	4	5	3	0	0	5	0	0	3	3	3
Dicranum undulatum	0	0	0	0	0	0	0	0	0	0	0	0	0	0	0	0	0	0	0
Pohlia nutans agg.	5	6	4	4	5	5	4	5	6	4	5	3	6	4	5	3	4	3	0
Plagiothecium laetum agg.	0	0	0	0	2	0	0	0	0	0	1	0	0	0	3	0	0	0	0
Pleurozium schreberi	5	4	5	4	4	4	6	6	5	6	7	6	5	4	5	7	8	5	4
Polytrichastrum alpinum	0	0	0	0	0	0	0	0	0	0	0	0	0	0	0	0	0	0	0
Polytrichum longisetum	1	0	0	0	0	0	0	0	0	0	0	0	0	1	0	0	0	0	0
Polytrichum juniperinum agg. [inkl.P.strictum]	7	10	8	6	5	7	10	9	7	8	9	5	10	0	6	7	4	6	4
Polytrichum piliferum	0	0	0	0	0	0	0	0	0	0	0	0	0	0	0	0	0	0	0
Sanionia uncinata	0	0	0	2	0	0	0	0	0	0	0	0	0	4	0	0	0	0	0
Tetraphis pellucida	0	0	0	0	0	0	0	0	0	0	0	0	0	0	0	0	0	1	0
Hylocomium splendens	0	0	0	0	0	0	0	0	1	0	0	0	0	0	0	0	2	3	0
Anastrophyllum minutum	0	0	0	0	0	0	1	1	0	0	0	0	0	0	0	3	3	0	0
Barbilophozia floerkei	7	6	4	5	6	7	8	6	4	4	3	6	3	4	2	5	5	4	0
Barbilophozia lycopodioides	3	0	2	0	4	5	5	3	6	5	4	4	0	7	4	2	4	2	0
Calypogeia neesiana	1	5	3	4	5	4	3	4	6	4	4	0	4	4	5	4	3	3	0
Cephalozia agg.	4	4	3	1	5	4	4	6	5	3	4	3	0	3	3	3	2	0	0
Cephaloziella spp.	0	0	0	0	0	0	0	1	0	0	0	0	0	0	0	0	0	0	0
Lophozia incisa	0	0	0	0	0	0	0	0	0	0	0	0	0	0	0	0	0	0	0
Lophozia ventricosa agg.	4	3	1	1	0	3	1	0	4	5	5	4	4	4	6	5	4	3	0
Mylia anomala	0	0	0	0	0	0	0	0	0	0	0	0	0	0	0	0	0	0	0
Ptilidium ciliare	0	0	0	0	0	0	0	0	0	0	0	0	0	0	0	1	3	5	3
Tetralophozia setiformis	0	0	0	0	0	0	0	0	0	0	0	0	0	0	0	0	0	0	0
Cladonia arbuscula	0	0	0	0	0	0	0	0	2	3	0	0	2	0	0	4	3	3	0
Cladonia bellidiflora	0	1	0	0	0	0	0	0	0	0	0	0	0	0	0	1	0	0	0
Cladonia carneola	0	1	0	0	1	0	0	0	0	0	0	0	0	0	0	0	0	0	0
Cladonia chlorophaea agg.	4	3	2	0	0	4	3	5	4	5	0	5	1	1	5	5	5	4	5
Cladonia coccifera agg.	0	0	0	0	1	0	0	2	1	0	0	3	0	0	5	4	2	4	2
Cladonia coniocraea	0	0	0	0	0	0	0	0	0	0	0	0	0	0	0	0	0	0	0
Cladonia crispata	0	0	0	0	0	0	0	0	0	0	0	0	0	0	3	4	0	1	2
Cladonia digitata	0	2	0	0	0	0	0	0	0	0	0	2	0	0	1	0	0	1	0
Cladonia fimbriata	0	1	0	2	0	0	0	0	0	0	0	0	0	0	0	0	0	0	0
Cladonia gracilis	5	4	4	5	3	4	0	0	0	4	2	3	5	0	4	5	5	5	3
Cladonia pleurota	0	2	0	0	0	0	0	1	0	0	0	0	0	0	0	3	0	0	0
Cladonia rangiferina	0	4	4	0	0	0	0	0	0	4	4	5	5	0	4	5	5	5	5
Cladonia squamosa	4	3	3	5	3	1	1	2	0	3	0	5	0	0	4	4	4	4	5
Cladonia straminea	0	0	0	0	0	0	0	0	0	0	0	0	0	0	0	0	0	0	0
Cladonia subulata	0	0	0	0	0	0	0	0	0	0	0	0	0	0	0	0	0	0	0
Cladonia sulphurina	0	0	0	0	0	0	0	0	0	0	0	2	0	0	0	4	0	0	0
Cladonia uncialis	0	4	2	3	0	0	0	0	0	0	1	3	4	0	2	5	4	3	5
Cetraria aculeata	0	0	0	0	0	0	0	0	0	0	0	0	0	0	0	0	0	0	0
Cetraria islandica	0	0	0	0	0	0	0	0	0	0	0	0	0	0	0	0	0	0	0
Flavocetraria nivalis	0	0	0	0	0	0	0	0	0	0	0	0	0	0	0	0	0	0	0
Icmadophila ericetorum	0	0	0	0	0	0	0	0	0	0	0	0	0	0	0	0	0	0	0
Lichenomphalia hudsoniana	0	0	0	0	0	0	0	0	0	0	0	0	0	0	0	0	0	0	0
Nephroma arcticum	0	0	0	0	0	0	0	0	0	3	2	0	0	0	3	4	5	3	0
Ochrolechia spp.	0	0	0	0	0	0	0	0	0	0	0	0	0	0	2	4	0	4	4
Sphaerophorus globosus	0	0	0	0	0	0	0	0	0	0	0	0	0	0	0	0	0	0	0

Appendix 8 Figures from DCA ordinations

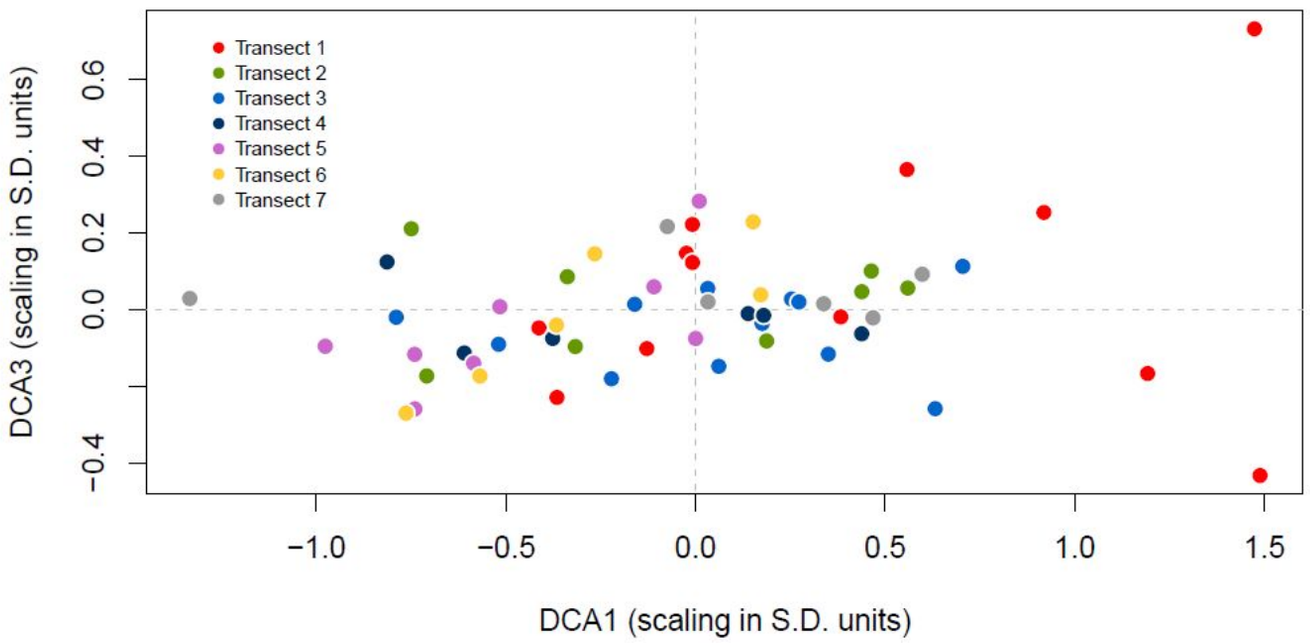

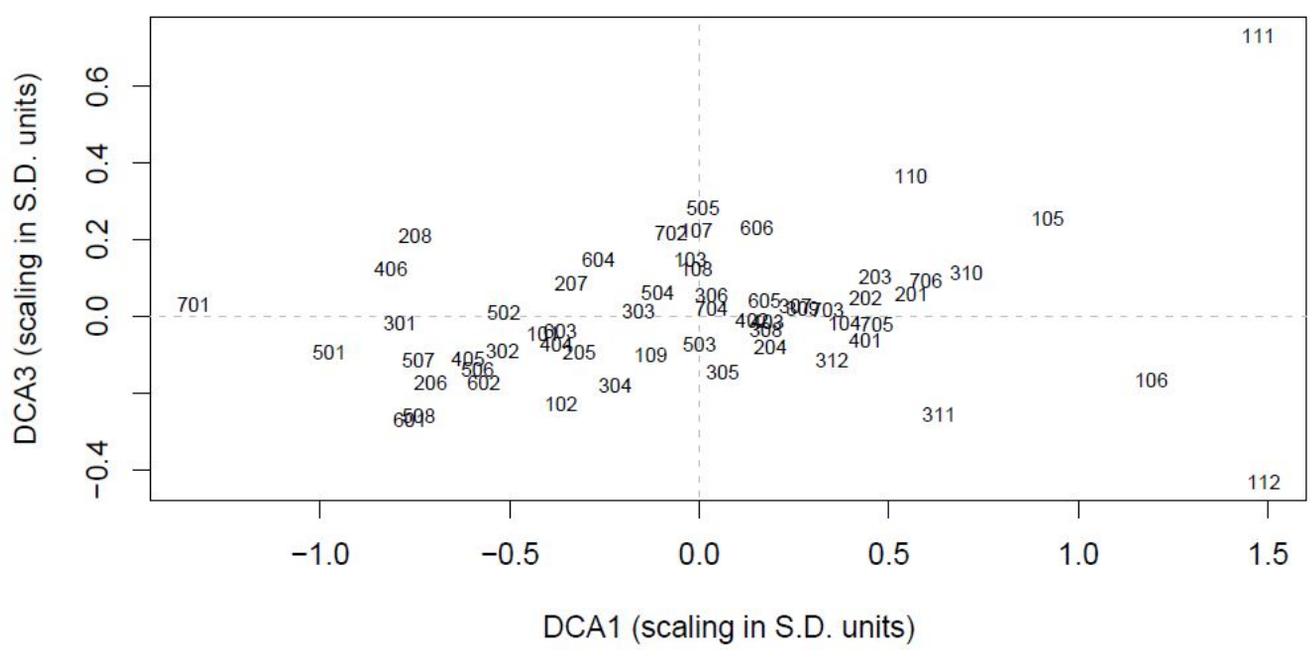

Appendix 9 Grapths with species frequencies in Peat heath and Peat forest

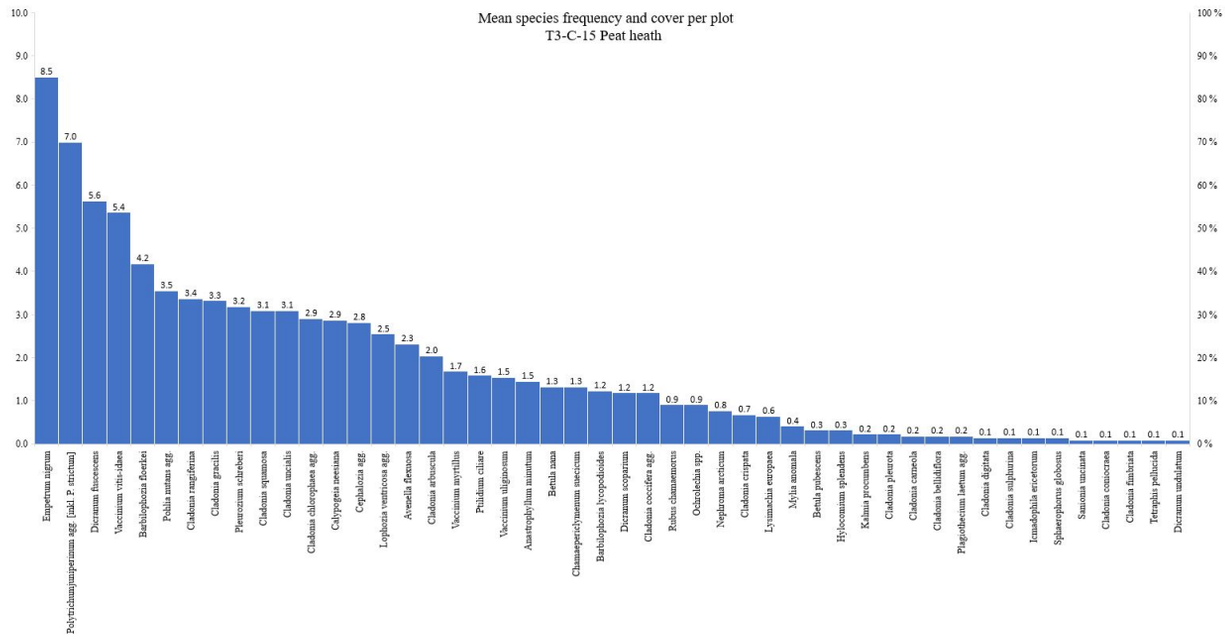

Mean species richness per plot in T3–C–15 Peat heath presented in frequency and cover on a 0–10 scale.

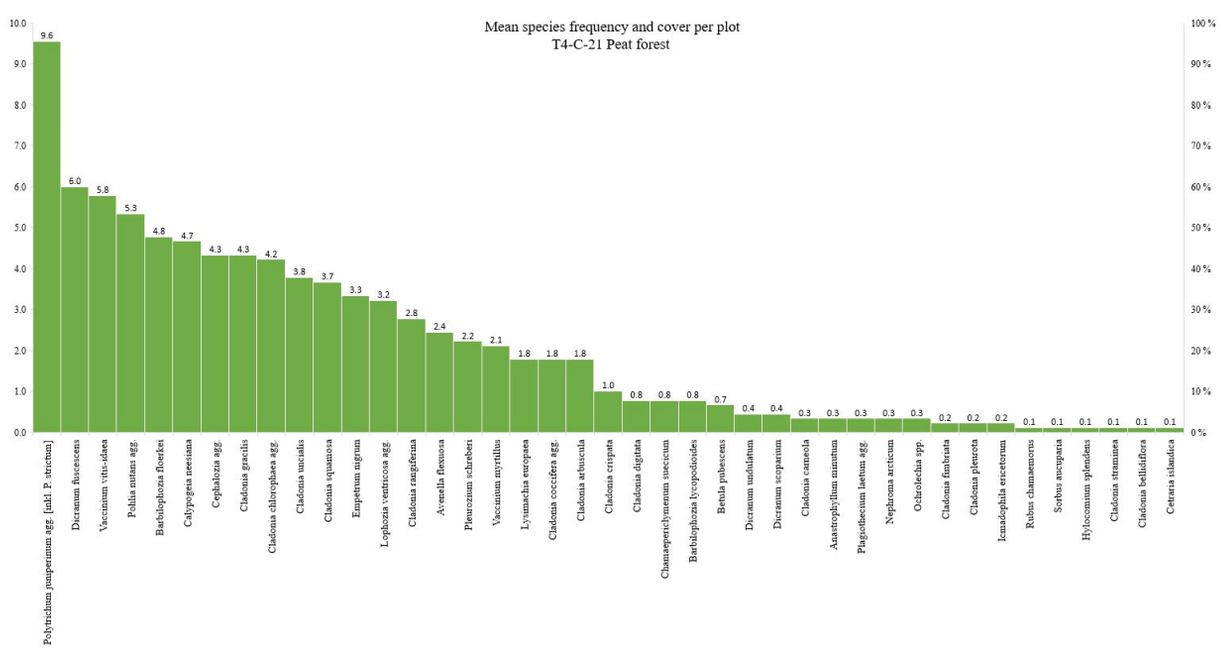

Mean species richness per plot in T4–C–21 Peat forest presented in frecuency and cover on a 0–10 scale.

Appendix 9, cont. Species frequency in Peat heath and Peat forest plots.

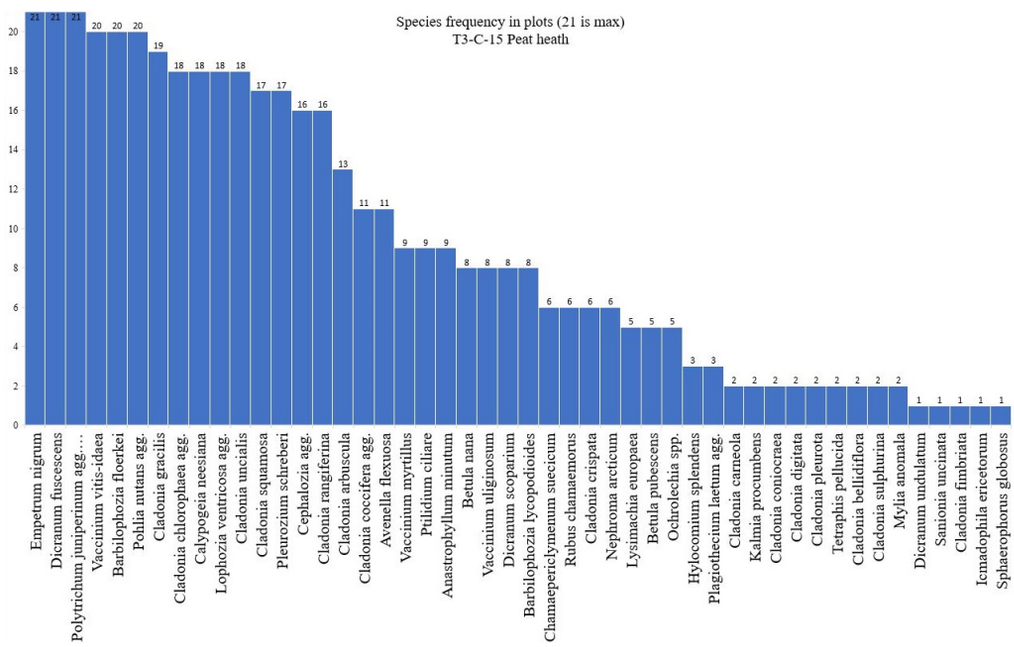

Species frequency in nr. of plots T3–C–15 peat heath

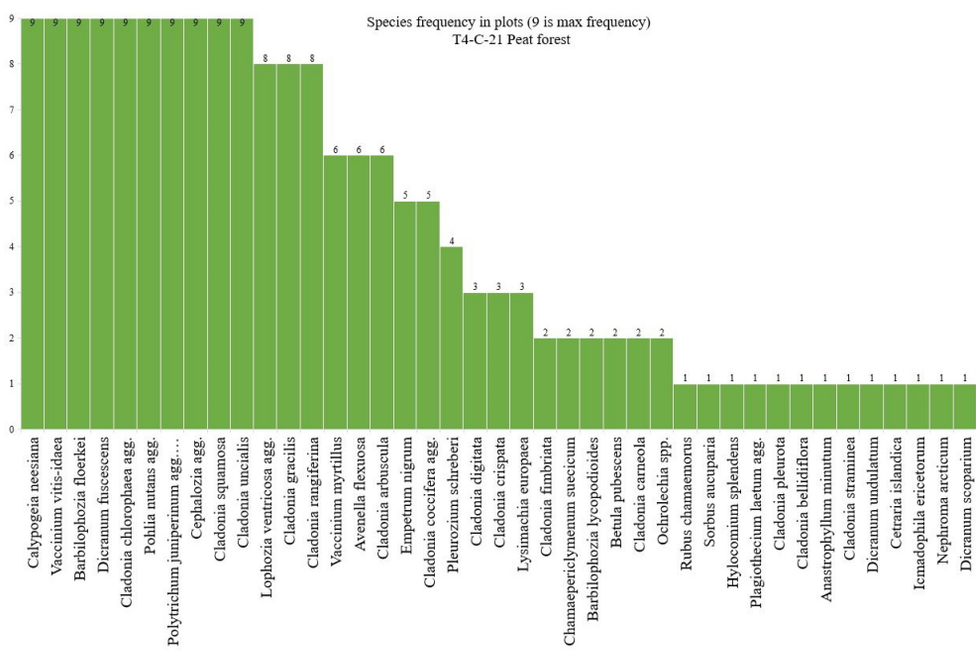

Species frequency in nr. of plots T4–C–21 peat forest

Appendix 10 Biplots with isolines of environmental variables

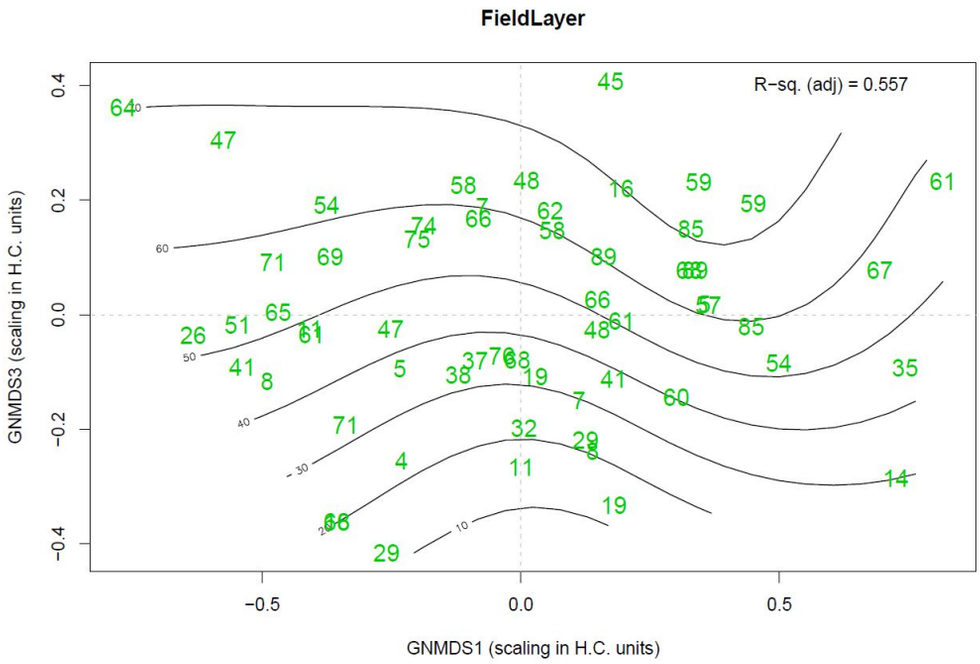

Isoline diagram with isolines representing Field layer and values for FieldLayer in each plot for the ordination. Increasing towards the high end of GNMDS3

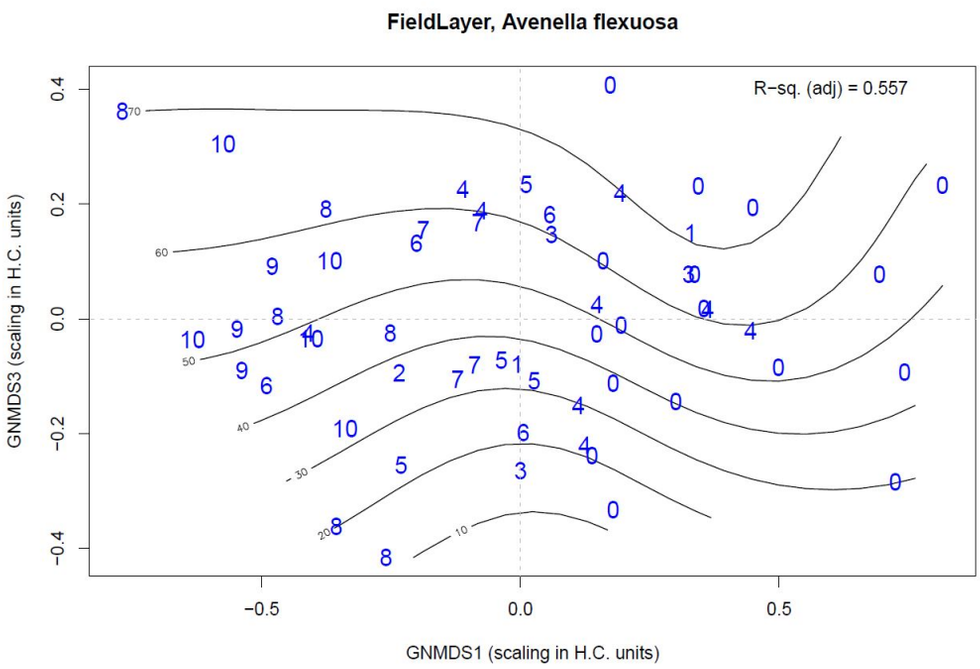

Isoline diagram with isolines representing Field layer and values for cover of Avenella flexuosa in each plot for the ordination on a 0–10 scale.

Appendix 11 Sentinel–2 satelite photos

Snow cover
Transect 1

4. march 2020

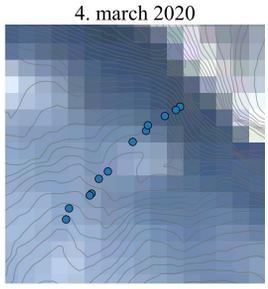

24. may 2020

2. june 2020

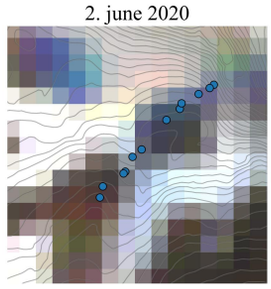

13. june 2020

20. june 2020

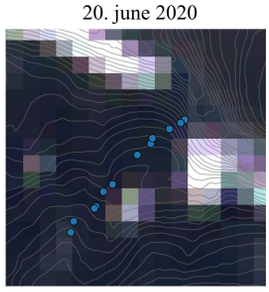

15. july 2020

Snow cover
Transect 2

4. march 2020

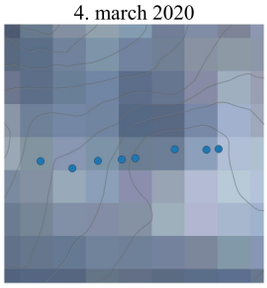

26. may 2020

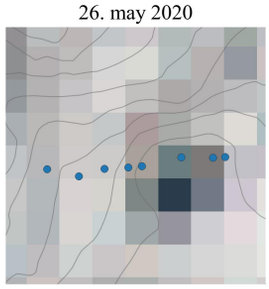

2. june 2020

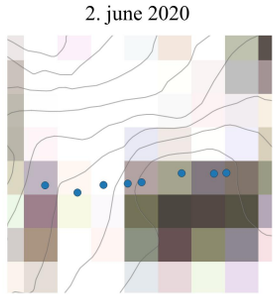

13. june 2020

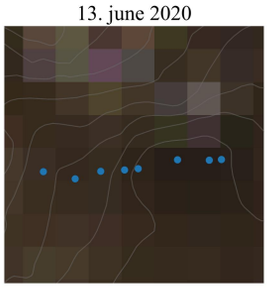

20. june 2020

15. july 2020

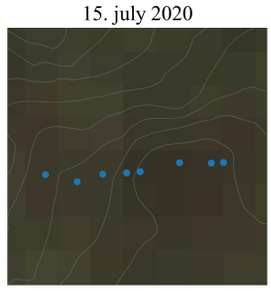

Snow cover
Transect 3

4. march 2020

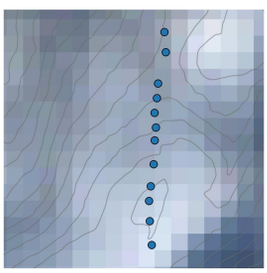

26. may 2020

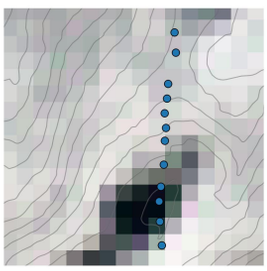

2. june 2020

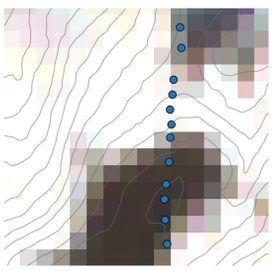

13. june 2020

20. june 2020

15. july 2020

Snow cover
Transect 4

4. march 2020

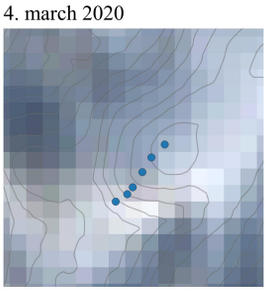

26. may 2020

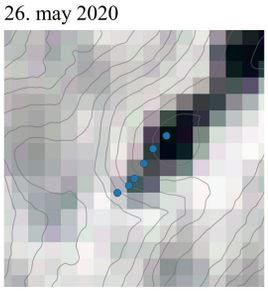

2. june 2020

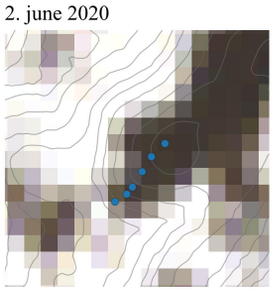

13. june 2020

20. june 2020

15. july 2020

Snow cover
Transect 5

4. march 2020

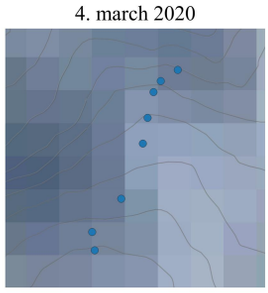

26. may 2020

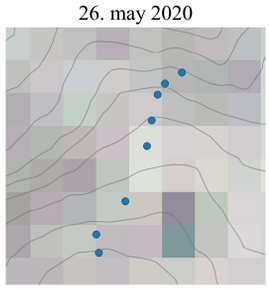

2. june 2020

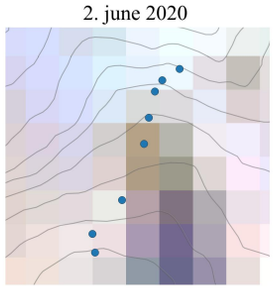

13. june 2020

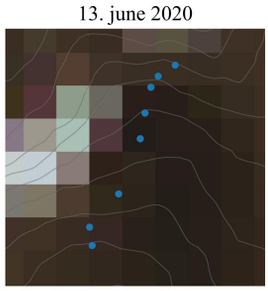

20. june 2020

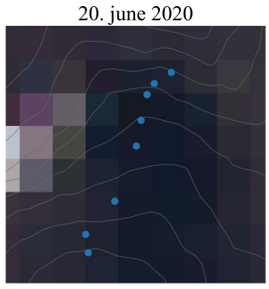

15. july 2020

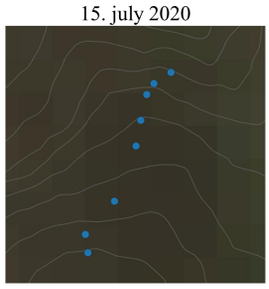

Snow cover
Transect 6

4. march 2020

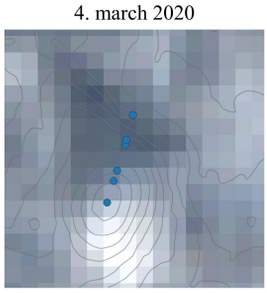

26. may 2020

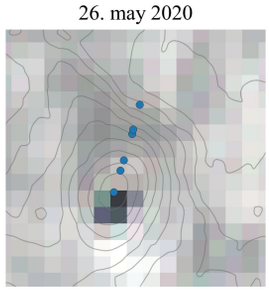

2. june 2020

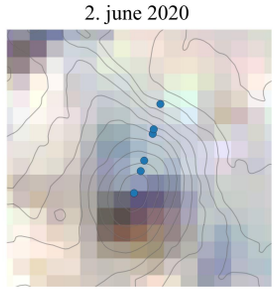

13. june 2020

20. june 2020

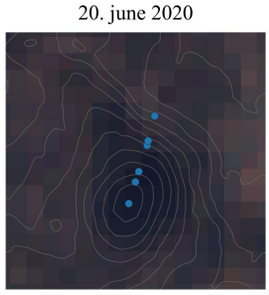

15. july 2020

Snow cover
Transect 7

4. march 2020

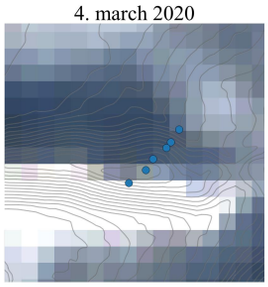

24. may 2020

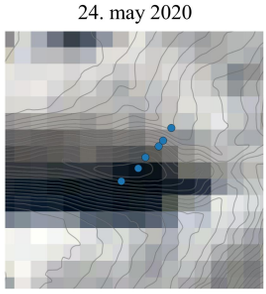

2. june 2020
(some clouds in upper part of crop)

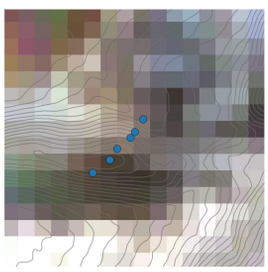

13. june 2020

20. june 2020

15. july 2020

Appendix 12 NIRS values for Nitrogen and Phosphorous

	Nitrogen [mg/kg]			Phosphorous [mg/kg]		
Plot	Scan 1	Scan 2	Mean	Scan 1	Scan 2	Mean
101	14462.50	12387.71	13425.10	855.83	650.24	753.04
102	5293.67	2014.55	3654.11	328.27	232.95	280.61
103	8977.68	9051.42	9014.55	425.17	341.08	383.12
104	12818.93	14665.38	13742.15	683.87	826.82	755.34
105	11488.13	9463.69	10475.91	450.73	293.94	372.34
106	5733.48	6073.76	5903.62	566.50	452.19	509.34
107	13313.64	13886.39	13600.01	643.29	547.32	595.30
108	12983.47	14689.13	13836.30	456.86	434.78	445.82
109	11269.01	8312.27	9790.64	663.12	313.06	488.09
110	17306.97	15649.50	16478.23	760.02	556.22	658.12
111	6971.28	3548.67	5259.97	1473.93	1117.55	1295.74
112	9077.56	5536.13	7306.84	1288.64	1022.67	1155.66
201	15095.44	15780.27	15437.85	675.44	588.32	631.88
202	12522.54	12921.99	12722.27	314.45	393.24	353.85
203	13569.77	11831.35	12700.56	345.73	117.64	231.69
204	16036.52	14462.20	15249.36	604.41	407.28	505.84
205	14128.87	16133.42	15131.14	632.90	784.91	708.90
206	13431.59	13942.92	13687.26	613.42	438.29	525.86
207	15878.00	17253.35	16565.68	906.75	831.62	869.18
208	14291.22	9287.10	11789.16	702.52	715.00	708.76
301	10840.39	9390.05	10115.22	745.82	304.56	525.19
302	14739.53	15917.35	15328.44	653.62	675.35	664.49
303	15663.80	15410.26	15537.03	567.22	546.11	556.67
304	15252.69	16041.80	15647.25	784.04	498.74	641.39
305	14318.62	12803.57	13561.09	674.24	359.48	516.86
306	15118.27	15211.45	15164.86	874.40	1034.60	954.50
307	13757.94	13112.78	13435.36	502.74	419.95	461.35
308	16212.25	13097.59	14654.92	919.26	402.32	660.79
309	15395.10	13232.00	14313.55	960.99	567.16	764.08
310	11945.39	13040.61	12493.00	454.09	407.39	430.74
311	14379.43	14555.60	14467.51	625.33	582.73	604.03
312	12472.46	13494.98	12983.72	685.37	547.06	616.21
401	13774.88	14384.30	14079.59	534.72	652.41	593.57
402	14252.63	14993.13	14622.88	755.21	654.77	704.99
403	14678.43	9261.22	11969.82	675.40	540.77	608.08
404	14680.19	16407.48	15543.83	689.55	642.15	665.85
405	15464.75	16294.13	15879.44	580.46	632.99	606.72
406	15708.40	13696.80	14702.60	461.65	335.50	398.58
501	16349.60	17403.42	16876.51	1016.84	959.55	988.20
502	14394.99	14702.60	14548.79	580.39	406.34	493.36
503	11314.40	9276.75	10295.57	435.12	268.58	351.85
504	13139.32	13513.88	13326.60	827.66	398.71	613.19
505	9688.85	13774.62	11731.74	619.60	671.52	645.56
506	17038.66	15277.78	16158.22	816.57	611.67	714.12
507	15961.73	15079.81	15520.77	845.96	595.26	720.61
508	11620.80	10470.15	11045.47	867.43	564.01	715.72
601	10956.41	10143.30	10549.86	396.26	200.45	298.35
602	13340.18	12799.51	13069.85	466.45	314.92	390.69
603	15071.53	14546.42	14808.97	627.84	607.17	617.50
604	15449.78	13475.13	14462.46	150.21	379.22	264.72
605	11113.58	13821.05	12467.31	443.66	710.32	576.99
606	14236.96	10261.52	12249.24	509.48	492.73	501.11
701	15840.54	14639.53	15240.03	482.83	191.44	337.14
702	13024.09	11590.32	12307.20	205.82	110.57	158.19
703	10919.67	11285.86	11102.76	547.33	403.37	475.35
704	11107.64	10810.37	10959.01	530.30	242.65	386.48
705	14716.21	14870.36	14793.29	627.52	688.38	657.95
706	10599.39	9328.68	9964.03	717.28	471.11	594.19

Appendix 13 NIRS and muffle oven analyses values for LOI (Loss on ignition)

	LOI (%)			
Plot	NIRS scan 1	NIRS scan 2	NIRS mean	Muffle oven analyses
101	81.1	74.6	77.9	86.7
102	56.1	45.2	50.7	54.0
103	93.5	97.6	95.5	97.2
104	92.6	91.8	92.2	97.6
105	74.3	93.0	83.7	96.4
106	60.0	57.3	58.6	89.9
107	*101.6*	*104.5*	*103.1*	98.2
108	*100.1*	99.2	99.6	96.7
109	88.5	83.4	86.0	95.9
110	85.0	*101.3*	93.2	97.5
111	16.7	26.8	21.7	24.0
112	28.9	42.1	35.5	31.5
201	95.6	104.0	99.8	97.8
202	93.3	98.2	95.7	97.8
203	85.6	98.0	91.8	95.9
204	95.4	*107.0*	*101.2*	97.7
205	*104.8*	*100.1*	*102.4*	97.7
206	91.6	93.1	92.3	95.1
207	64.6	78.3	71.5	67.9
208	75.1	81.0	78.0	93.7
301	76.7	77.9	77.3	93.4
302	90.3	92.9	91.6	97.0
303	92.9	89.6	91.3	95.1
304	96.6	*101.1*	98.9	97.5
305	87.1	*103.7*	95.4	97.5
306	97.0	*102.9*	*100.0*	97.3
307	96.0	98.3	97.2	97.2
308	96.8	*100.2*	98.5	98.0
309	*102.1*	*105.9*	*104.0*	98.3
310	94.1	99.7	96.9	97.4
311	*103.9*	*105.6*	*104.7*	98.0
312	*100.1*	*102.6*	*101.3*	97.9
401	98.3	*103.8*	*101.0*	97.7
402	99.1	*100.8*	99.9	97.8
403	91.2	*107.7*	99.5	97.7
404	*104.0*	*102.5*	*103.3*	97.6
405	*100.2*	*103.4*	*101.8*	97.6
406	89.9	*104.3*	97.1	94.7
501	98.7	97.6	98.2	97.2
502	95.8	99.6	97.7	97.0
503	83.8	86.4	85.1	97.2
504	93.9	*100.2*	97.0	97.8
505	91.1	96.5	93.8	97.4
506	80.4	*100.0*	90.2	97.1
507	95.0	98.8	96.9	96.9
508	77.8	78.4	78.1	76.6
601	75.8	79.8	77.8	89.5
602	93.2	99.3	96.3	96.8
603	*102.5*	*108.5*	*105.5*	97.5
604	93.8	98.6	96.2	97.6
605	81.6	86.3	83.9	98.0
606	96.0	95.0	95.5	97.7
701	*108.4*	*109.5*	*109.0*	97.0
702	91.9	*106.9*	99.4	96.8
703	*100.0*	*101.8*	*100.9*	96.9
704	*101.2*	99.7	*100.4*	97.1
705	*101.5*	*102.3*	*101.9*	98.0
706	59.6	63.8	61.7	51.1

Appendix 13 Standardizes semivariograms

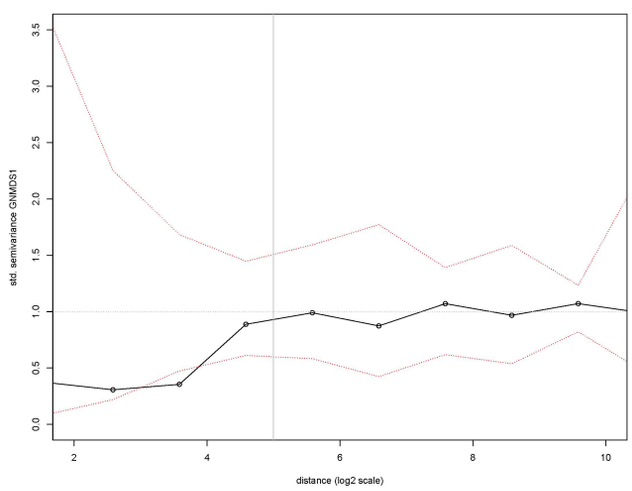

Figure A.1: Standardized semivariogram for GNMDS1. Red lines show confidence intervals for the variable, and the horizontal grey line shows the mean distance where variation goes from within transect to between transect variation

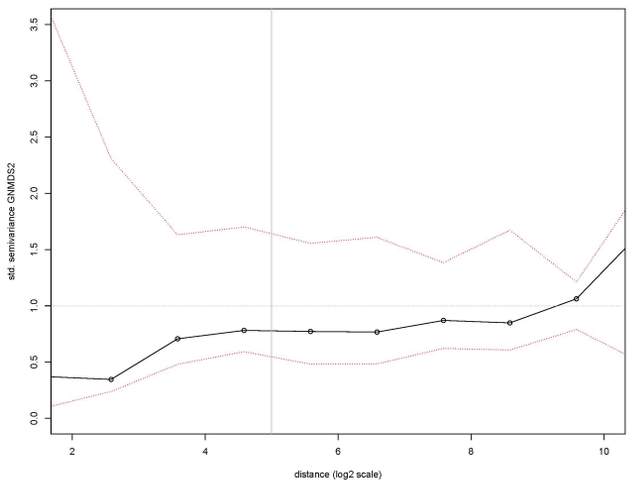

Figure A.2: Standardized semivariogram for GNMDS2. Red lines show confidence intervals for the variable, and the horizontal grey line shows the mean distance where variation goes from within transect to between transect variation

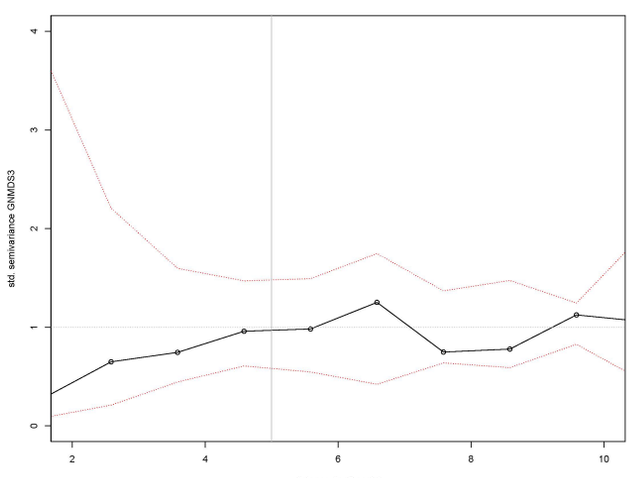

Figure A.3: Standardized semivariogram for GNMDS3. Red lines show confidence intervals for the variable, and the horizontal grey line shows the mean distance where variation goes from within transect to between transect variation

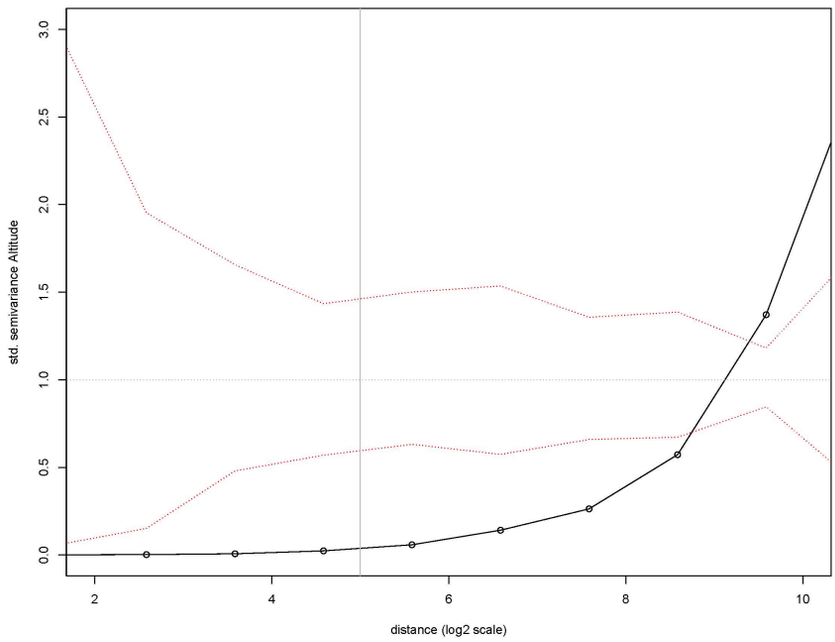

Standardized semivariogram for Altitude. Red lines show confidence intervals for the variable, and the horizontal grey line shows the mean distance where variation goes from within transect to between transect variation

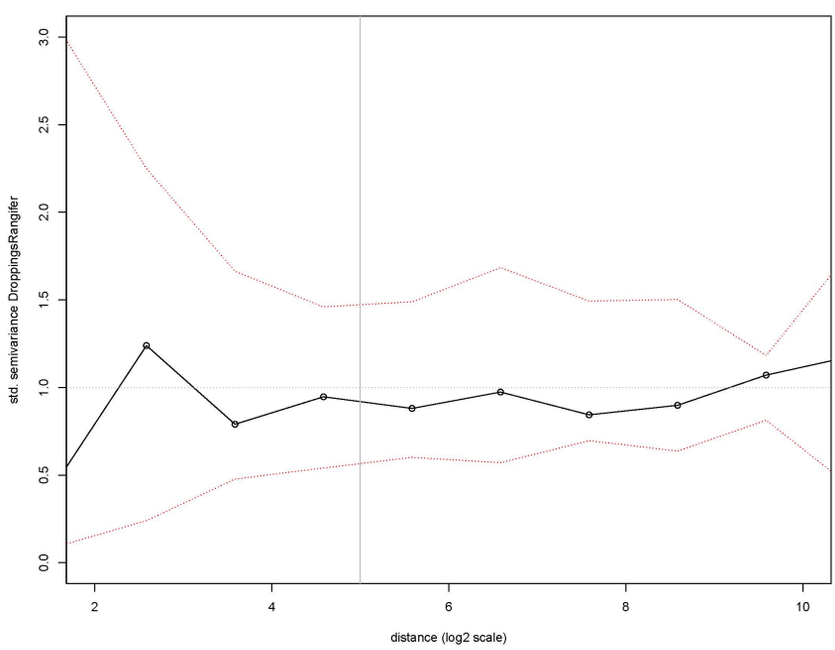

Standardized semivariogram for droppings from R. tarandus (DroppingsRangifer). Red lines show confidence intervals for the variable, and the horizontal grey line shows the mean distance where variation goes from within transect to between transect variation.

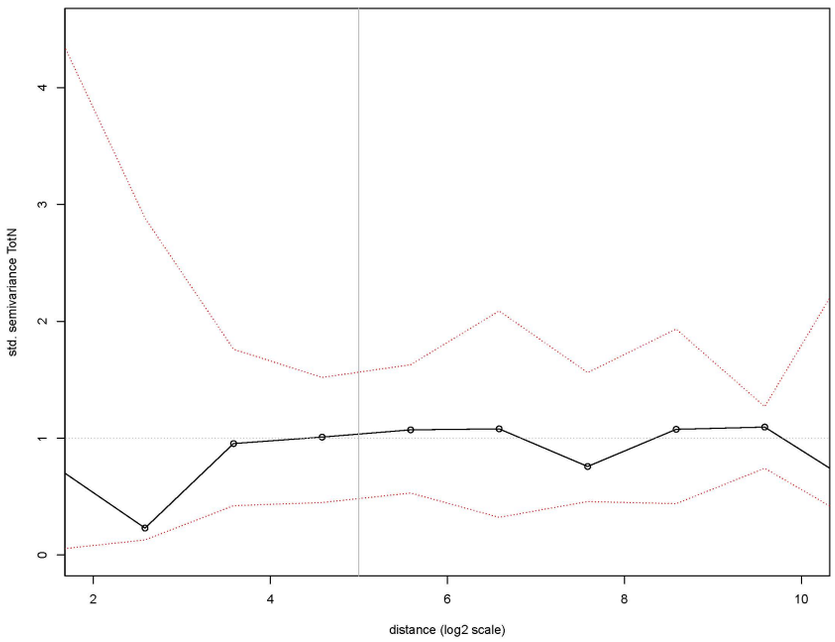

Figure A.4: Standardized semivariogram for nitrogen content in the soil (TotN). Red lines show confidence intervals for the variable, and the horizontal grey line shows the mean distance where variation goes from within transect to between transect variation.

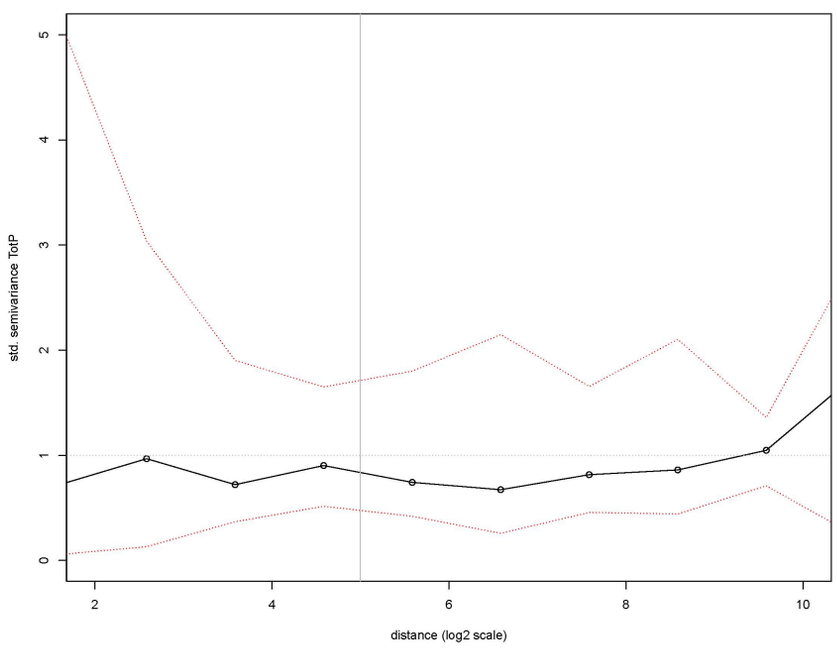

Figure A.5: Standardized semivariogram for phosporous content in the soil (TotP). Red lines show confidence intervals for the variable, and the horizontal grey line shows the mean distance where variation goes from within transect to between transect variation.

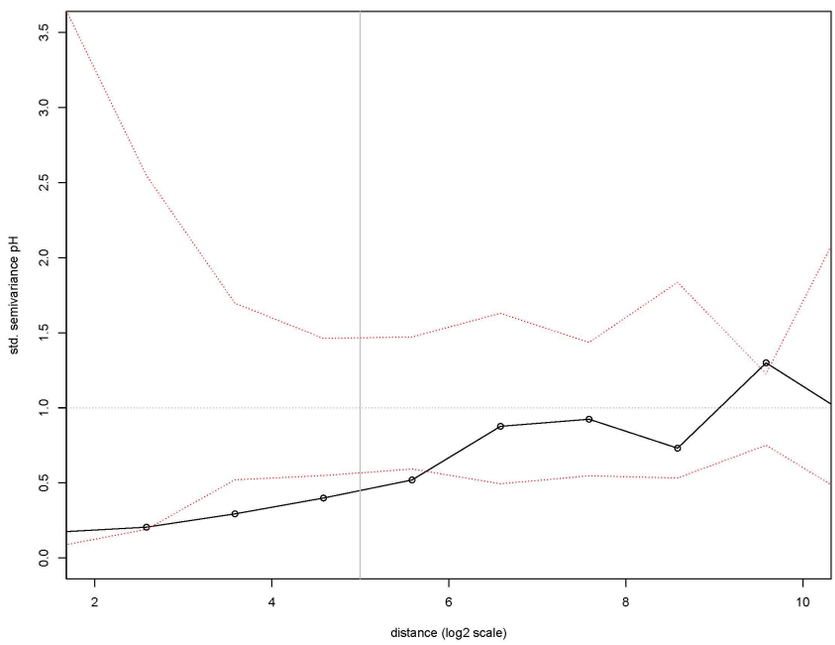

Standardized semivariogram for pH. Red lines show confidence intervals for the variable, and the horizontal grey line shows the mean distance where variation goes from within transect to between transect variation

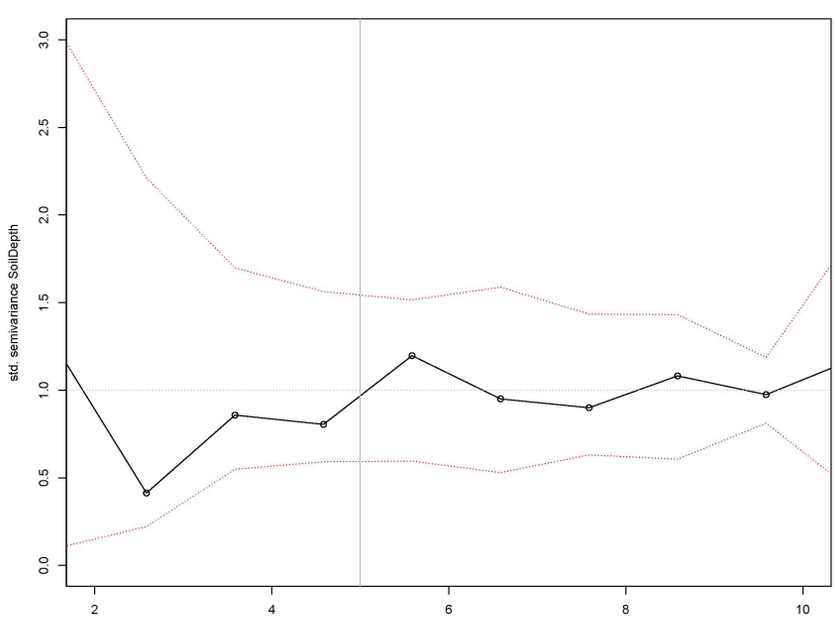

Standardized semivariogram for soil depth. Red lines show confidence intervals for the variable, and the horizontal grey line shows the mean distance where variation goes from within transect to between transect variation

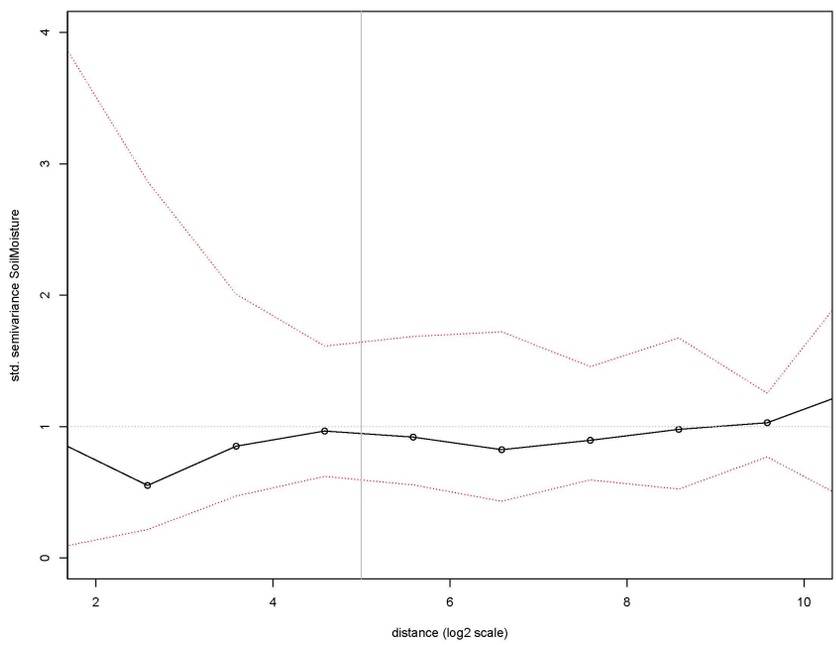

Figure A.6: Standardized semivariogram for soil moisture. Red lines show confidence intervals for the variable, and the horizontal grey line shows the mean distance where variation goes from within transect to between transect variation

Terrain variation

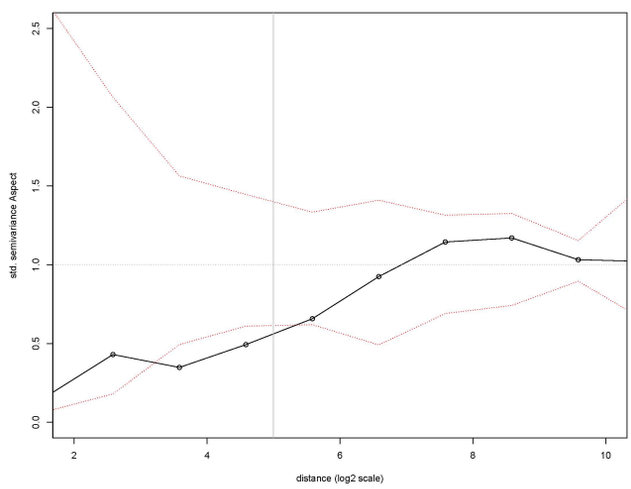

Figure A.7: Standardized semivariogram for Aspect. Red lines show confidence intervals for the variable, and the horizontal grey line shows the mean distance where variation goes from within transect to between transect variation.

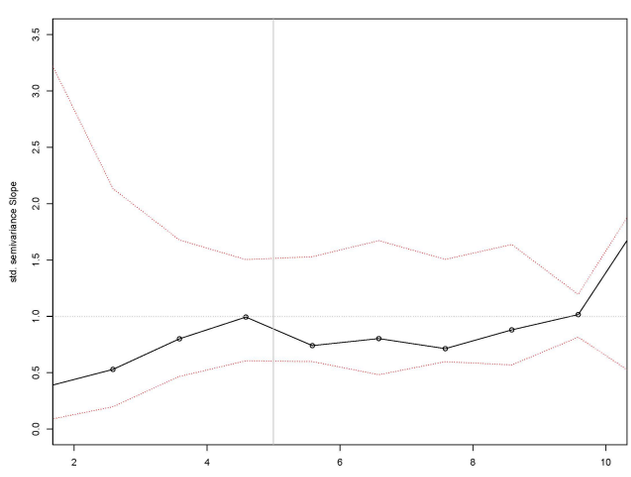

Figure A.8: Standardized semivariogram for Slope. Red lines show confidence intervals for the variable, and the horizontal grey line shows the mean distance where variation goes from within transect to between transect variation.

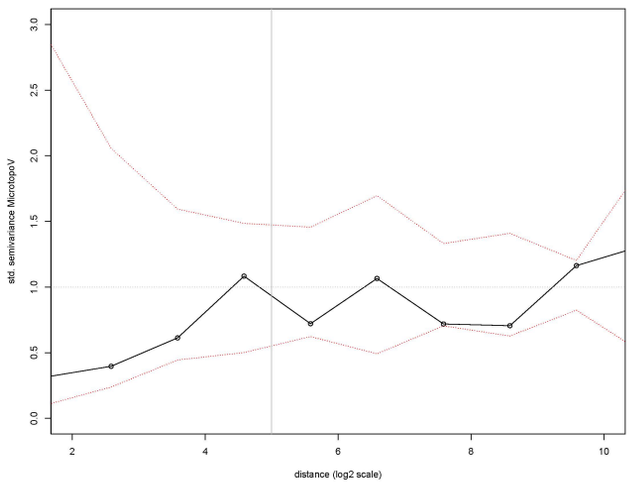

Figure A.9: Standardized semivariogram for MicrotopoV. Red lines show confidence intervals for the variable, and the horizontal grey line shows the mean distance where variation goes from within transect to between transect variation.

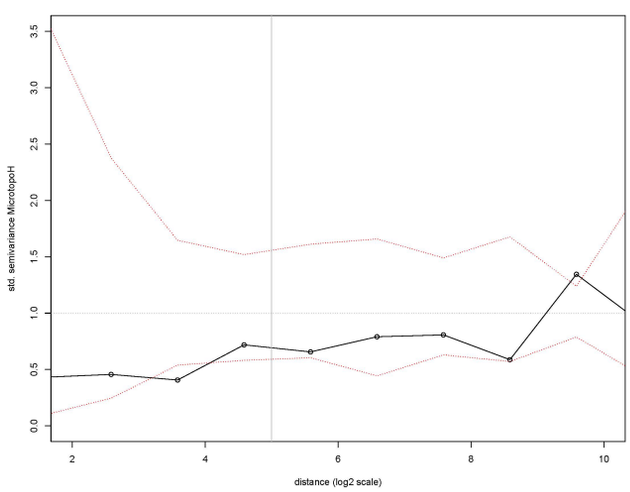

Standardized semivariogram for MicrotopoH. Red lines show confidence intervals for the variable, and the horizontal grey line shows the mean distance where variation goes from within transect to between transect variation.

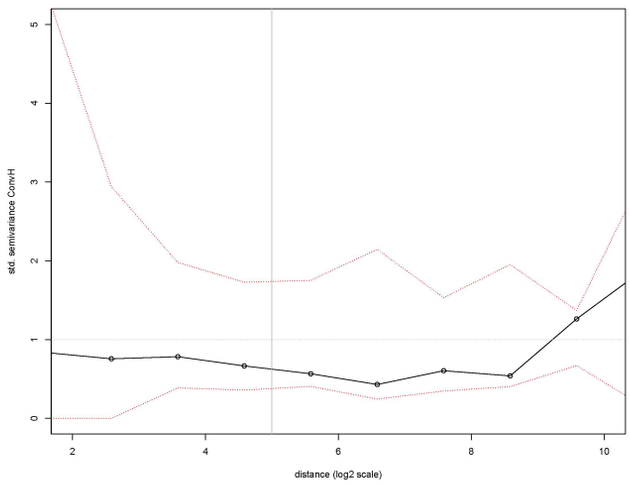

Figure A.10: Standardized semivariogram for ConvH. Red lines show confidence intervals for the variable, and the horizontal grey line shows the mean distance where variation goes from within transect to between transect variation.

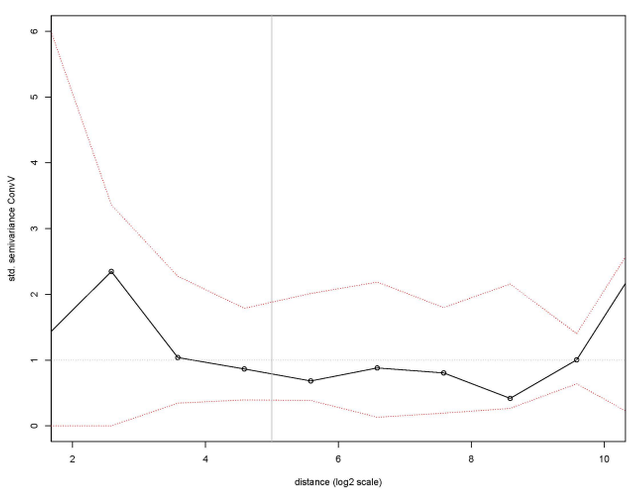

Figure A.11: Standardized semivariogram for ConvV. Red lines show confidence intervals for the variable, and the horizontal grey line shows the mean distance where variation goes from within transect to between transect variation.

A.0.1 Significant variables to GNMDS1

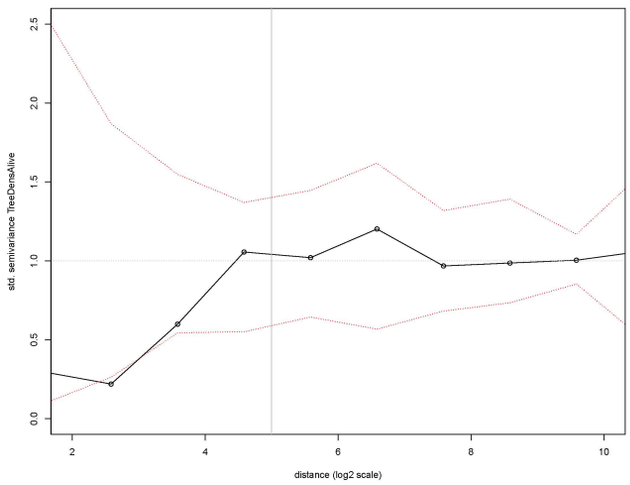

Figure A.12: Standardized semivariogram for TreeDensAlive. Red lines show confidence intervals for the variable, and the horizontal grey line shows the mean distance where variation goes from within transect to between transect variation.

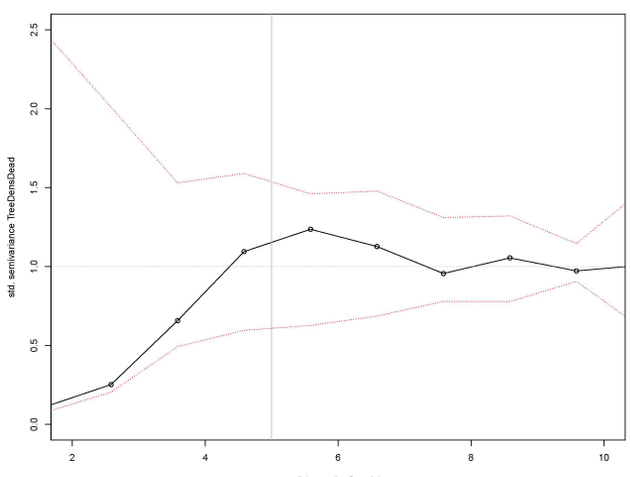

Figure A.13: Standardized semivariogram for TreeDensDead. Red lines show confidence intervals for the variable, and the horizontal grey line shows the mean distance where variation goes from within transect to between transect variation.

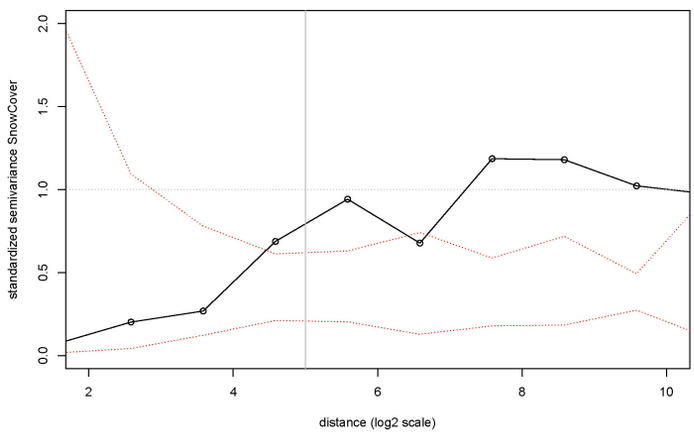

Figure A.14: Standardized semivariogram for snow cover. Red lines show confidence intervals for the variable, and the horizontal grey line shows the mean distance where variation goes from within transect to between transect variation.

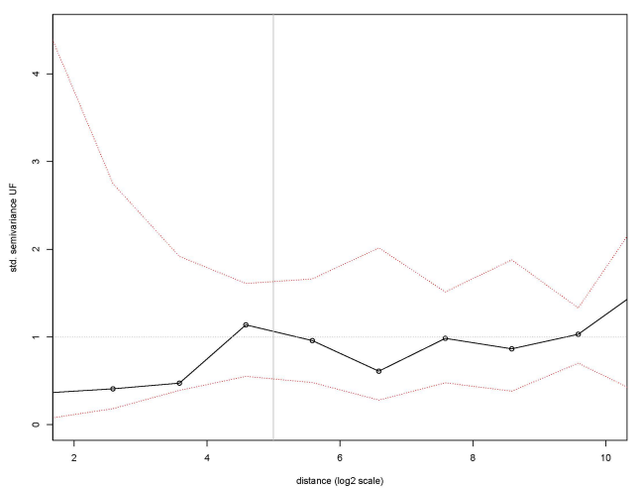

Figure A.15: Standardized semivariogram for risk of severe drought (UF). Red lines show confidence intervals for the variable, and the horizontal grey line shows the mean distance where variation goes from within transect to between transect variation.

A.0.2 Significant variables to GNMDS2

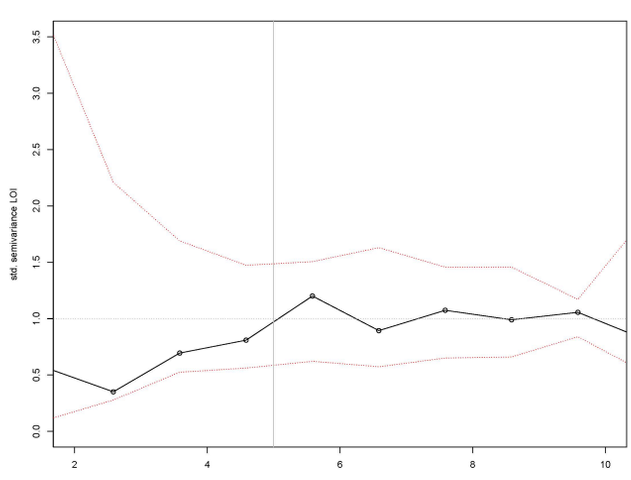

Figure A.16: Standardized semivariogram for loss on ignition (LOI). Red lines show confidence intervals for the variable, and the horizontal grey line shows the mean distance where variation goes from within transect to between transect variation.

A.0.3 Significant variables to GNMDS3

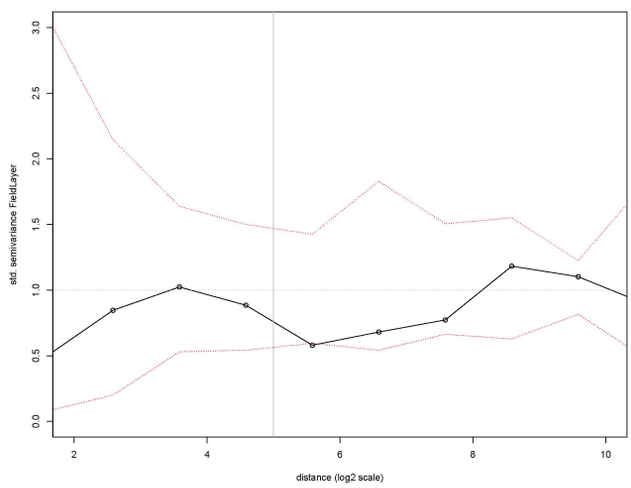

Figure A.17: Standardized semivariogram for FieldLayer. Red lines show confidence intervals for the variable, and the horizontal grey line shows the mean distance where variation goes from within transect to between transect variation.

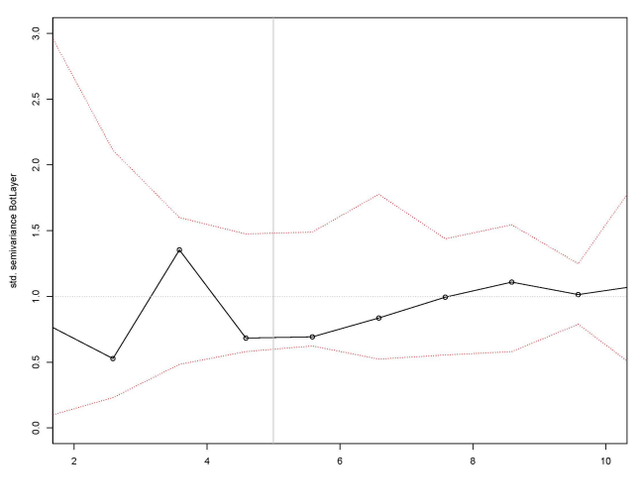

Figure A.18: Standardized semivariogram for BotLayer. Red lines show confidence intervals for the variable, and the horizontal grey line shows the mean distance where variation goes from within transect to between transect variation